HIGHWAY RESEARCH BOARD

Bulletin 242

Bridges: Bearing Pads, Foundations, Scour and Waterways

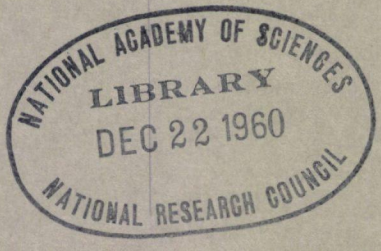

National Academy of Sciences—
National Research Council

publication 728

HIGHWAY RESEARCH BOARD

Officers and Members of the Executive Committee

1960

OFFICERS

PYKE JOHNSON, *Chairman* W. A. BUGGE, *First Vice Chairman*

R. R. BARTELSMEYER, *Second Vice Chairman*

FRED BURGGRAF, *Director* ELMER M. WARD, *Assistant Director*

Executive Committee

BERTRAM D. TALLAMY, *Federal Highway Administrator, Bureau of Public Roads* (ex officio)

A. E. JOHNSON, *Executive Secretary, American Association of State Highway Officials* (ex officio)

LOUIS JORDAN, *Executive Secretary, Division of Engineering and Industrial Research, National Research Council* (ex officio)

C. H. SCHOLER, *Applied Mechanics Department, Kansas State College* (ex officio, Past Chairman 1958)

HARMER E. DAVIS, *Director, Institute of Transportation and Traffic Engineering, University of California* (ex officio, Past Chairman 1959)

R. R. BARTELSMEYER, *Chief Highway Engineer, Illinois Division of Highways*

J. E. BUCHANAN, *President, The Asphalt Institute*

W. A. BUGGE, *Director of Highways, Washington State Highway Commission*

MASON A. BUTCHER, *Director of Public Works, Montgomery County, Md.*

A. B. CORNTHWAITE, *Testing Engineer, Virginia Department of Highways*

C. D. CURTISS, *Special Assistant to the Executive Vice President, American Road Builders' Association*

DUKE W. DUNBAR, *Attorney General of Colorado*

FRANCIS V. DU PONT, *Consulting Engineer, Cambridge, Md.*

H. S. FAIRBANK, *Consultant, Baltimore, Md.*

PYKE JOHNSON, *Consultant, Automotive Safety Foundation*

G. DONALD KENNEDY, *President, Portland Cement Association*

BURTON W. MARSH, *Director, Traffic Engineering and Safety Department, American Automobile Association*

GLENN C. RICHARDS, *Commissioner, Detroit Department of Public Works*

WILBUR S. SMITH, *Wilbur Smith and Associates, New Haven, Conn.*

REX M. WHITTON, *Chief Engineer, Missouri State Highway Department*

K. B. WOODS, *Head, School of Civil Engineering, and Director, Joint Highway Research Project, Purdue University*

Editorial Staff

FRED BURGGRAF ELMER M. WARD HERBERT P. ORLAND

2101 Constitution Avenue Washington 25, D. C.

 HIGHWAY RESEARCH BOARD

Bulletin 242

Bridges: Bearing Pads, Foundations, Scour and Waterways

Presented at the
38th ANNUAL MEETING
January 5-9, 1959

1960

Washington, D. C.

Department of Design

T.E. Shelburne, Chairman
Director of Research, Virginia Department of Highways
Charlottesville

COMMITTEE ON SURFACE DRAINAGE OF HIGHWAYS

Carl F. Izzard, Chairman
Chief, Division of Hydraulic Research
Bureau of Public Roads

Robert E. Bond, Hydraulic Engineer, Bureau of Public Roads, Denver, Colorado
Tate Dalrymple, U.S. Geological Survey, Washington, D.C.
Roy C. Edgerton, Research Engineer, Oregon State Highway Commission, Salem
Kenneth Eff, Chief, Hydraulic Section, Chief of Engineers, Washington, D.C.
John G. Hendrickson, Jr., American Concrete Pipe Association, Chicago
S.W. Jens, Consulting Engineer, 101 S. Meramec St., St. Louis, Mo.
Clint Jay Keifer, Engineer of Sewer Hydraulics, City Bureau of Engineering, Chicago
James D. Lacy, Drainage Engineer, Bureau of Public Roads, Fort Worth, Texas
Robert A. Norton, Hydraulic Engineer, Connecticut State Highway Department, Hartford
A.L. Pond, Jr., Drainage Engineer, Virginia Department of Highways, Richmond
W.O. Ree, Agricultural Research Service, Stillwater, Oklahoma
John M. Robertson, Chief Sales Engineer, Armco Drainage and Metal Products Inc., Middletown, Ohio
R. Robinson Rowe, Bridge Engineer, California Division of Highways, Sacramento
Clyde T. Sullivan, Chief, Division of Engineering, U.S. Department of Agriculture
F.W. Thorstonson, Hydraulic Engineer, Minnesota Department of Highways, St. Paul
W.S. Winslow, Hydrographic Engineer, North Carolina State Highway Commission, Raleigh

COMMITTEE ON BRIDGES

G.S. Paxson, Chairman
Assistant State Highway Engineer,
Oregon State Highway Commission, Salem

Raymond Archibald, 1242 E. McDowell Road, Pheonix, Arizona
J.N. Clary, Engineer of Bridges, Virginia Department of Highways, Richmond
E.M. Cummings, Manager of Sales, Bethlehem Steel Company, Bethlehem, Pennsylvania
Frederick H. Dill, Assistant to Vice President, U.S. Steel Corporation, Pittsburgh, Pennsylvania
E.L. Erickson, Chief, Bridge Division, Bureau of Public Roads
F.M. Fuller, Raymond Concrete Pile Company, New York, N.Y.
H. deR. Gibbons, The Union Metal Manufacturing Company, Canton, Ohio
T.B. Gunter, Jr., Assistant Chief Engineer—Bridges, North Carolina State Highway Commission, Raleigh
John J. Hogan, Consulting Structural Engineer, Portland Cement Association, New York, N.Y.
W.T. Lankford, Applied Research Laboratory, U.S. Steel Corporation, Monroeville, Pennsylvania
Adrian Pauw, Professor of Civil Engineering, University of Missouri, Columbia
M.N. Quade, Consulting Engineer, Parsons, Brinckerhoff, Hall and MacDonald, New York, N.Y.
William H. Rabe, First Assistant Engineer of Bridges, Ohio Department of Highways, Columbus
C.P. Siess, Professor, Department of Civil Engineering, University of Illinois, Urbana
Charles B. Trueblood, Armco Drainage and Metal Products, Inc., Middletown, Ohio
J.A. Williams, Bridge Engineer, Missouri State Highway Department, Jefferson City

Contents

Elastomeric Bridge Bearings

R. L. PARE, Bridge Engineer, and
E. P. KEINER, Structural Engineer, Charles A. Maguire and Associates, Providence, R. I.

Tests were made for the purpose of determining the adequacy of elastomeric bearings in bridge construction and to establish bearing design criteria. Samples of neoprene, 6 in. by 12 in. of varying thickness, molded or in bonded layers, were tested. Test equipment included a 500,000-lb Southwark-Emery tension compression machine, a 40,000-lb hydraulic jack and various recording gauges. The required compressive and shear loads were applied directly, alternately and in combination for varying periods. Test phases included vertical deflection under compression, horizontal and vertical deflection in combined compression and shear, shape effects, time-creep relationships and fatigue.

All bearing types tested bore close stress-strain relationships. Within the limits of the test procedures it is assumed that neoprene-based bearing products meeting current specifications have similar physical properties. It was found that vertical deflection increased inversely with durometer readings; with time and dynamic loading; and were proportionally greater with added thickness. Tests for additional vertical deflections similar to intermittent live bridge loads or dynamic creep, indicate that static deflections should be increased by 50 percent.

Bearings tested indicated, in each instance, similar horizontal deflections due to horizontal shear loads. Resistance to shear distortion increased with thickness and stiffness but was not affected by direct compressive loading or by shape or orientation of bearing. The absence of fatigue in the 3-hr alternating phase of the tests indicates the need for a longer testing period in this respect.

TEST OF ELASTOMERIC BRIDGE BEARINGS

●THE PURPOSE of the program leading to this report was twofold; first, to investigate the physical properties of elastomeric materials now available; and second, to establish a design procedure, based on experimental data, for the use of elastomeric bearings.

The use of elastomeric materials for bridge bearings has some precedent. The Texas and Florida Highway Departments, the British Railway System and the French National Railway have all used elastomeric bearings. The British Railways have conducted tests similar to those described herein; however, the materials tested were apparently of lower durometer hardness and may have differed in compounding.

The principal physical characteristics required of materials for elastomeric bearings include the following:

1. Resist compressive loading up to 1,200 psi without undue deflection and with definite limits of creep under sustained load.
2. Resist shear loads which produce deflections up to 50 percent of the thickness of the bearings without loss of elastic properties.
3. Resist repeated reversal of shear loads without undue loss of elastic properties.
4. Divergence from stress-strain ratio at 70 F not to exceed 25 percent for increase or decrease of temperature by 90 F.
5. Remain not brittle at minus 30 F.

The desirable chemical characteristics include:

1. Excellent resistance to weathering, ozone and natural aging.
2. Resistance to water absorption within acceptable limits.
3. Resistance to deterioration by oil to limit loss of strength characteristics to 20 percent after a standard immersion test.

Temperature and chemical tests of the elastomeric materials were beyond the scope of this program. These characteristics must be determined by tests conducted with equipment not normally available nor easily manufactured in laboratories maintained by public agencies. The importance of these tests is, however, not to be overlooked and the elastomeric materials must be found satisfactory in these tests before their use can be universally accepted.

The material selected for testing consisted of blocks of neoprene molded into the required shape or built up of layers of plies (each = 0.21 in. thick) to the required thicknesses and bonded with a cementing agent. The test specimens were of uniform width and length except in tests for shape factor. The width was 6 in., the length 12 in. and the thickness varied. This size was selected as an approximation of the average size anticipated for bridge bearings (Fig. 1).

The equipment was designed around a Southwark-Emery tension compression machine of 500,000-lb capacity. A 40,000-lb hydraulic jack was used to provide the shear force. The apparatus consisted of two concrete blocks set between the heads of the compression machine. A yoke was cast into the concrete blocks to hold the hydraulic jack and to provide a reaction for the base of the jack. The samples to be tested were placed above and below a steel or steel and concrete-shear plate and inserted between the concrete blocks in the compression machine. Loads were applied vertically by the compression

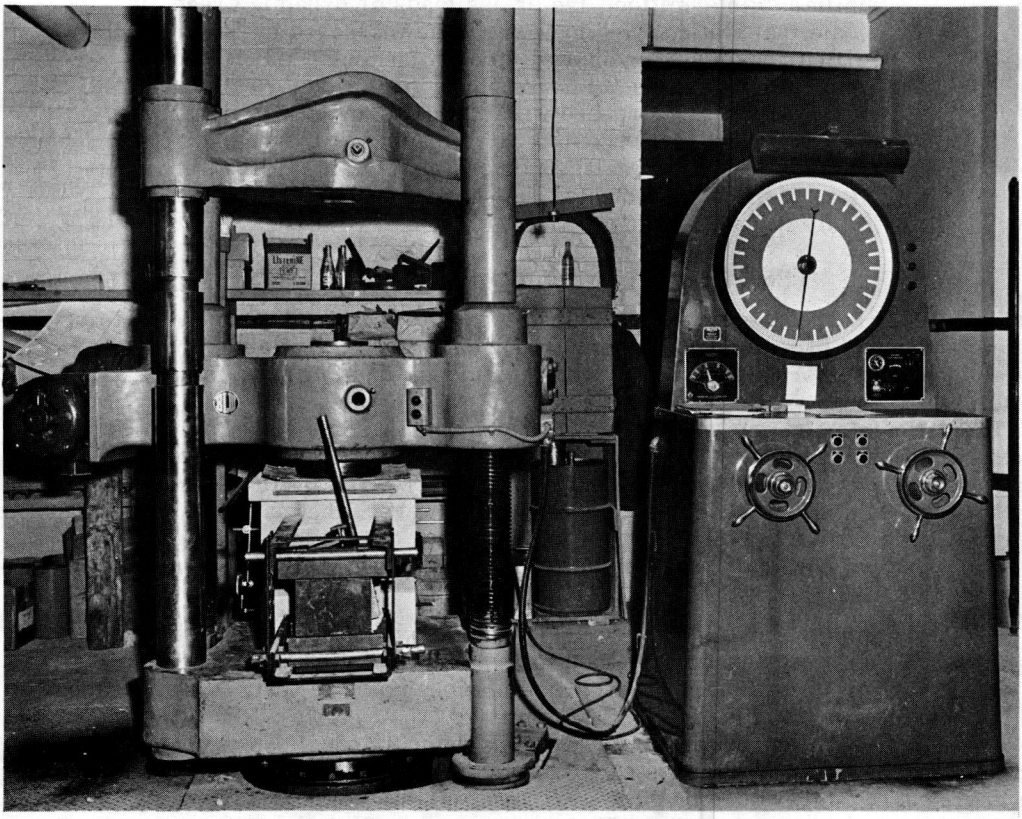

Figure 1. Test equipment.

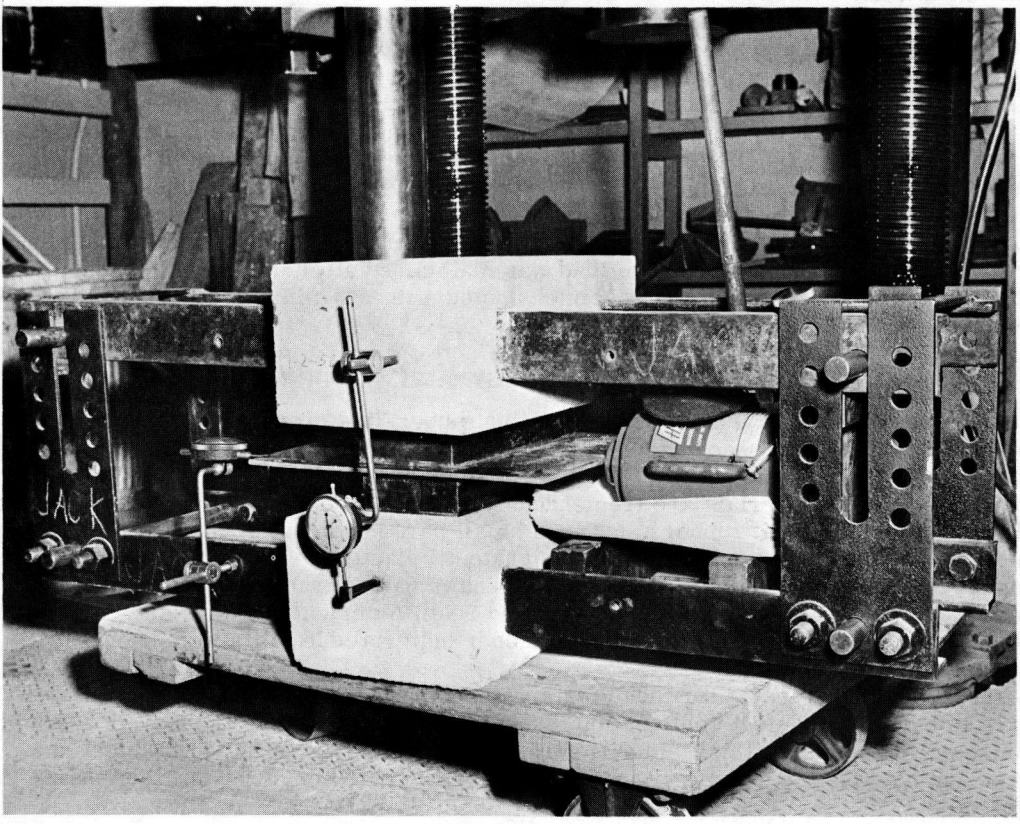

Figure 2. Shear stressing test equipment.

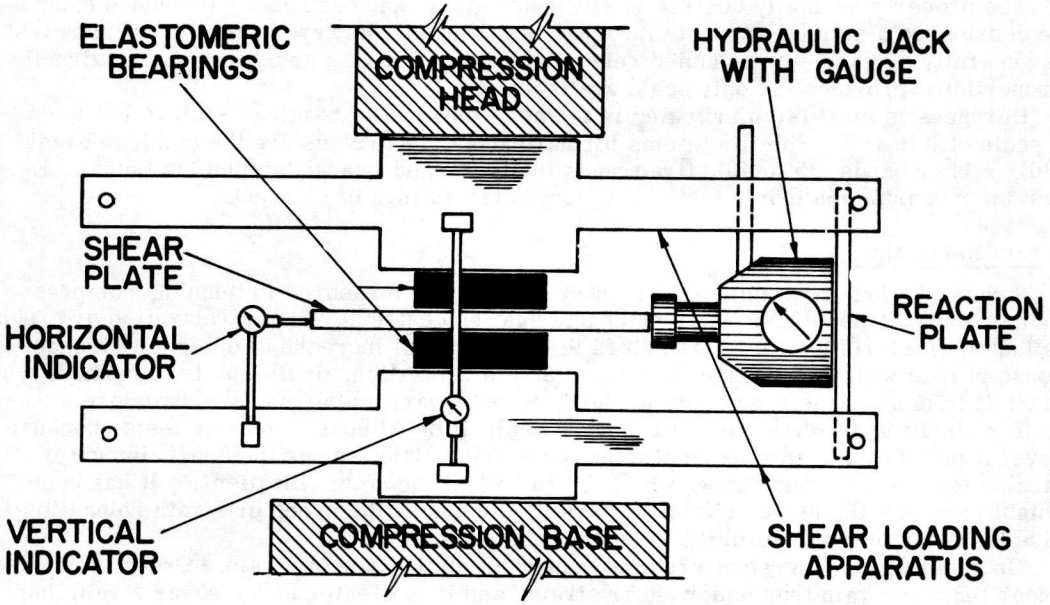

Figure 3. Diagram of testing apparatus.

machine and horizontally by the hydraulic jack (Figs. 2 and 3).

The instrumentation consisted of load gauges on the Southwark-Emery machine and hydraulic jack, and horizontal and vertical deflection dial indicators. Two dial indicators were used to measure vertical deflection and two for horizontal deflection. The resultant movements were the average of the dial readings.

The basic procedure was first to load the specimens in compression, recording load and deflection; hold the compressive load for 5 min and slowly unload. The specimen was then again loaded in compression and the compression load held constant while shear loads were applied up to 40 percent of the compressive load. The shear load to each of the two bearings of 20 percent (total 40 percent) was held for 5 min and then slowly unloaded. The compressive load was maintained after the shear load had been removed and the recovery of the specimens noted after a 5-min interval. All tests followed this general procedure.

ELASTOMER TERMINOLOGY AND PROPERTIES

Elastomer means all materials that exhibit rubber-like properties. The term elastomer, when generally recognized and accepted, will eliminate many of the prejudices associated with synthetic rubber. The physical and chemical properties of the man-made elastomeric materials are tremendously varied, exceeding in many cases the useful properties of natural rubbers, not by a small percentage but by many times.

Natural rubber is the term used to designate all elastomer materials manufactured from vegetable sap. Commercially the best known natural rubber is "Hevea," produced from rubber grown principally in Central and South America. Other elastomer materials are normally compared with natural rubber material due to its well-known characteristics.

The elastomer selected for these tests was neoprene. At this time, neoprene appears to have the greatest combination of required properties of the elastomers available. Future developments in this field will surely increase the desirable qualities of neoprene and may lead to an entirely new substance superior in every desirable characteristic.

ELASTOMER PROPERTIES AND STANDARD TESTS

Hardness

The property normally desired is stiffness rather than hardness. Hardness cannot be considered a strictly accurate measure of stiffness. However, until a stiffness test is generally adopted, the assumed relationship that hardness and stiffness are directly proportional provides the only scale available.

Hardness is most often indicated in terms of durometer readings—soft to hard—on a scale of 0 to 100. Familiar items for hardness comparisons are the common eraser (30), rubber bands (35 to 40), tire treads (60 to 70) and typewriter platens (90±5). Elastomer bearing materials tested had durometer ratings of 60 to 90.

Strain Relaxation

Stress-strain relaxation and permanent set must be measured in tension, compression or shear depending on the type of information desired. "Strain relaxation or creep is that characteristic of all elastomers to show gradual increase of deformation under constant load with the passage of time... Strain relaxation, or creep, is important... since it influences the space relationships between various parts of the structure. It is difficult to predict creep for a given application without... service tests, because several factors have an important effect on creep. Chief among these are amount of strain, temperature and changes in these two resulting from vibration... It has been established that the higher the initial strain, the higher the creep or strain relaxation; also the higher the temperature the higher the creep.

"In general, the degree of creep is dependent on the type of strain. Creep is greater under tension strain than under shear strain, and it is greater under shear strain than under equal compression strain. Creep is also greater under dynamic loading than under static loading." (1).

Compression Load Deflection

In the region where compressive loads are 300 to 800 psi, the stress-strain curve is nearly straight, and design assumptions assuming proportional stress-strain can be made within reasonable error. Below this range, stress-strains are far from proportional and experimental curves must be developed for the range desired.

Shape

In addition to stiffness and range of deflection, another factor known as shape affects the stress-strain relationship. Elastomers subject to compressive loads lose little or no volume. To deflect vertically it is necessary for the elastomer to expand horizontally. If the contact surfaces restrain movement, the free surfaces bulge. Through much experimentation an empirical formula has been developed which relates this degree of restraint and is known as shape factor.

$$\text{Shape Factor} = \frac{\text{One Load Area}}{\text{Total Free Area}}$$

For a rectangular block of length A, width B, and thickness t, the formula for Shape Factor becomes

$$S = \frac{A \times B}{2t\,(a + B)}$$

The relation of Shape Factor (Fig. 4) to stiffness is well documented and it need only be noted that stiffness increases with Shape Factor. In bridge bearings the ratio of the area of loaded surface to the thickness of the bearing is so great the effect of Shape Factor error is small.

Shear Load Deflection

Shear deflection in elastomers is measured as the ratio of linear deformation d to the rubber thickness t. The angle of torsion is θ (Fig. 5).

When combined with compression, the thickness must be reduced by the deflection Δt, due to compression, therefore

$$\frac{d}{t - \Delta t} = \tan \theta$$

Shape in shear has been found to have little effect except when the thickness to width ratio is greater than one to four. This ratio should probably be kept to one to five as a minimum to prevent edge disturbance and a tendency to roll.

SERVICE TESTS

The simulated service tests included the following categories:

1. Vertical deflection under varying compressive loads at room temperature;
2. Other variables: (a) thickness, (b) hardness, (c) compounding (manufacture), and (d) shape;
3. Horizontal deflection under varying horizontal shear and vertical compressive loads at room temperature; and
4. Other variables as previously indicated.

Analysis of the results of the above tests, together with special tests, combined to yield information on the effect of (a) shape, (b) creep, (c) compounding, and (d) fatigue on neoprene bearings.

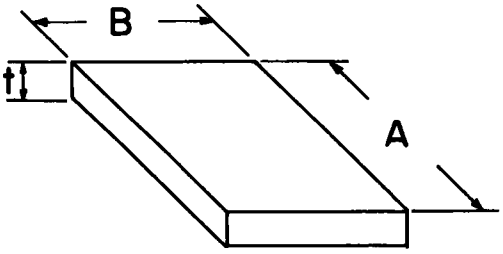

Figure 4. Shape factor.

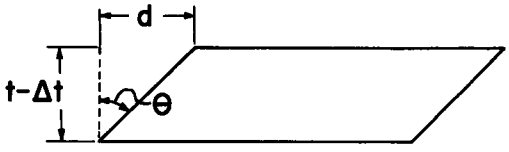

Figure 5. Shear deflection angle.

Compression Tests

During the compression tests, loads on the thicker bearings were observed to produce deflections well over 20 percent of the original thickness of the bearings. No sign of distress appeared in the molded bearings. The bearings built of plies tended to separate slightly at the edges under high loads, but on release of load the separations closed and were not discernible. One molded bearing consisting of two layers, each ¾-in. thick, bonded through a layer of metal mesh, tended to separate along the mesh layer.

Typical curves of deflection under compressive loading are shown in Figure 6. A study of these curves indicates a remarkable uniformity of compressive deformations. The ultimate bearing capacity of the neoprenes tested was beyond the range of these tests. The maximum load applied was 2,000 psi to the samples and in no case did the curves of stress-strain change shape at or near this point.

Sources of Error

Vertical deflection results were inconsistent in the various tests due to:

1. Durometer ratings are inconsistent and not an accurate gauge of stiffness.
2. The rate of application of load was apt to vary due to factors beyond control of the test.
3. The temperature fluctuated day by day.

Tests for Combined Shear and Compression

The shear loads on the bearings produced horizontal deflections exceeding in some cases the thickness of the bearings. In three cases, the thicker bearings made up of several plies tended to separate under high shear loads, but as with the vertical loads the separations closed as the loads were removed and were not discernible in the free samples. In no case was the ultimate load capacity in shear found in the process of these tests. The bearings appeared to be as serviceable at the conclusion of the tests as at the start.

Typical curves of deflection under combined loading of compression and shear are shown in Figure 7. A study of all the curves for combined loading revealed that the shear distortions are very similar for all of the bearings tested. In contour they are almost identical. The difference in deflection for similar bearings is due to the variation in durometers (stiffness) far more than for any other reason.

The inconsistencies for the combined load testing were the same as listed for the compression tests with one notable addition. Steel and concrete plates were used interchangeably to transmit the shear loads. As the concrete surfaces were rougher than the steel surfaces, the degree of restraint of the rubber in contact with the concrete was probably greater. The horizontal deflections under low compressive loads may have been affected due to this interchange of shear plates but this was not apparent in the test results.

SPECIAL TESTS

Shape Effect on Vertical Deflections

To study the effect of shape, the formula:

$$\text{Shape Factor} = \frac{\text{width x length}}{2 \text{ x thickness (width + length)}}$$ was adopted.

The vertical tests on neoprene bearings of varying thickness substantiate the shape curves for values of shape below three established by the Goodyear Tire and Rubber Company in their Handbook of Molded and Extruded Rubber (4). For high values of shape however, the deflections recorded were increasing below the computed deflections as the shape factor increased.

Shape Effect on Horizontal Deformations

Horizontal shear tests were run on a number of bearings of various size. The results indicate that the shape or orientation of the material has no visible effect on the horizontal stress-strain relationship. One exception was noted. Where the width (dimension parallel to the shearing force) becomes less than four times the thickness, the bearing tends to roll and slip noticeably when the horizontal force exceeds 5 percent of the vertical (Fig. 8).

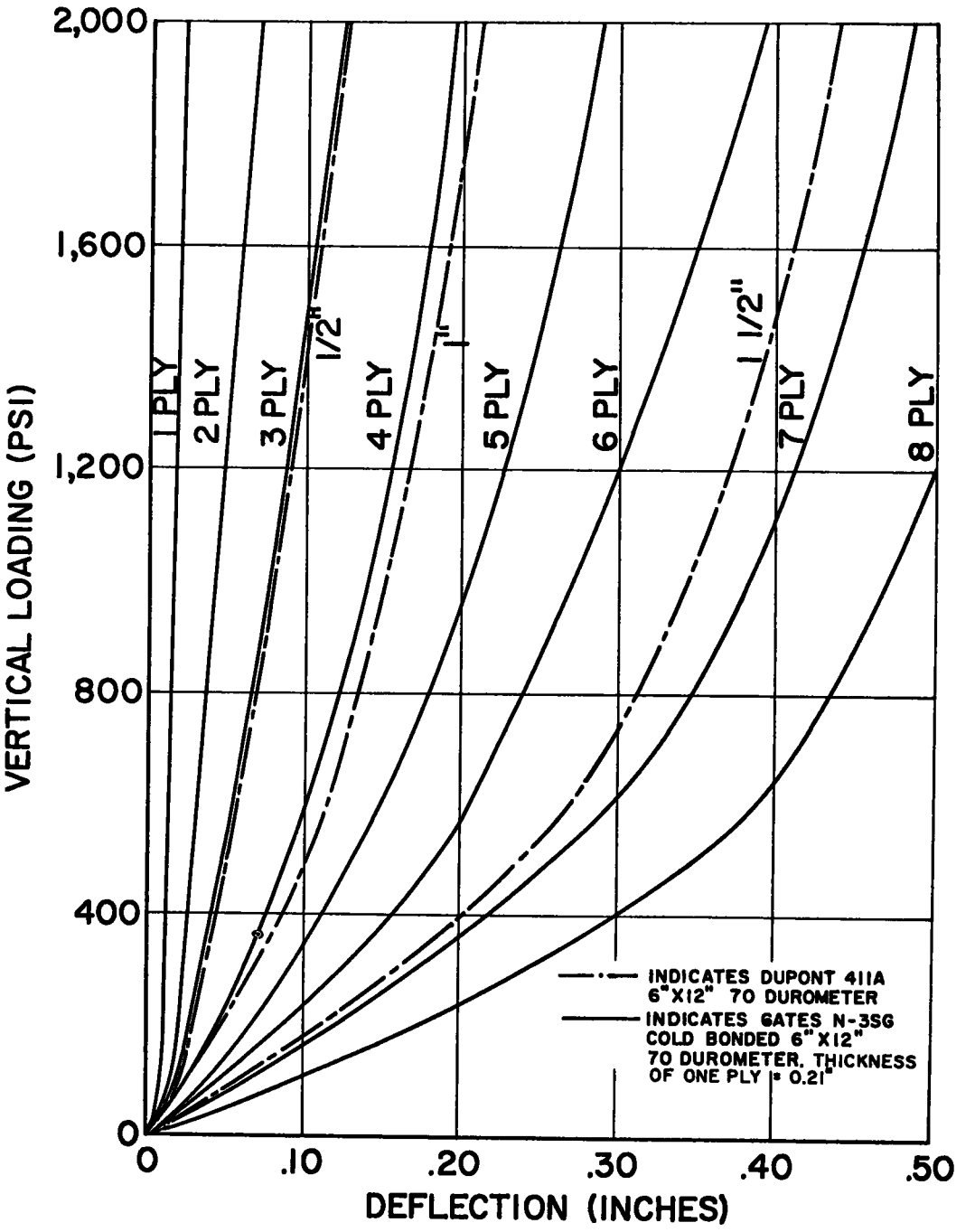

Figure 6. Vertical stress-strain test results.

Time

To study the effect of normal creep of elastomeric bearings under load, two static vertical deflection tests were performed. In the first test the 3-ply compound was subjected to a sustained vertical load of 2,000 psi for 2¾ hr. The creep deflections related to the deflection when full load was reached were 2.7 percent in 5 min and 6.1 percent in 2¾ hr. From the time curve it appears 50 percent of the creep occurs in the first 5 min.

The second test was run on a 6- by 12- by 1½-in. 70 durometer bearing. Test conditions were identical to those employed with the 3-ply unit. Resulting creep deflections related to the deflection when full load was reached were 3.8 percent in 5 min and 7.4 percent in 2 hr.

Keeping in mind the accuracy required in the computations of vertical deflections for bearings of this type it is evident that sufficient figures may be obtained if the vertical deflections obtained under full load are increased 15 percent for static creep. However, it will be shown in succeeding paragraphs that creep from dynamic loading will yield higher (governing) values.

Fatigue

An important question in the use of this material is the effect of fatigue under operating conditions. An attempt to simulate this condition was performed on two 6- by 9- in. by 1-in. 70 durometer units. The bearings were subjected to a sustained vertical load of 800 psi. A horizontal force of 17,200 lb was alternately applied against the opposite 6-in. faces. Eighteen force cycles were accomplished in three hours. The tabulation of horizontal deflections indicated no sign of fatigue.

Vertical deflections, however, show dynamic creep. This creep has the same proportions as static creep but with greater value. In three hours the percentage of creep to the initial deflection when full load was reached came to 47.8 percent.

To account for dynamic loading to which bridge structures are subject, the vertical deflections for full vertical load should be increased 50 percent. It is thought that the final deflections thus computed will closely approximate working values.

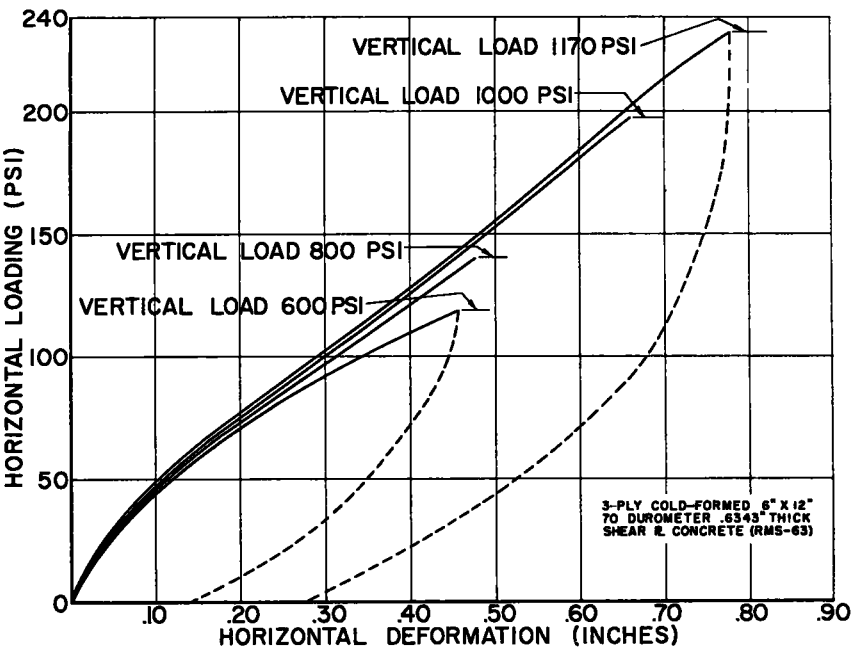

Figure 7. Typical horizontal deflections.

COMPOUND (MANUFACTURE)

From the data collected in tests on bearings provided by four manufacturers, the deflection curves for 70 durometer materials were compared. The results as shown by the curves indicate that all the materials used have approximately the same stress-strain relationship in compression and shear-compression in combination. The only control over the manufacture of the bearings other than size and hardness was the specification proposed by N. L. Catton of Dupont (5). It is encouraging to see the selection of bearings perform similarly. This result should not be construed to mean that every 6- by 12-in. unit of 70 durometer hardness will yield equally under the same stresses. Other properties such as durability and fatigue may vary in these samples as well as deviations from the stated 70 durometer hardness. However, it is felt that the methods of manufacture may be controlled by a specification to provide required engineering properties.

CONCLUSIONS

Hardness

Hardness of elastomeric bearings is an important consideration. The selection of various hardnesses may vary from those tested in this program due to varying requirements. To tabulate the varying stress-strain relationships due to hardness, four pairs of bearings were tested. The effect of varying vertical load may be considered to contribute little to horizontal deformations. In Figure 22, these hardness curves are plotted with the deformation reading as the ratio of horizontal movement to the vertical thickness under load. In this case the curves plot as a single contour for the hardness involved.

Vertical Deflections

The vertical deflections measured due to static vertical compressive loads were in general found to be less than anticipated. The deflection curves indicated the following:

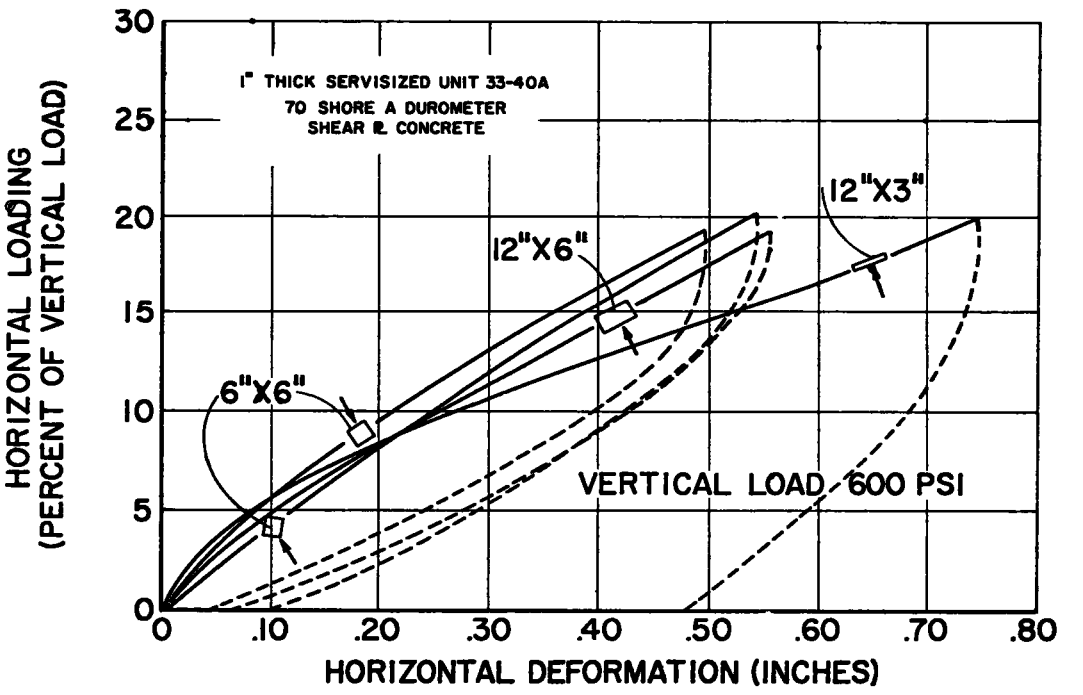

Figure 8. Effect of shape on horizontal deformations.

1. Deflection increased inversely with durometer ratings.
2. Deflection is proportionately greater (deflection divided by thickness) as the thickness of the bearing increases.
3. Shape deviation has limited effect on compressive resistance of elastomeric bearings.
4. Deflection increases with time and dynamic loading.

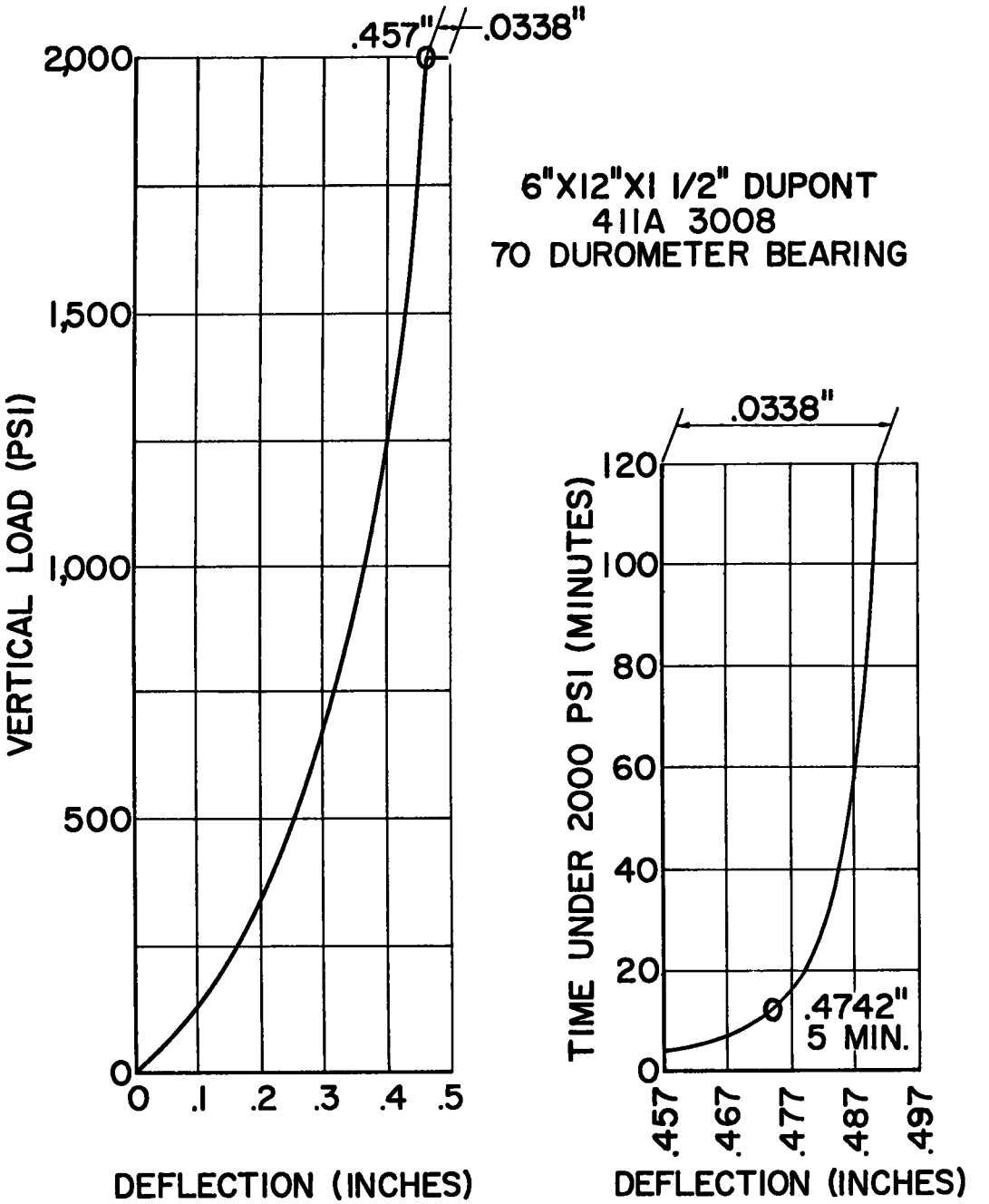

Figure 9. Vertical static loading.

The small vertical deflections and the limited effect of shape factor error is thought to be due to the large size of the samples tested. The curves indicate that shape factor determination with factors from 1 to 3 are consistent for use in predicting deformation

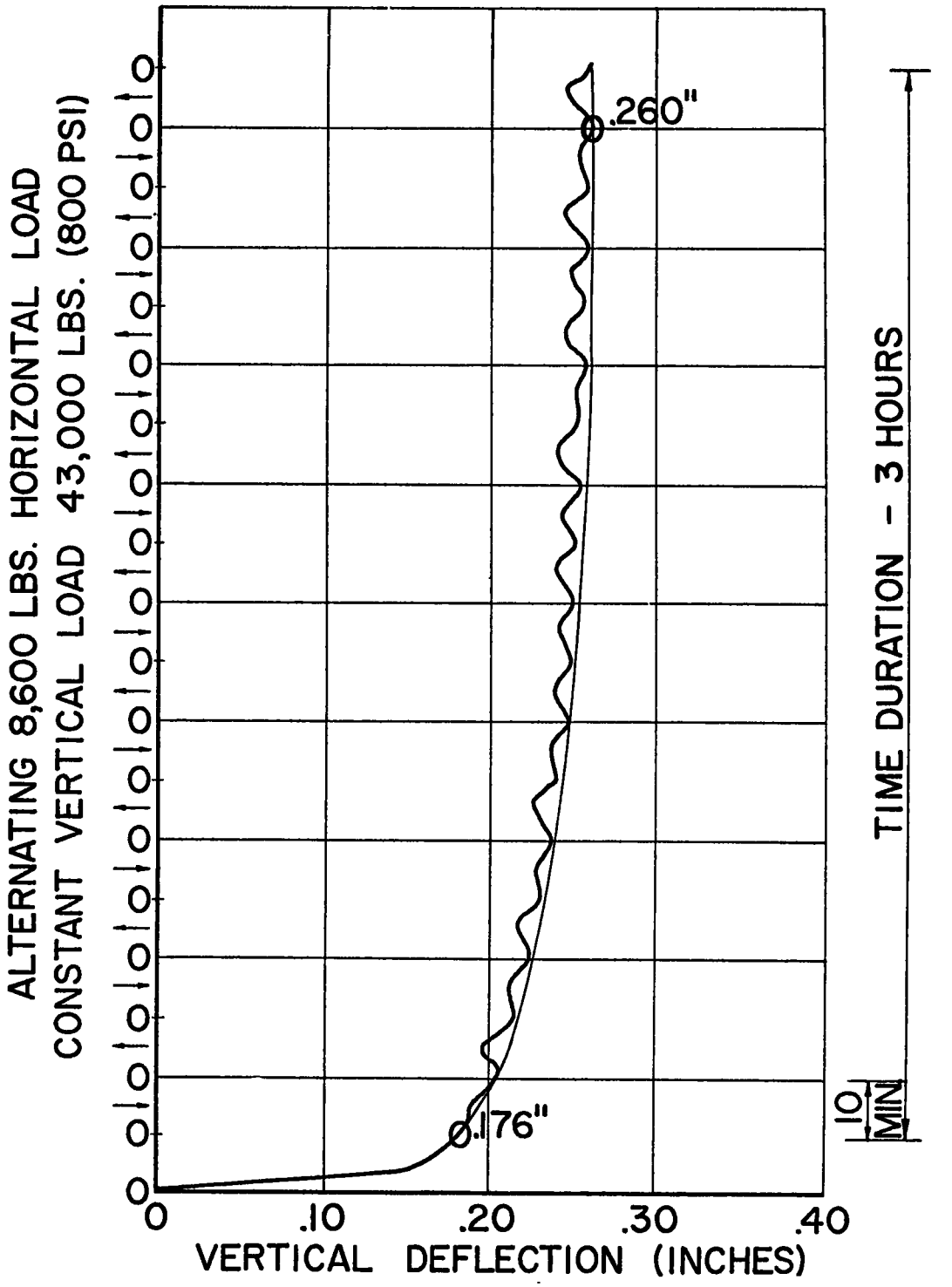

Figure 10. Horizontal fatigue loading.

under compression. As the shape factor increases above 3, the percent of error of the computed from the measured increases (Fig. 11).

Horizontal Deflections

The horizontal deflections measured due to horizontal shear loads were similar for all the bearings tested. Four important factors were determined for this condition of loading:

1. Direct compressive load has little appreciable effect on shear resistance.
2. Shear modulus of the elastomer increases with thickness.
3. Resistance to shear distortion increases as the stiffness of the elastomer increases.

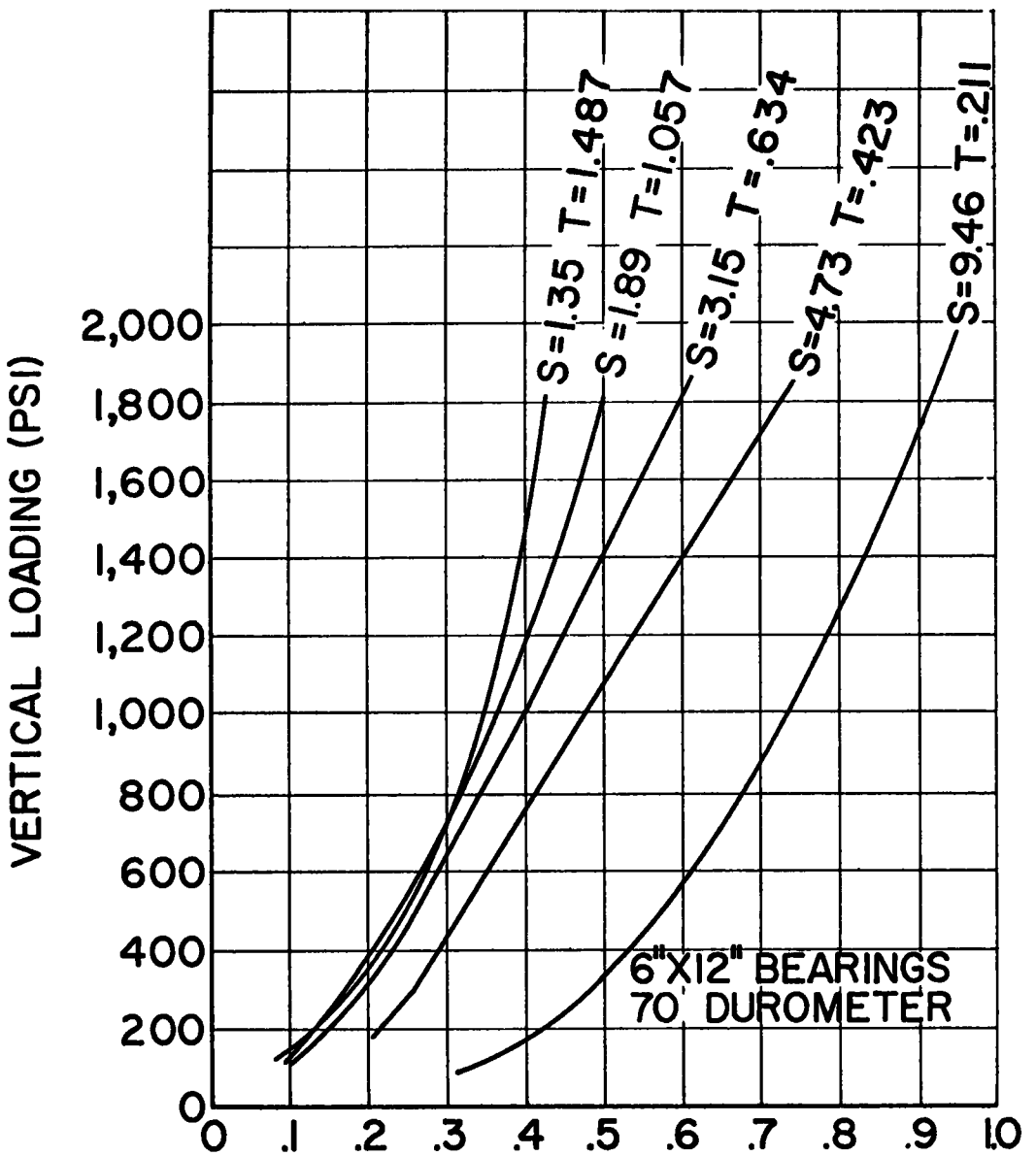

Figure 11. Effect of shape on vertical deflections.

4. The shape or orientation of the bearing has little or no effect on its shear resistance, unless the ratio of thickness to the minimum plan dimension is one-quarter or more.

A designer who knows what horizontal movement to anticipate can design an elastomeric bearing for almost any degree of restraint.

Dynamic Creep

An elastomeric bridge bearing under working conditions is subject to dynamic loading. The continual expansion-contraction action of the bridge deck will repeatedly deform the unit with reversing horizontal strains. The intermittent live load with associated vibrations will deform the elastomeric units to greater vertical deflections. These types of loadings are referred to as dynamic and the additional deflections appearing as a result are called dynamic creep.

Dynamic creep of the vertical deflections resulting from an alternating horizontal loading indicates that all static vertical deflection values arrived at by the use of charts in this report should be increased by 50 percent. A test to study dynamic vertical creep under intermittent vertical live load was not conducted.

The curve that resulted from the test of dynamic vertical creep under alternating horizontal load indicates that an additional 50 percent deflection is maximum for an indefinite period. This prognostication is based on one test. Many engineers believe that if the compression set of bridge bearing pads is kept below 20 percent, no significant amount of creep will occur. Compression set in the tests conducted for this report could not be measured accurately. The hysteresis curves indicate that compression sets would generally be less than 20 percent. It is obvious that additional tests are necessary for horizontal and vertical creep.

A fatigue test was attempted in 3 hours of alternating horizontal loading. The lack of fatigue may indicate that the duration of testing was insufficient. Additional tests particularly for fatigue in conjunction with extreme temperatures are recommended.

Negligible Factors

From this test program, three factors appear to be negligible for the design of bridge bearings.

1. The plan shape (not to be confused with shape factor) has little relationship to the vertical or horizontal stress-strain properties. The bearing unit may be round, rectangular or multi-sided. This provides the designer considerable freedom in selecting the plan shape to best fit the particular location.
2. Static creep is of negligible importance as dynamic creep yields much greater strain values.
3. There appears to be only slight variation of measured physical properties between bearings compounded to the same specification.

Design Factors

An important design and construction factor in the use of elastomeric bearings is the relation of the two bearing surfaces. When these surfaces are not parallel, one edge of the neoprene is subjected to high unit compression while the other side may be free of contact. Such a non-parallel condition may arise from (a) excessive camber or deflection in the beam; (b) roadway grade not parallel to the bearing seat; and (c) an uneven bearing seat.

To consider in detail the effect of these three factors is presently inadvisable as too little is known of the plastic action of elastomers. Until more precise information becomes available, the authors suggest the following procedure. Select a thickness of bearing for which the computed vertical deflection under dead load will be at least equal to the difference in thickness due to the greatest of the aforementioned three factors. This procedure is based on the assumption that a further increase in vertical deflection of 50 percent due to dynamic creep will adjust the bearing surfaces to a reasonably uniform bearing pressure.

Future Developments

The program of testing, completed by the Rhode Island Department of Public Works, together with the engineering firm of Charles A. Maguire and Associates, establishes within reasonable limits the physical properties at room temperature of the best neoprene now available for bridge bearings. Much more needs to be done.

The tests of elastomer properties proposed for current consideration by the American Association of State Highway Officials Bridge Committee are a starting point but are not considered sufficient for determining the adequacy of elastomers to be used in bridge construction.

The present tests are those that have been developed basically for the automobile industry. It is recommended that the American Society for Testing Materials develop additional tests more directly applicable to elastomeric bridge bearings.

Among the factors which should be considered in compiling new test requirements are tests for: a more stringent ozone resistance; freezing and thawing in a saturated condition; resistance to brine solutions; shear and compression at temperatures from -20 F to +160 F; dynamic creep; and simulated aging under service exposures.

Elastomer bearings should have a minimum useful life of 50 years, with a probable service life of 100 years.

The initial cost of the bearings is insignificant by comparison with the cost of replacement. For elastomeric bearings to be feasible they should outlast the estimated economic life of the structure they support.

DESIGN OF ELASTOMERIC BRIDGE BEARINGS

Utilizing the data collected from tests and other references the following is a suggested method for design of (neoprene) elastomeric bridge bearings.

Criteria

The brief specification below outlines general rules followed by Charles A. Maguire and Associates for the design of neoprene elastomeric bearings.

1. The maximum occasional vertical compressive load = 800 psi (live and dead loads).
2. The maximum continuous vertical compressive load = 500 psi (dead load).
3. The maximum horizontal shear deformation shall be equal or less than one-half the nominal thickness.
4. The maximum horizontal force from a deformed bearing shall equal or be less than 20 percent of the minimum vertical compressive load.
5. The minimum plan dimension shall equal or be greater than 5 times the thickness.
6. The estimated maximum vertical deflection shall be the vertical deflection derived from the charts or computed by formula increased 50 percent for dynamic creep.
7. The vertical deflection derived from the charts or computed by formula shall be greater than the tangent of the surface slope angle times the length of the bearing.

Formulas

The following equations are derived from the graphs on neoprene elastomeric bearings.

$$\text{Vertical deflection under vertical load (in.)} = \left(\begin{matrix}\text{nominal}\\ \text{thickness}\\ \text{(in.)}\end{matrix}\right) \frac{(C_1 \times \text{Vertical load (psi)} + C_2)}{(100 \times \text{Shape Factor})}$$

$$\text{Horizontal Force from deformed bearing (psi of plan area)} = \frac{\text{Modulus of Shear-G (psi)}}{\text{Nominal thickness (in.)}} \times \frac{\text{Horizontal deformation (in.)}}{\text{Vertical deflection under vertical load (in.)}}$$

Values for G, C_1 and C_2 by durometer hardness:

Shore A Durometer	G	C_1	C_2
60	90 psi	0.030 sq in. per lb	12.0
70	160 psi	0.025 sq in. per lb	10.5
80	310 psi	0.020 sq in. per lb	6.0
90	580 psi	0.015 sq in. per lb	1.5

Procedure

There are a number of methods for locating elastomeric bearings under the stringers or girders. The standard arrangement shown in Figure 13 would have one end of the superstructure stringer pinned to the substructure with an elastomeric bearing at the other end to permit horizontal movement. A second method or equalized arrangement (Fig. 14) involves an equal capacity elastomeric bearing under each end. This allows each bearing to absorb more or less one-half the horizontal movement. The longitudinal forces due to traction and wind are, however, resisted only by the bearings extended in the direction of the applied force.

A compromise procedure would require two elastomeric bearings of variable thickness and size which may be designed to provide any degree of restraint between standard and equalized arrangements.

The procedure for the construction of any one bearing will depend on basically the required thickness. When the thickness of one unit exceeds 1¼ in. it is suggested a multi-unit be used. With this construction method the vertical deflections and horizontal forces from shear movements are kept to a minimum.

Design Problem

A simple beam can be analyzed as follows. This typical beam spans 60 ft between supports and has a camber under dead loads of 1¼ in.—neoprene bearings to be designed in an equalized arrangement.

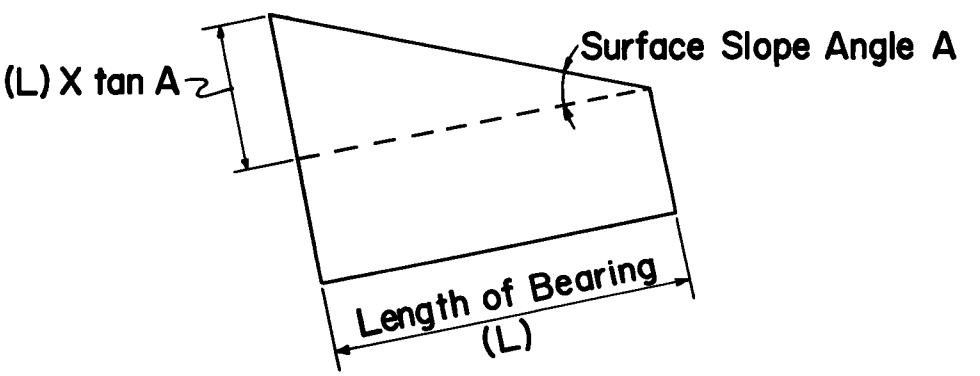

Figure 12. Diagram of the surface slope angle.

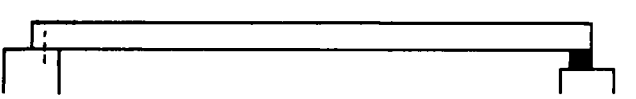

Figure 13. Standard arrangement.

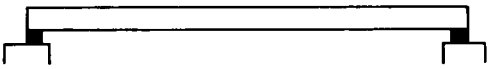

Figure 14. Equalized arrangement.

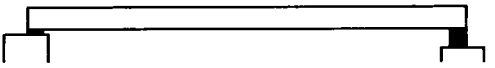

Figure 15. Varied arrangement.

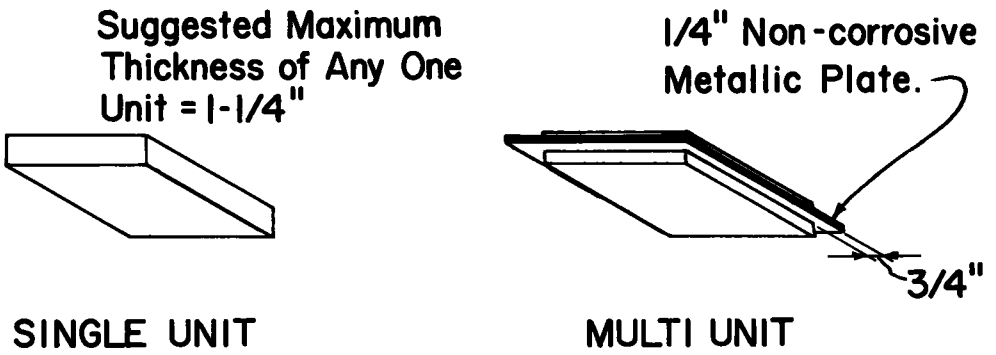

Figure 16. Bearing construction.

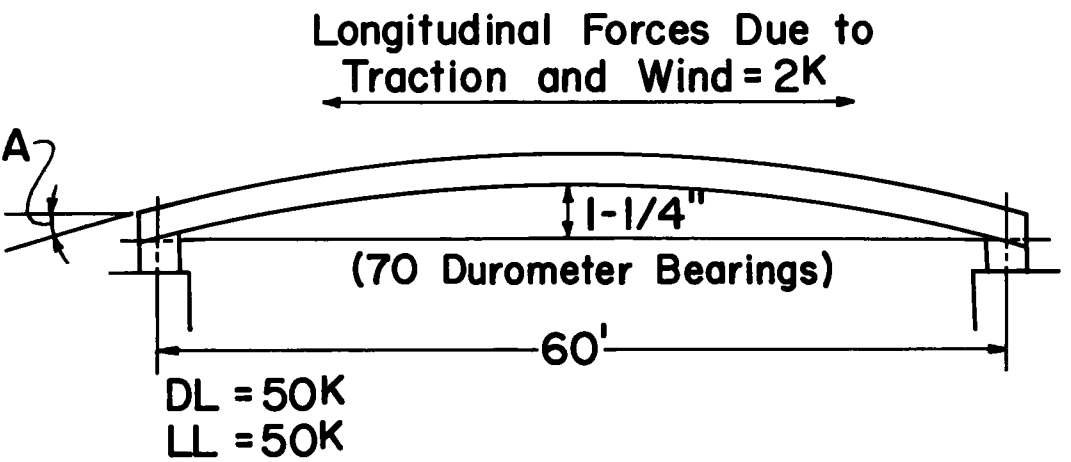

Figure 17. Simple beam example.

Change in length due to temperature = $\frac{60 \text{ ft} \times 12 \text{ in./ft} \times 40 \text{ F} \times 0.000008}{2}$ = 0.115 in. each end.

$$\text{Area} = \frac{P_{max.}}{800} \text{ or } \frac{P_{D.L.}}{500} = \frac{100,000}{800} \text{ or } \frac{50,000}{500} = 125 \text{ sq in.}$$

assume width = 14 in., length = 9 in., thickness = ¾ in.

$$\text{Shape Factor} = \frac{14 \times 9}{2 \times 3/4 \times -14+9)} = 3.66$$

$$\text{Maximum vertical load} = \frac{100,000}{14 \times 9} = 795 \text{ psi}$$

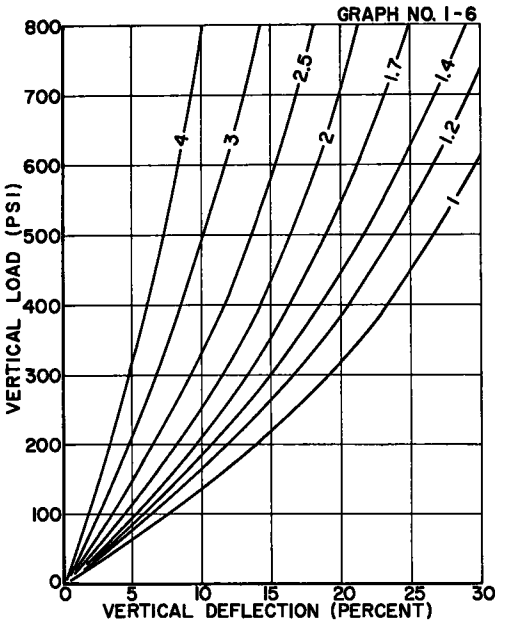

Figure 18. Vertical stress-strain by shape factor— 60 shore A durometer neoprene elastomers.

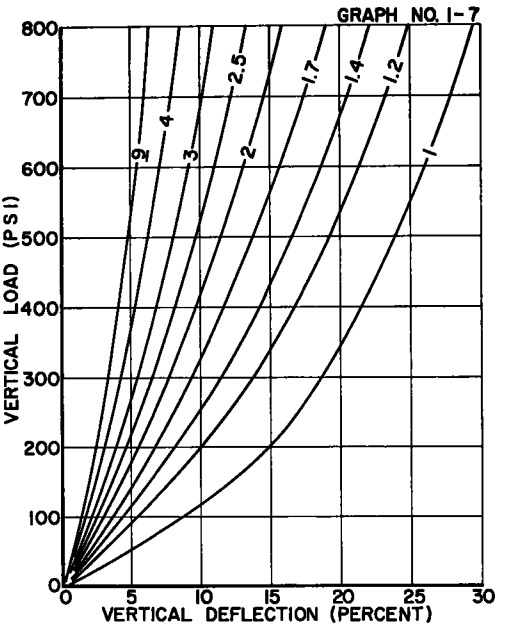

Figure 19. Vertical stress-strain by shape factor— 70 shore A durometer neoprene elastomers.

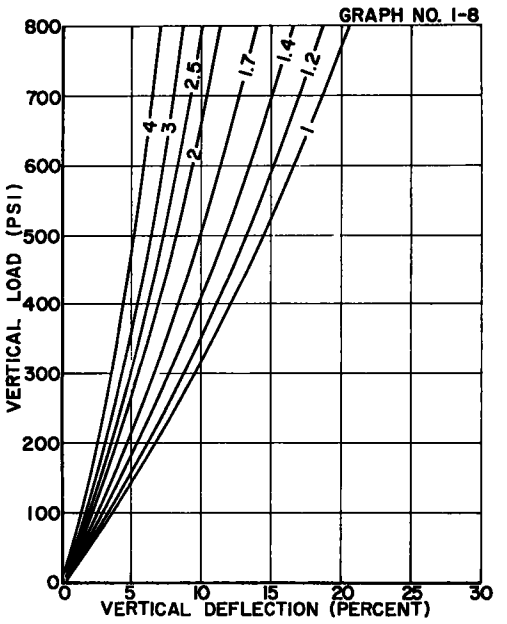

Figure 20. Vertical stress-strain by shape factor— 80 shore A durometer neoprene elastomers.

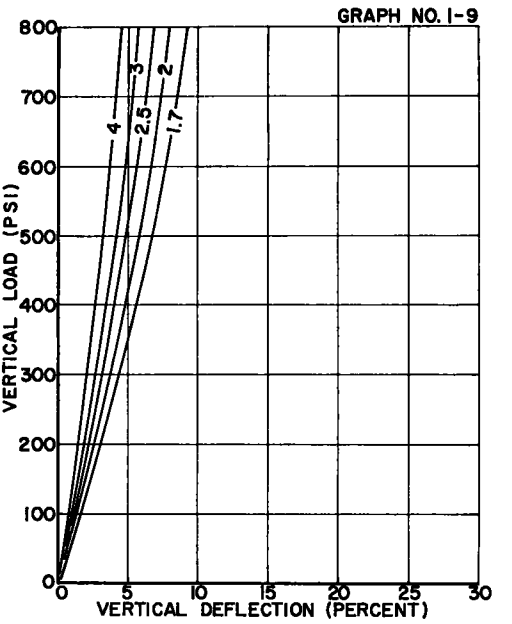

Figure 21. Vertical stress-strain by shape factor— 90 shore A durometer neoprene elastomers.

From graph 1-7: for a shape factor = 3.66 and a vertical load = 795 psi; the resulting vertical deflection = 9 percent or 0.067 in. The tangent of the surface slope angle A times the length L = 0.063 in. This value is less than the vertical deflection and therefore satisfactory.

From graph 2: for a 70 durometer bearing and a ratio of

$$\frac{0.115 \text{ in. (horizontal deformation)}}{0.75\text{-}0.06 \text{ in. (vertical thickness under load)}} = 0.17.$$

The resulting horizontal shearing force = 37 psi. Add to this the stress due to the longitudinal forces ($= \frac{2000 \text{ lb}}{126 \text{ sq in.}} = 15.8$ psi) and the total shearing force = 52.8 psi.

No sliding of the surfaces will occur if 20 percent of the minimum load on the bearing $\left(= \frac{0.2(50,000)}{126} = 79.5 \text{ psi}\right)$ is greater than the maximum shearing force. Which it is: 79.5 > 52.8.

From graph 2: for a 70 durometer bearing and a force of 52.8 psi, the resulting ratio = 0.28. The total horizontal movement at each end = 0.28 x 0.68 = 0.191 in.

The final vertical thickness after dynamic deflections = 0.75 in. - 1.5 (0.0675 in.) = 0.649 in.

REFERENCES

1. "The Language of Rubber." E.I. duPont deNemours and Company, Inc., (1957).
2. Graves, James R., "Rubber Seats for Prestressed Beams." Engineering News-Record, (May 16, 1957).
3. "Rubber Bearing Plates for Bridges." Societe Technique, Pour L'Utilisation de la Precontrainte (S.T.U.P.), Paris.
4. Goodyear Tire and Rubber Company, Handbook of Molded and Extruded Rubber, (1949).
5. "Elastomeric Bridge Bearing Pads." Report - N.L. Catton to E.L. Erickson and Members of Bridge Committee AASHO dated November 12, 1957.
6. "Elastomeric Bridge Bearings - Report of Tests and Design Procedures." Charles A. Maguire and Associates, (1958).

Discussion

S.D. McCREADY, Product Engineer, Dupont Company, Wilmington, Delaware— An elastomer bearing is primarily a flat rubber pad with lateral dimensions less than the pier or abutment it is seated on. It is placed between the support area with the girder resting on it. As the girder expands and contracts, the pad deflects horizontally in shear.

Under a compressive load the elastomer pad absorbs surface irregularities and distributes all forces uniformly. In shear, the neoprene bearing reacts as a spring, the resistance of which can be calculated at all times. There is no starting friction to overcome or no corrosion deposit to break loose. Another important advantage of a neoprene bearing is its freedom from costly maintenance. There is no need for lubrication or cleaning.

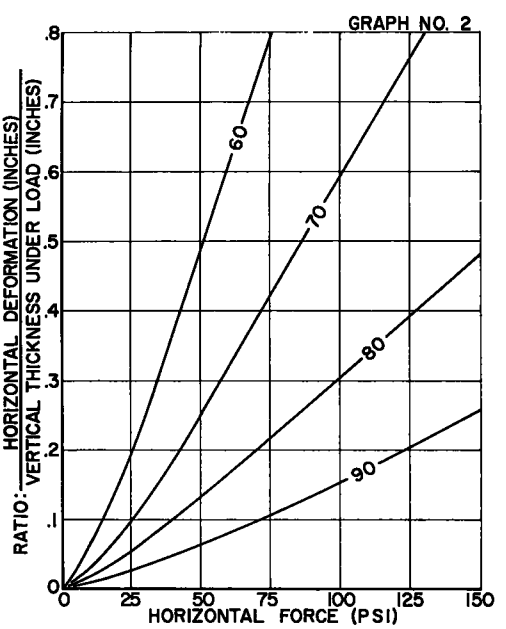

Figure 22. Horizontal stress-strain by shore A durometer.

The elastomer bearing pad was first used in France in rebuilding the bridges destroyed during World War II. The Freysinett Company, pioneers in prestressed concrete, did a lot of the original engineering on the subject. The English also are using elastomeric bridge pads and they too have developed engineering data on the subject.

About two years ago, according to records, the state of Texas became interested in elastomer bridge pads. At this time, the market was investigated and a high quality neoprene vulcanizate was recommended. The subject is actively being pursued, because it is believed that neoprene is the best all-around elastomer presently available for the application.

The Dupont Company manufactures neoprene—a synthetic rubber that is employed in elastomeric bearing pads. Because of this they are interested in assisting in the development of the bearing pad market and insuring that proper design considerations be applied to neoprene for maximum efficiency in service. They have, therefore, offered their assistance to the American Association of State Highway Officials, engineers, architects, and contractors on the subject.

A brief comment on the serviceability of neoprene pads at low temperatures follows. All elastomers tend to stiffen at successively lower temperatures. The rate and extent of stiffening is dependent upon the type of elastomer, the compounding ingredients used, and the state of vulcanization attained.

The rate and extent of stiffening of neoprene pads can readily be determined by laboratory tests. From these tests, it is believed that at temperatures normally experienced in this country, neoprene bridge bearings will be serviceable. As Pare has said however, further field work should be carried out on the subject. Under service conditions, the rate of shear movement in an elastomer bearing is extremely slow. Since stiffness is related not only to temperature but to rate of movement, a greater factor of safety is insured than would be predicted from laboratory tests.

A number of bridges in Ontario, Canada have successfully utilized neoprene pads and have performed satisfactorily over a winter period. A new span under construction in the White River area of Ontario, on the northeast side of Lake Superior, will employ neoprene pads over an expected temperature range of -65 to +120 F.

The amount of horizontal distortion to which a neoprene pad can safely be subjected has been discussed in many quarters lately. Rubber industry experience over the years has shown that neoprene vulcanizates, of a similar type and hardness to that specified in bridge bearing pads, can be distorted in shear 20 to 25 F in either direction from the neutral axis without difficulty. Therefore, it is believed that Pare's conclusions with regard to maximum attainable distortion are sound.

Report on Tests of Neoprene Pads Under Repeated Shear Loads

A.M. OZELL and J.F. DINIZ, Department of Civil Engineering, Engineering and Industrial Experiment Station, University of Florida, Gainesville

The use of neoprene pads as bearing elements for bridge members poses the question of their behavior under repeated loads. Of special interest is the shear deformation of the pads caused by horizontal motion of the girders resting on them resulting from application of live load and also due to thermal effects on the girders.

The tests described in this report were devised to study the effects on neoprene pads of repeated shear loads with simultaneous compressive loads, simulating the actual load conditions in a bridge. The test program was limited in scope, and variables such as shape factor, thickness, hardness and magnitude of shear deformation have not been included in these studies. Furthermore, tests were run at room temperature and hence effects of temperature, humidity and presence of deleterious substances in contact with the neoprene or in the atmosphere were not studied.

DESCRIPTION OF TESTS

●THE TEST arrangement (Fig. 1) consisted of two stationary concrete side blocks and a center block which moved up and down applying the shearing force to the neoprene pads. The pads were placed between the center block and each side block. The surfaces of the blocks in contact with the pads were trowel-finished.

The compressive load was applied to the pads with four steel bolts bearing on the outside of the blocks. The bearing load was obtained by tightening these bolts and the magnitude of tension in each bolt was measured with SR-4 strain gages. Gage readings were taken frequently during the entire test period to determine the variation in normal load resulting from changes in the elastic properties of the neoprene pads and the creep of the material. Preliminary tests indicated that almost continuous tightening of the bolts would be required in order to compensate for the changes in the properties of the pads; hence maintaining a constant normal load was prohibitively time-consuming and impractical. For this reason no such adjustments were made.

The vertical travel of the center block and consequent shear load on the pads was produced by a fatigue machine. This machine is of the constant-deflection type, rated capacity 50,000 lb, with the motion of its loading beam obtained through a variable-throw eccentric. It is possible to measure the load being applied by the machine through a dynamometer which connects the eccentric to the loading beam.

Before and after being subjected to repetitive loading, each pad was tested statically to determine its load-deformation characteristics under direct loading. The elastic property of the pads thus determined was used as the basis of comparison and in the determination of the extent of damage caused by repeated loading. The pads were loaded in compression between two steel plates $1\frac{1}{4}$ in. x 6 in. x 12 in. The initial deflection reading was taken at a load of 50 psi and the maximum load was 1,000 psi. The rate of loading and unloading was kept constant, 3,000 lb per min, to assure consistency in the results.

TEST RESULTS

The neoprene pads furnished by the manufacturer were of two types herein called type A and type B. The physical properties of the two types of pads are as follows:

	Pads A	Pads B
Tensile Strength, psi	3,000	2,500
Elongation at break, %	310	230
Hardness, Shore A	72	76
Resilience, %	58	45
Compression set "B" 22 hr at 70 C, %	21	20
Brittle point	-43 C	-39 C

Pads A-1 and A-2 were 1 in. x 4 in. x 8 in., with a shape factor[1] of 1.33, and were tested under an initial bearing pressure of 815 psi. After 1,090,000 cycles of loading, the pads had not failed but the test was discontinued at which time the bearing pressure had been reduced to 645 psi. It is assumed that 1,000,000 repetitions of design load corresponds to the useful life of a structure. The repeated shearing deformation was 0.180 in. and the initial and final shearing stresses were 130 and 70 psi, respectively, based on applied load divided by contact area. The shearing force was applied along the 8-in. dimension of the pads. The load-deformation relationship of the pads before and after the test is given in Figure 2.

Pads A-3, A-4, A-5 and A-6 were 1 in. x 4 in. x 6½ in. The initial bearing pressure was 530 psi. The test was discontinued at 1,074,000 cycles of loading, at which time the bearing pressure was 380 psi. No failure occurred in these pads which were loaded along the 4-in. dimension. The shearing deformation was 0.180 in. and the initial and final shearing stresses were 120 and 65 psi, respectively. The load-deformation curves before and after testing are presented in Figure 3.

Pads A-7, A-8, A-9 and A-10 were 1 in. x 4 in. x 6½ in. The initial bearing pressure was 580 psi and the shear deflection 0.425 in., with the pads loaded in shear along the 4-in. dimension. The test was discontinued at 236,000 cycles of loading. The bearpressure was then 425 psi and the four pads had failed. Figure 4 shows specimens A-8 and A-10 which were damaged the most. The distortion of the pads was permanent and

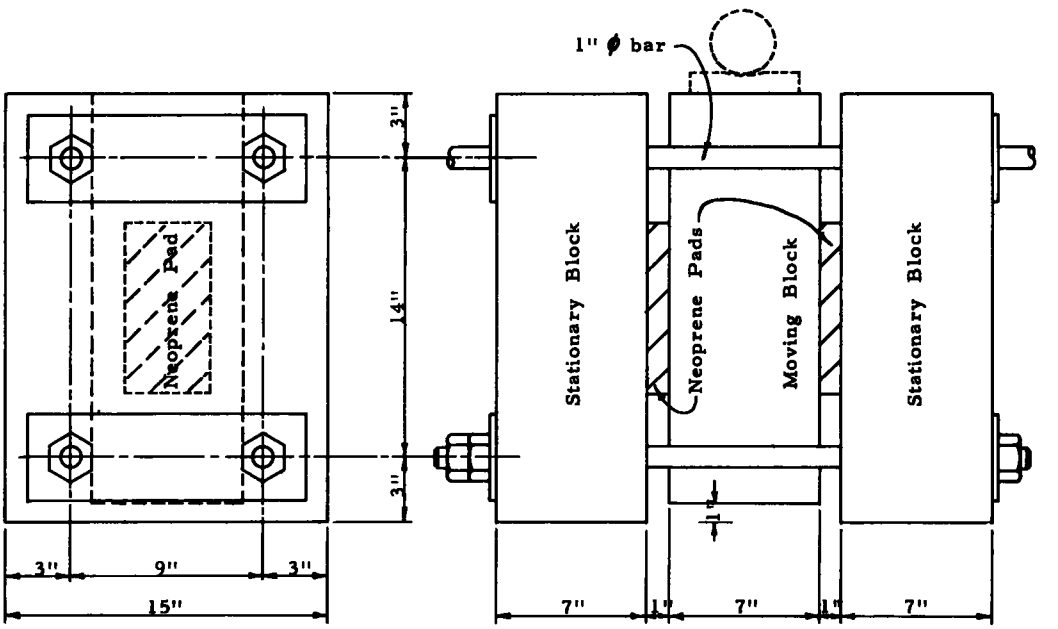

Figure 1. Test set-up.

[1] Shape factor is defined as the ratio of the bearing area to the perimeter surface area. Shape factor is significant because the perimeter surfaces bulge under bearing loads and the edge disturbance coupled with tendency to roll under shearing load renders the pads with relatively small bearing area but large perimeter area vulnerable to failure.

the cracks were similar in the four specimens although they were not quite as much developed in pads A-7 and A-9. Figure 5 shows the load-deformation curves before and after the test.

Pads A-11, B-1, B-2 and B-3 were 1 in. x 4 in. x 6 in. The initial bearing pressure was 310 psi and the final, 220 psi. The shear deformation was applied along the 4-in. dimension and was equal to 0.390 in. At 170,000 cycles, pad B-1 had failed while the others had been only distorted. The initial and final shearing stresses were

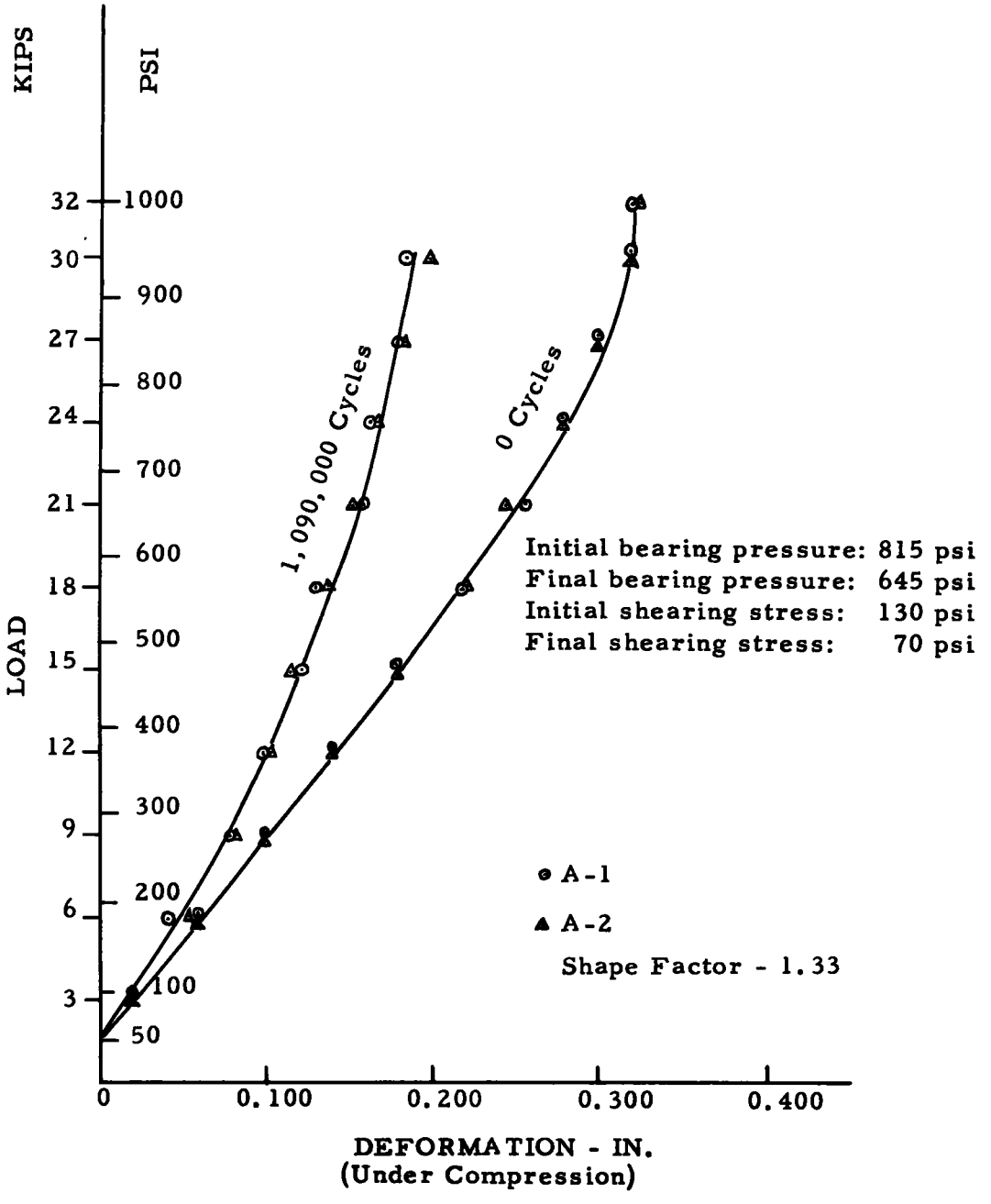

Figure 2. Load-deformation diagram for pads A-1 and A-2.

148 psi and 106 psi, respectively. The load-deformation curves before and after the fatigue test are presented in Figure 6.

Pads B-4, B-5, B-6 and B-7 were 1 in. x 4 in. x 6 in. They were loaded in shear along the 4-in. dimension and the corresponding deformation was 0.450 in. The bearing pressure was 500 psi at the start of the test and 200 psi at the end. At 120,000 cycles all pads showed extensive damage with large cracks present. Figure 7 shows the load-deformation curves before and after the test.

Pads B-8, B-9, B-10 and B-11 were 1 in. x 4 in. x 6 in. The initial bearing pressure was 540 psi and the final 375 psi. The shear load was applied along the 4-in. dimension. The initial shearing stress was 340 psi. These pads were subjected to an initial shear deformation of 0.100 in. and a subsequent additional repetitive deformation

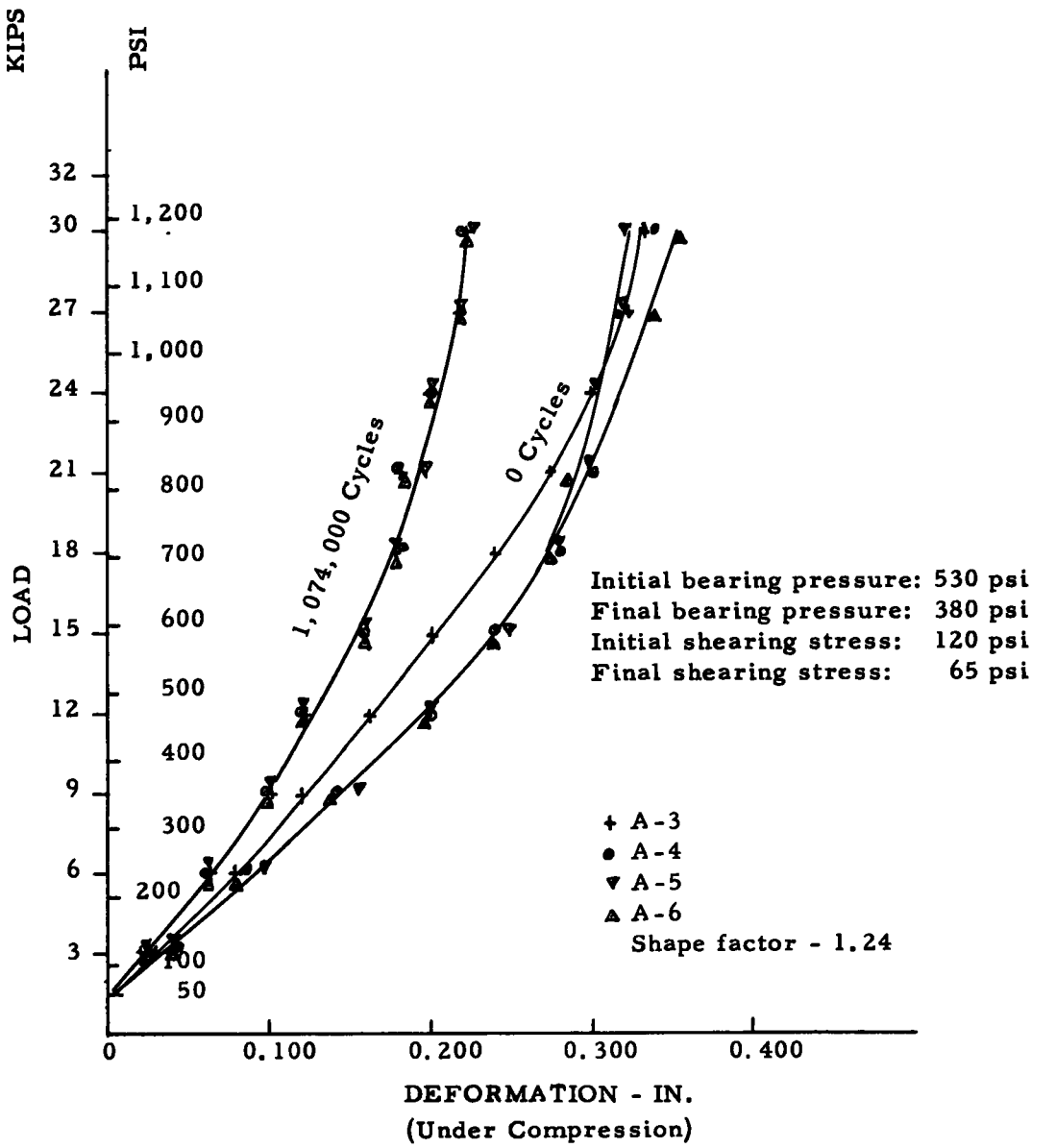

Figure 3. Load-deformation diagram for pads A-3, A-4, A-5, and A-6.

of 0.360 in. Cracks appeared at 20,000 cycles and the test was discontinued at 35,000 cycles. The load deformation curves for these specimens are shown in Figure 8.

Pads B-12 and B-13 were 1 in. x 4 in. x 8 in. (Previously, these pads had served as supports for prestressed concrete beams tested in fatigue and had been subjected to about 6,000,000 cycles of direct load at about 100 psi bearing stress.) The shear deformation was 0.450 in. applied along the 8-in. dimension. The initial shearing stress was 291 psi. After 17,000 cycles of loading, the specimens showed damage and the test was discontinued. Figure 9 shows the load-deformation relationship before and after the test.

DISCUSSION OF TEST RESULTS

Before examining the test results a word should be said about the compressive tests used to establish the load-deformation relationship of the pads.

The amount of deformation for a given compressive load is a function of the contact surface (smooth or rough, glued or unglued), the size of the lateral expansion area, the size and shape of the pads, the hardness (as measured by a durometer), and the speed of loading.

It is important that the exposed surfaces of the pads be free of cuts or imperfections which will cause the pads to tear when they bulge under the load.

These tests indicated that the pads hardened apparently as a consequence of fatigue action. This hardening took place before the pads were torn, as evidenced by the load-deformation curves of pads with or without cracks.

The compressive load on the pads at the end of the tests was considerably smaller than the initial load. This can be explained not only by the change in the elastic properties of the pads but also by the drift or creep of the neoprene. The reduction of the bearing pressure, as well as the shearing stress during the entire test period, was almost linear indicating a gradual change in the elastic properties of the neoprene and creep of the material.

In these tests the two studies on combination of variables were on the bearing pressure (compressive force) and the shear deformation. However, the bearing pressure in the average range of 265 psi minimum to 730 psi maximum did not seem to have much influence on the results. On the other hand, the amount of shear deformation was the most important single factor in the failure of the pads.

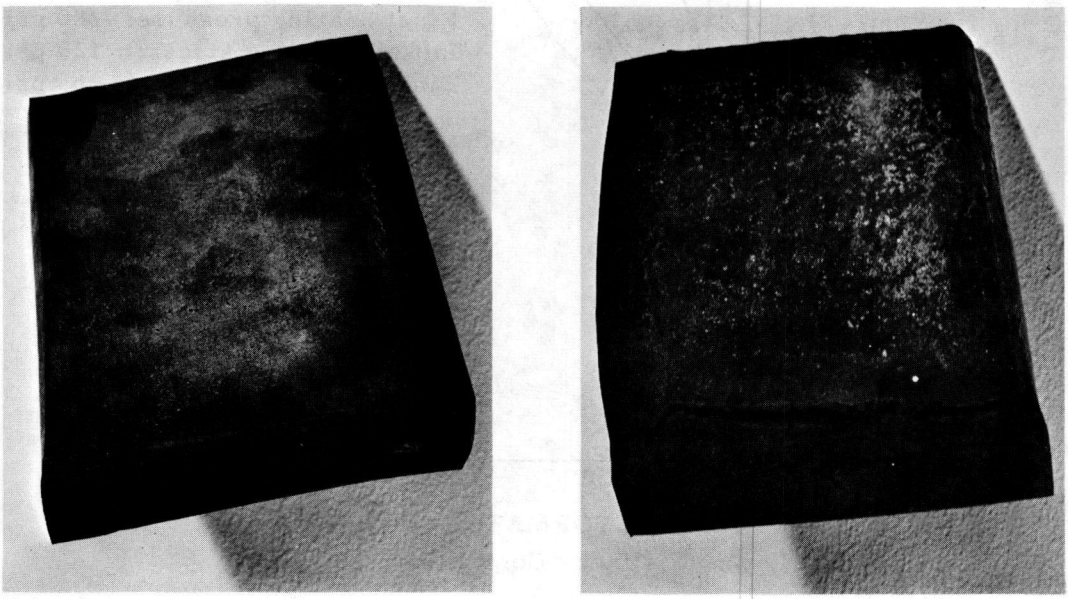

Figure 4. Two of the most severely damaged neoprene pads (A-8 and A-10).

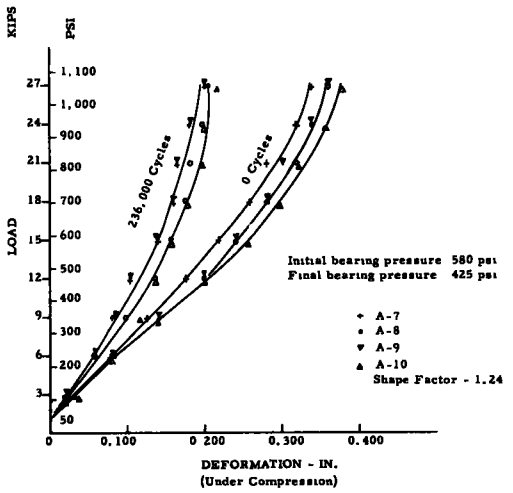

Figure 5. Load-deformation diagram for pads A-7, A-8, A-9, and A-10.

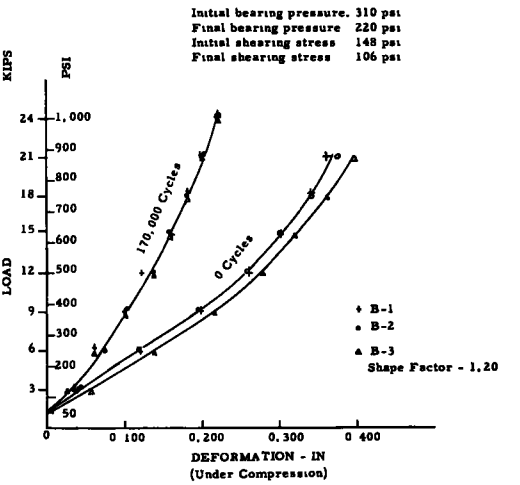

Figure 6. Load-deformation diagram for pads B-1, B-2, and B-3.

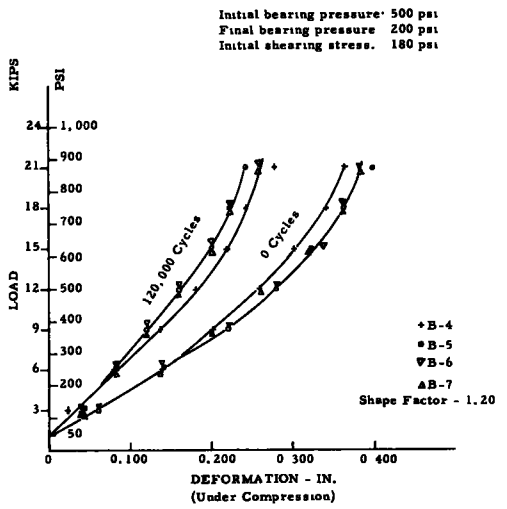

Figure 7. Load-deformation diagram for pads B-4, B-5, B-6, and B-7.

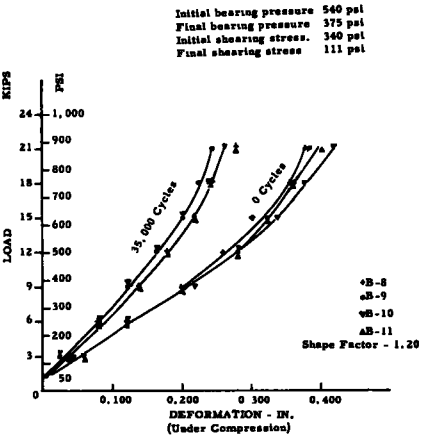

Figure 8. Load-deformation diagram for pads B-8, B-9, B-10, and B-11.

Pads A-1 and A-2 subjected to an average bearing pressure of 730 psi and a simultaneous shear deformation of 0.180 in. exhibited little visual damage (slight permanent distortion but no cracks) after 1,090-000 applications of shear deformation although some hardening of the neoprene had obviously taken place. Pad B-1 subjected to an average bearing pressure of 265 psi failed at 170,000 applications of 0.390 in. shear deformation. Pads B-8, B-9, B-10 and B-11, under an average bearing pressure of 458 psi, failed after 20,000 applications of shear deformation of 0.460 in.

From the above typical behavior and results it could be concluded that bearing pressures of about 700 psi with simultaneous shear deformation of about 0.25 in., one-fourth of pad thickness, could safely be assumed as the maximum limiting design criteria for the use of such pads.

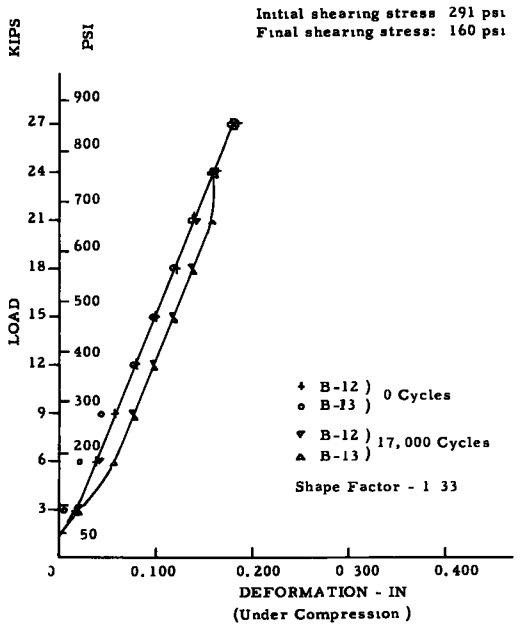

Figure 9. Load-deformation diagram for pads B-12 and B-13.

Figure 10 shows photographs of some of the pads that failed, illustrating the type of cracks that occurred and the manner in which they were formed and developed.

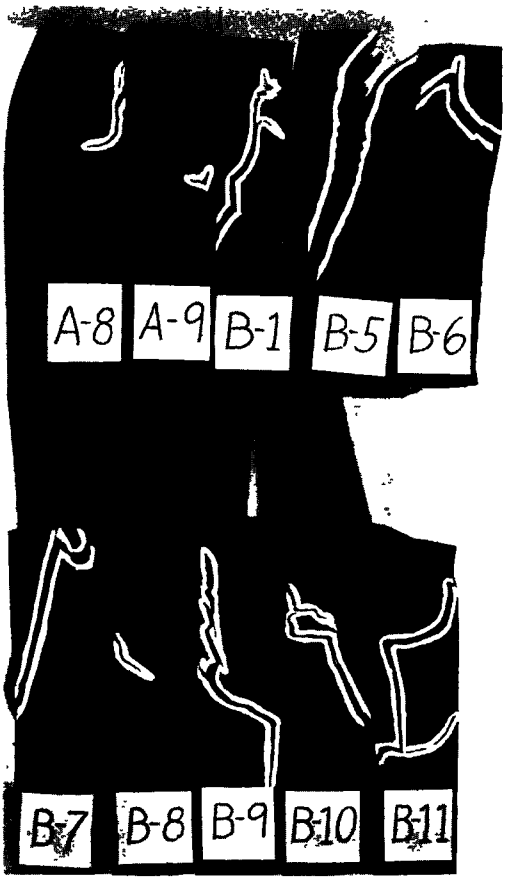

Figure 10. General view of pad failures.

CONCLUSIONS

The tests showed that repeated shear deformations of neoprene pads, under conditions similar to those of actual use, can cause failure at a relatively low number of repetitions of load when the shear deformations are comparatively large.

The critical factor, therefore, is the amount of shear deformation imposed to the pads, rather than the bearing stress.

For pads of the general shape and thickness of those tested, it appears that a limiting shear deformation of one-fourth the pad thickness is adequate for design purposes. Under such repetitive shear deformations an allowable bearing value of 700 psi is safe.

Repeated loads cause some hardening and creep of the pads although it was not definitely established that repetition alone was responsible for the change in these properties. Nevertheless, this hardening does not render the pads unsafe.

ACKNOWLEDGMENT

These tests were conducted as part of a research program sponsored by the Florida State Road Department. The neoprene pads were donated by Oil States Rubber Company, Arlington, Texas. The authors wish to thank A. L. Conyers and D. E. Branson for their assistance.

Discussion

S.D. McCREADY, Product Engineer, Dupont Company, Wilmington, Delaware— Dr. Ozell has completed a thorough study of the dynamic characteristics of elastomer bearing pads, during which he developed a method for predicting their service life under

laboratory conditions. The application of Ozell's data to actual service conditions will be discussed.

Under the most severe shear loads imposed in his testing, no failure was experienced in less than 17,000 cycles. Since expansion and contracting of bridge spans take place very slowly, 17,000 cycles represent many hundreds of years of good performance. This type translation of data is necessary in the rubber industry due to the difficulty in reproducing service conditions in the laboratory.

An illustration of this is the effect of rate of shear cycling to specimen life. Elastomers build up considerable frictional heat when flexed rapidly, which contributed to the breakdown of the vulcanizate. For example, the rubber industry employs tests, such as the St. Joe Flexometer, as described in ASTM Method D 623, to measure the rate of heat generation and fatigue characteristics of tire carcass and tread compounds. Ozell distorted his specimens in shear at the rate of 120 cycles per min. Because of this, it is safe to assume that considerable frictional heat developed which contributed to the failure of the neoprene pads. The rate of shear distortion of bearing pads in service would cause very little heat generation.

The conclusions drawn, therefore, by Ozell relative to shear deformation are somewhat conservative.

Ozell has confirmed the value of 700 psi maximum compressive stress on a 70 durometer pad which has been included in the tentative AASHO bridge pad specification. It should be pointed out that shape factor must be taken into account when computing compressive loads.

The maximum compressive deformation, not including drift, should not exceed 15 percent of initial bearing thickness for maximum long-term performance of the elastomer. For example, an 815 psi load on a 1 x 4 x 8 seventy durometer bearing, having a shape factor of 1.33, will compress it 24 percent. A 720 psi load on a 1 x 4 x 6½ seventy durometer bearing, having a shape factor of 1.24, will compress it 23 percent. Thus, the 700 psi value should apply only to a 70 durometer neoprene pad having a shape factor greater than 1.8. This is very important and should not be ignored in design calculations. By limiting the initial vertical deflection to 15 percent, the compressive stress in psi is automatically taken care of regardless of durometer of shape of the elastomer bearing pad.

A. M. OZELL, Closure — McCready's comment on the heating of the neoprene pads caused by friction resulting from excessive rate of load application is correct. However, although these pads were warm to the touch, they were never "hot." Such minor heating is believed not to have the drastic effect as McCready states.

As mentioned in the conclusions, the critical factor was found to be the shear deformation rather than the bearing stress which contributed to the fatigue failure of the pads. It should be emphasized that the severity of the shear deformation is related to the shape factor. In the tests reported the shape factors varied between 1.20 - 1.33 for which a limiting shear deformation of ¼ the pad thickness was suggested.

McCready's recommendation to limit, for design purposes, the bearing deformation to 15 percent of the pad thickness to account automatically for shape factor or durometer variation has merit.

Tests of Steel Tubular Piles Driven Near Saigon River, Vietnam

D. ALLAN FIRMAGE[1], Associate Professor of Civil Engineering, Brigham Young University, Provo, Utah

●POLITICALLY speaking, the Republic of Vietnam is very young, but geologically the country is very old. The central and northern portions consist of well-worn hills, small valleys and plateaus. The southern portion has been formed by the deposits of the Mekong, Saigon and Dong Nai Rivers.

One of the foreign aid projects of the U.S. Government consists of building 30 kilometers of new highway from the city of Saigon north. This highway crosses many smaller streams and canals as well as the two large rivers, the Saigon and the Dong Nai. Most of the highway alignment is through rice paddies between the many streams.

Core drillings showed quite a variation in subsoil characteristics. Foundation conditions were found to be good at the northern end of the highway with a good grade of rock at depths of less than 100 ft. At the southern end, no rock was found within the limit of the drilling equipment, which was 150 ft. The subsoil on the southern end consisted of varying depths of organic muck overlaying strata of clay and sand.

This subsoil condition dictated the use of piles for all structures. On the northern end, point-bearing piles of steel rolled sections were used. However, for the southern end it was apparent that if piles of high capacity with reasonable length were to be achieved, it would be necessary to use frictional displacement piles. This called for steel tubular piles of some type. Piles of steel WF sections were test driven to depths over 200 ft with only nominal driving resistance. The pier design selected for the smaller crossings was a multiple-pile bent. This substructure was to support 80-ft prestressed beams. The column heights required a minimum column diameter of 20 in. It was then decided to select a 20-in. tubular pipe pile for the substructure of these prestressed concrete beam bridges. A continuous plate girder was the design selected for the major 880-ft crossing of the Saigon River. This bridge was to incorporate 80-ft prestressed beam approach spans on pile trestle bents. For the major span, it was decided to use the 20-in. tubular pile or a fluted steel pile for supporting a reinforced concrete pier.

As there was no previous experience of piles of this size and type in this area, it was necessary to drive and test load several piles before the substructure design could be completed. For the Rach Chue crossing, a 4-span prestressed beam bridge, one test pile was deemed sufficient as borings indicated a uniformity of soil characteristics throughout the length of the structure. For the Saigon River, it was considered necessary to drive test piles near each bank with the idea of using a 20-in. tubular pile on the approach spans and a fluted pile under the main piers. One pile of each type was driven on both the north and south banks.

The fluted pile selected was a pile with the diameter varying from 8 in. at the tip to 18 in. in two 75-ft sections. Beyond the 75-ft length the pile diameter was constant at 18 in. The thickness of the pile was No. 3 gauge (0.239 in.).

DRIVING OF PILES

The driving of the Rach Chue pile was from the land near the edge of the stream and the Saigon piles were driven from a floating barge. All piles were driven with a McKiernan-Terry C-5 double acting steam hammer. This hammer has the following characteristics:

Weight of ram-piston in lb	5,000
Rated striking energy (ft lb per blow)	16,000

[1] Formerly Chief Bridge Design Engineer, Capitol Engineers, Saigon, Vietnam.

Rated speed (strokes per min.)	110
Steam pressure, inlet, psi	100
Stoke-ins	18

The length of leads limited the maximum length of handling to one section. The 20-in. pile came in 40-ft sections and the 18-in. fluted pile in 38- and 36-ft sections. It was necessary during the driving of the piles to stop and weld the sections together. The 20- x ¼-in. tubular pile required the welding of a collar at the top of the pile.

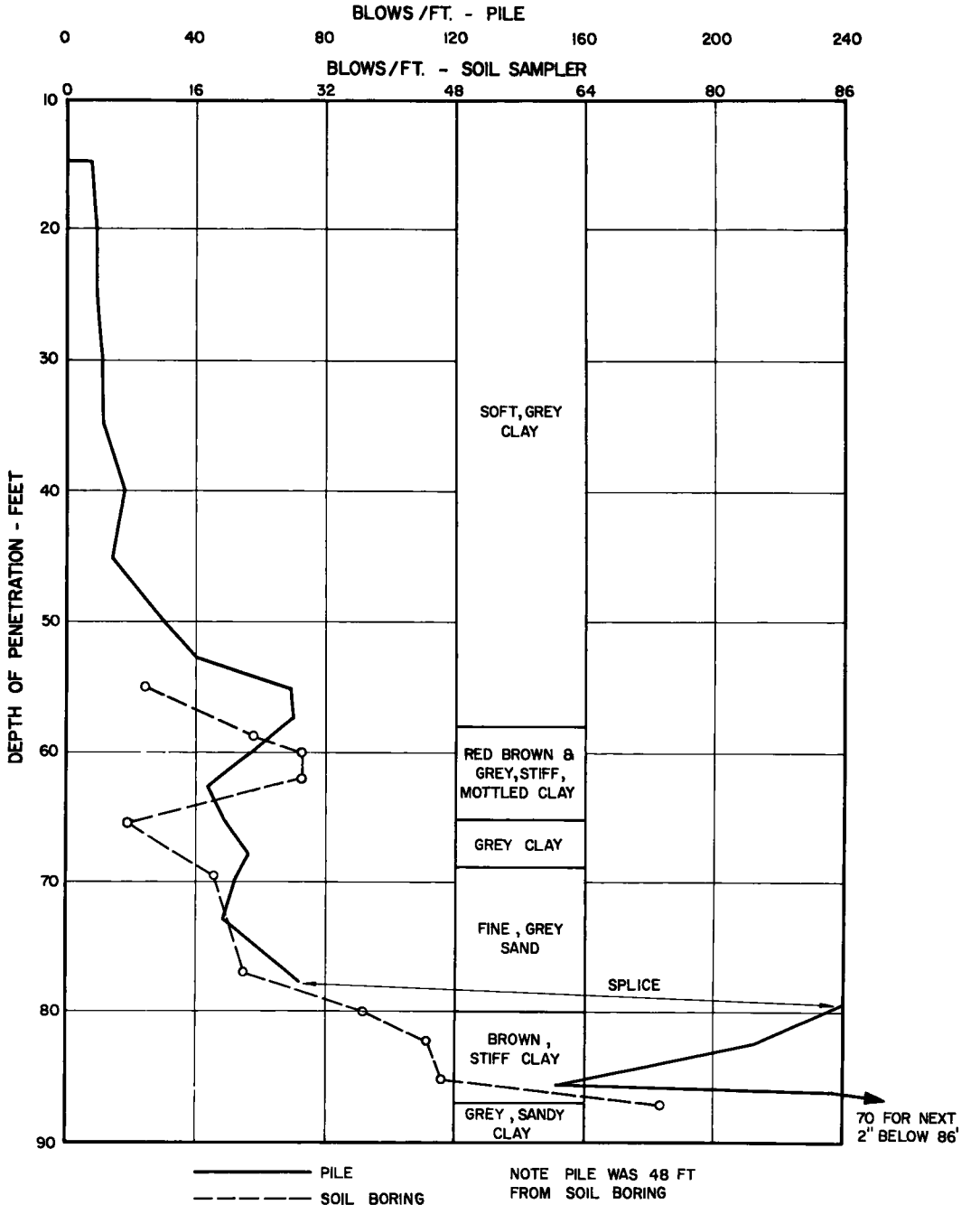

Figure 1. Location: Rach Chue River– 20-in. x ¼-in. steel pipe pile.

Without this collar, the end of the pile would curl during hard driving. This collar was cut off before the next section was welded on. The fluted pile drove as is, without any trouble. The piles were marked at 2-in. intervals for the counting of the blows per unit of penetration.

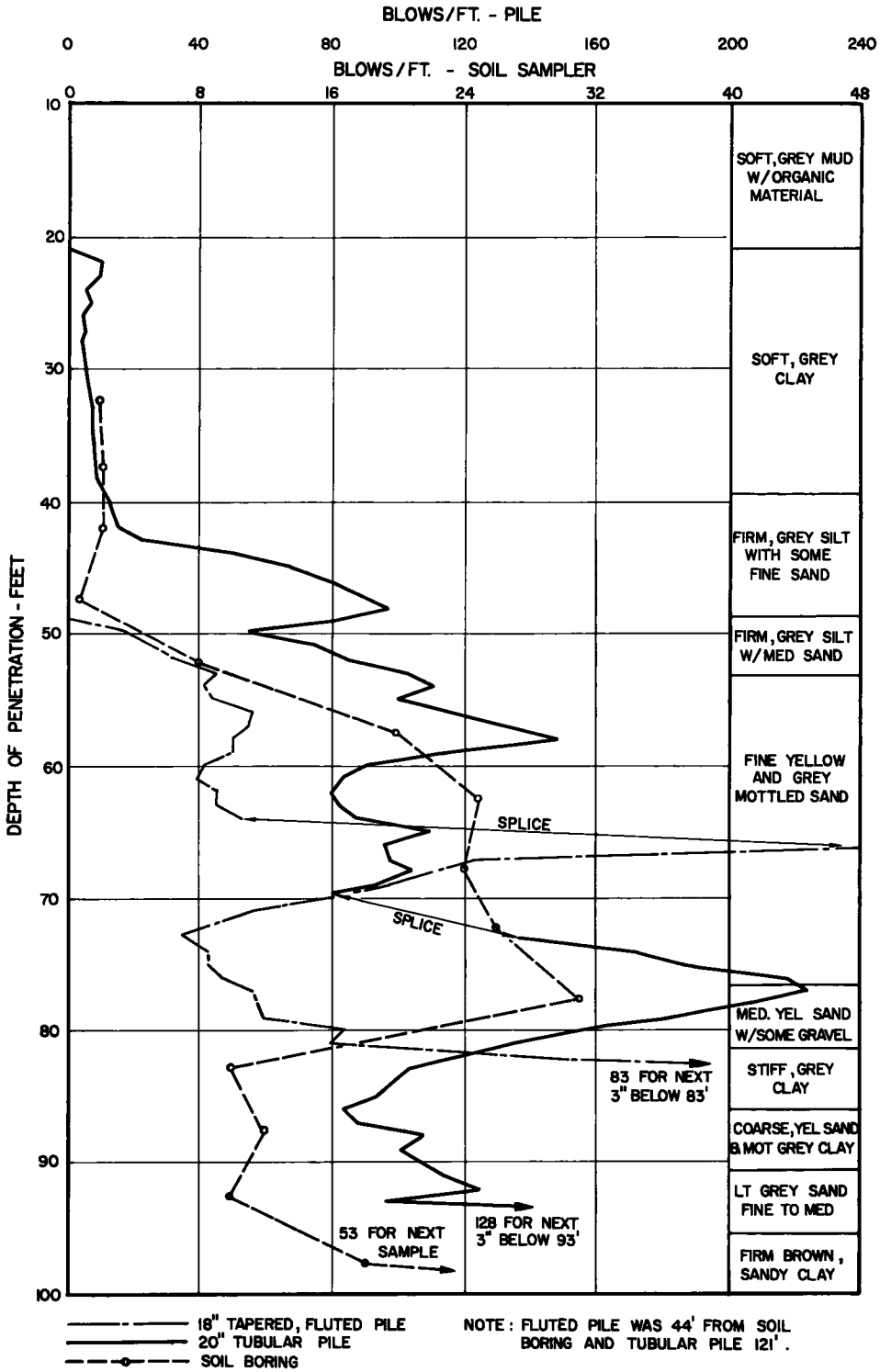

Figure 2. Location: Saigon River—north bank.

All the piles with the exception of the fluted pile on the south bank of the Saigon tightened up quite suddenly. Figures 1, 2 and 3 show the penetration-blow count relationship. Also shown are the blow counts that were necessary to drive the soil sampler.

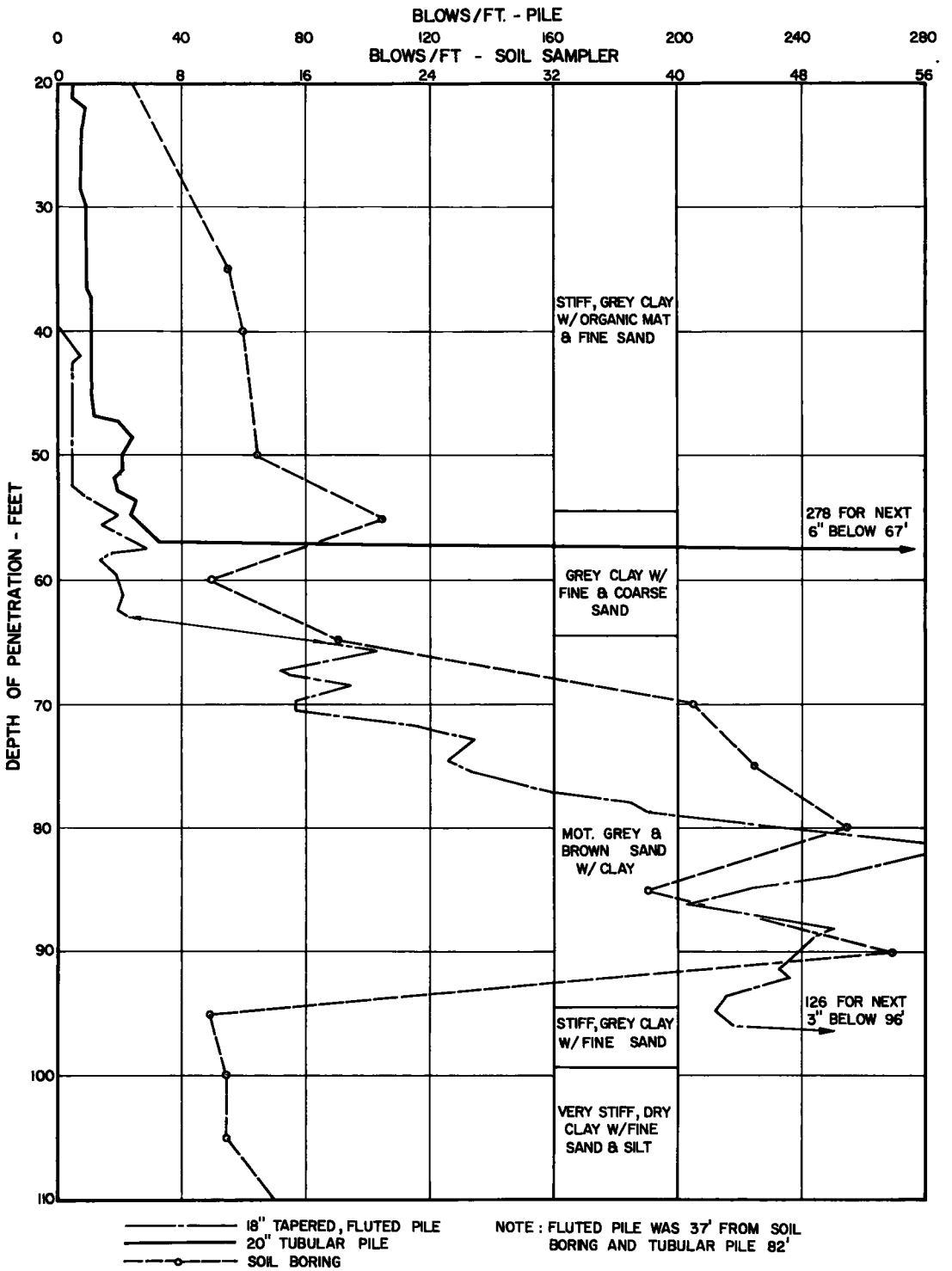

Figure 3. Location: Saigon River— south bank.

After driving the piles, they were cut off at the required elevation and left to set several days and then filled with concrete.

LOAD TESTS

The pile was prepared for load tests by driving four timber piles forming the corners of a 16-ft square with the test pile in the center of the square. The timber piles were then connected with diagonal braces, and a horizontal grid of timber bracing near the top of the test pile gave lateral restraint to the test pile. On the north bank where the piles were farther out of the ground, cable tie-backs to concrete anchors were made to the timber piles.

A ½-in. steel collar was welded to the pile about 7 ft from the top, and a ⅜-in. loose collar was then slid down over the top of the pile to rest on the welded collar.

A loading platform consisting of a structural steel frame with a filling of reinforced concrete was then placed on the top of the test pile which had been ground smooth and level.

Diagonal braces consisting of a pair of 6- x 6- x ½-in. angles were then welded from the corners of the platform to the loose collar. The platform being 16 ft square could accommodate nine 5- x 5-ft concrete blocks in each layer. The weight of the platform was 20.2 tons. Figure 4 shows the platform in place on top of the pile.

The loads consisted of concrete blocks. Three sizes of blocks were used to give the necessary flexibility of loading. These sizes were 5 x 5 x 5 ft; 2½ x 5 x 5 ft; and 5 x 5 x 3 ft.

While loads were being placed, screw-type jacks were placed on the top of the timber piles and jacked against the corners of the loading platform. In this manner the test piles were not required to carry any eccentric loads. All loads were balanced with respect to the pile before the corner jacks were retracted. Figures 4 through 7 show various stages of loading of the various piles.

The increments of load were generally as follows:

Increment	No. and Size of Blocks	Weight of Increment (tons)	Total Weight on Pile (tons)	Minimum Time Interval Between Increments (hr)
1	Platform	20.2	20.2	
2	3- 5 x 5 x 5	28.2	48.4	At least 24
3	2- 5 x 5 x 5	18.8	67.2	1
4	2- 5 x 5 x 5	18.8	86.0	2
5	2- 5 x 5 x 5	18.8	104.8	3
6	3- 5 x 5 x 5	28.2	133.3	12
7	2- 5 x 5 x 5	18.8	151.8	24
8	2- 5 x 5 x 5	18.8	170.6	24
9	2- 5 x 5 x 5	18.8	189.4	24-48
10	2- 2½ x 5 x 5	9.4	198.8	24-48

Above the total load of 198.8 tons the increments were usually in 9.4 to 11.2 tons

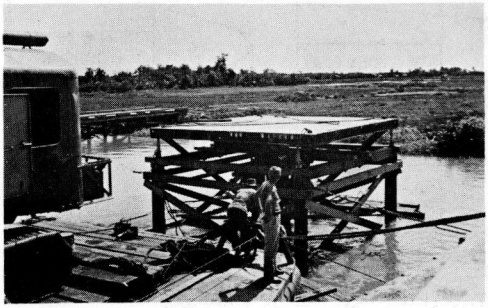

Figure 4. Platform ready for loading—north bank of Saigon River.

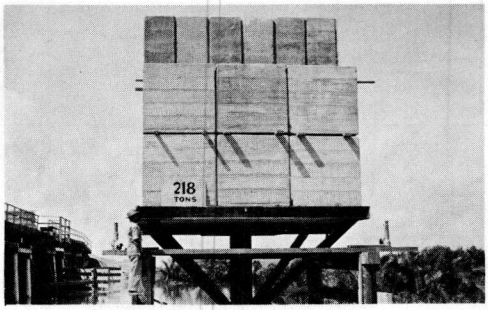

Figure 5. Final load on 20-in. tubular pile—Rach Chue.

(2 at 5 x 5 x 3). Loads for increment 8 and above were usually placed in the morning and a settlement reading taken at that time. Another reading was taken in the evening and again the following morning. If there was noted a settlement between the afternoon reading and the following morning reading, no additional load was placed until settlement stopped. If no settlement had occurred between the stated time interval, an additional increment was then placed on the pile at the 24-hr interval.

Readings of settlement were taken with a Zeiss level, reading on a scale graduated in millimeters. The instrument was sufficiently close to the scale to be able to read to the nearest 0.5 mm (approximately $\frac{1}{50}$ in.). Reference bench marks were placed nearby and read at each reading of the pile. Figure 8 shows readings being taken of settlements. On the Rach Chue it was possible to set the instrument on firm ground. For the Saigon River piles it was not possible to do this and instrument platforms were constructed by driving timber piles near the test piles. These instrument platforms were to be utilized also during the construction of the actual bridge.

When the plot of the load vs settlement, relationship indicated that the limiting pile load was imminent, the pile was unloaded to measure the rebound. This unloading was usually conducted over an 8-hr time period. The pile was then left unloaded (except for platform weight) for a period of 16 hr. The loads were then reapplied in the same increments with approximately one hour between increments. The loadings beyond the previous high before unloading were then applied to the pile in accordance with the general procedure as above outlined.

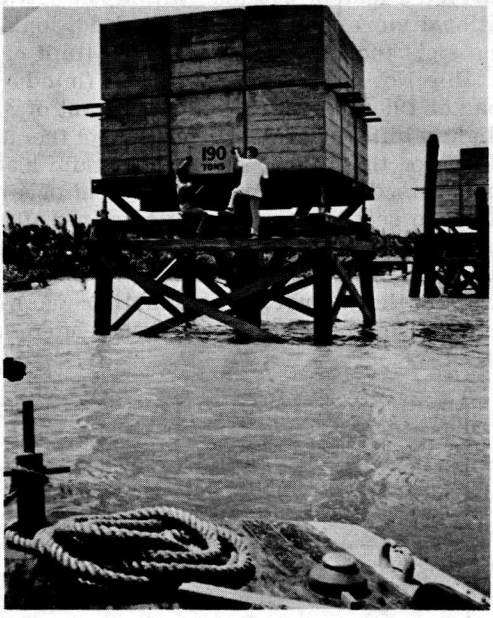

Figure 6. Loads on piles—north bank of Saigon River.

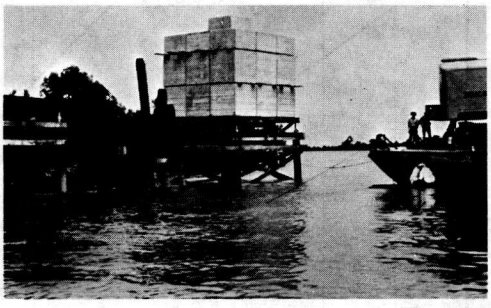

Figure 7. Load of 234 tons on 20-in. tubular pile—south bank of Saigon River.

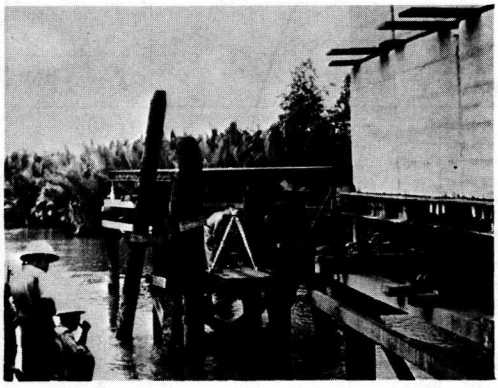

Figure 8. Reading settlements.

In order to reduce the time of testing, two platforms were used on the Saigon River tests, and two tests were conducted at the same time.

RESULTS OF LOAD TESTS

The load vs settlement readings for each of the five piles is plotted in Figures 9 through 13. The general shape of these curves is similar, with a fairly straight-line relationship up to about 80 percent of the ultimate load and then a gradual curve beyond this point.

Pile No. 1 (20 in. at the Rach Chue)

carried a load of 208 tons with a net settlement of 4.0 mm (0.158 in.). With an additional increment of 10 tons an additional settlement of 4 mm occurred. Two hundred and eight tons was considered the limit of load.

Pile No. 2 (18 in. tapered and fluted—north bank of the Saigon River) carried a load of 199 tons with a net settlement of 3.0 mm (0.118 in.). This pile showed a slightly different reload curve from the unload curve. Two additional increments were placed on this pile to give a maximum load of 217.6 tons. This additional load of 18.6 tons caused an additional settlement of 4 mm. The loading was stopped at this point although settlement of the pile ceased after about 24 hr.

Pile No. 3 (20 in. at north bank of Saigon River) had a total settlement of 15.5 mm (0.61 in.) and a net settlement of 5 mm (0.197 in.) at a load of 254.3 tons. The load on this pile was not carried farther due to the limit in capacity of the load platform.

Pile No. 4 (18 in. tapered and fluted—south bank of Saigon River) had a net settle-

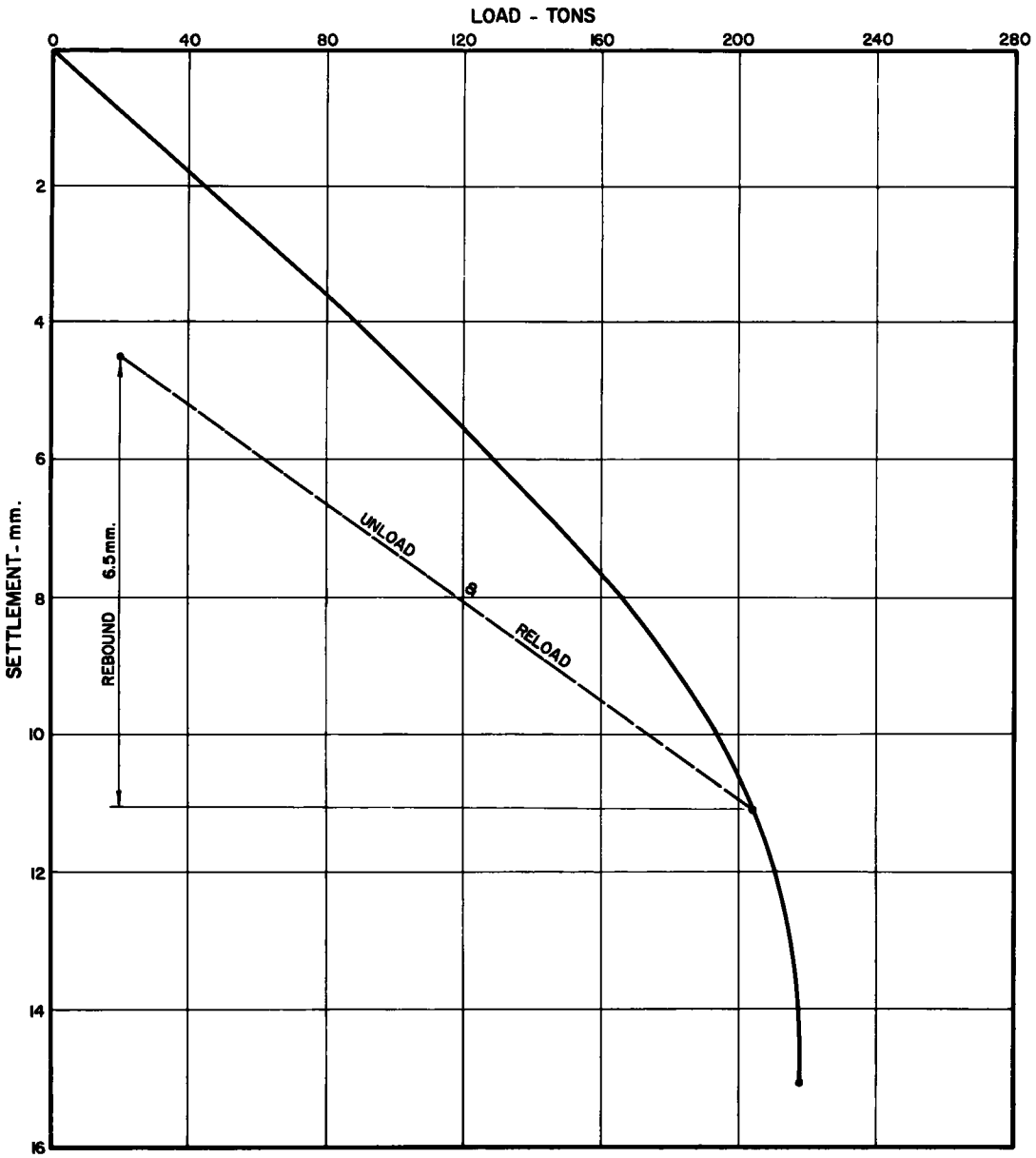

Figure 9. Rach Chue River—20-in. tubular pile.

ment of 7 mm (0.275 in.) at a load of 189.4 tons. Applying the AASHO limit of ¼ in net settlement, the limit load for this pile would be 180 tons.

Pile No. 5 (20 in. at south bank of Saigon River) had a net settlement of only 2.5 mm after a load of 189.4 tons. Using the same slope as the load-settlement curve, it can be said that the load could go over 200 tons before a permanent settlement of ¼ in. would result. The load was carried to 245.2 tons, but excessive settlement occurred in a 40-hr period at the last load increment of 11.2 tons. Large settlements at peak loads in all piles were very slow, therefore, no sudden failure occurred in any pile.

DISCUSSION

Sampler-Pile Blow Count Relationship

It can generally be said that the correlation between blows to drive the sampler and

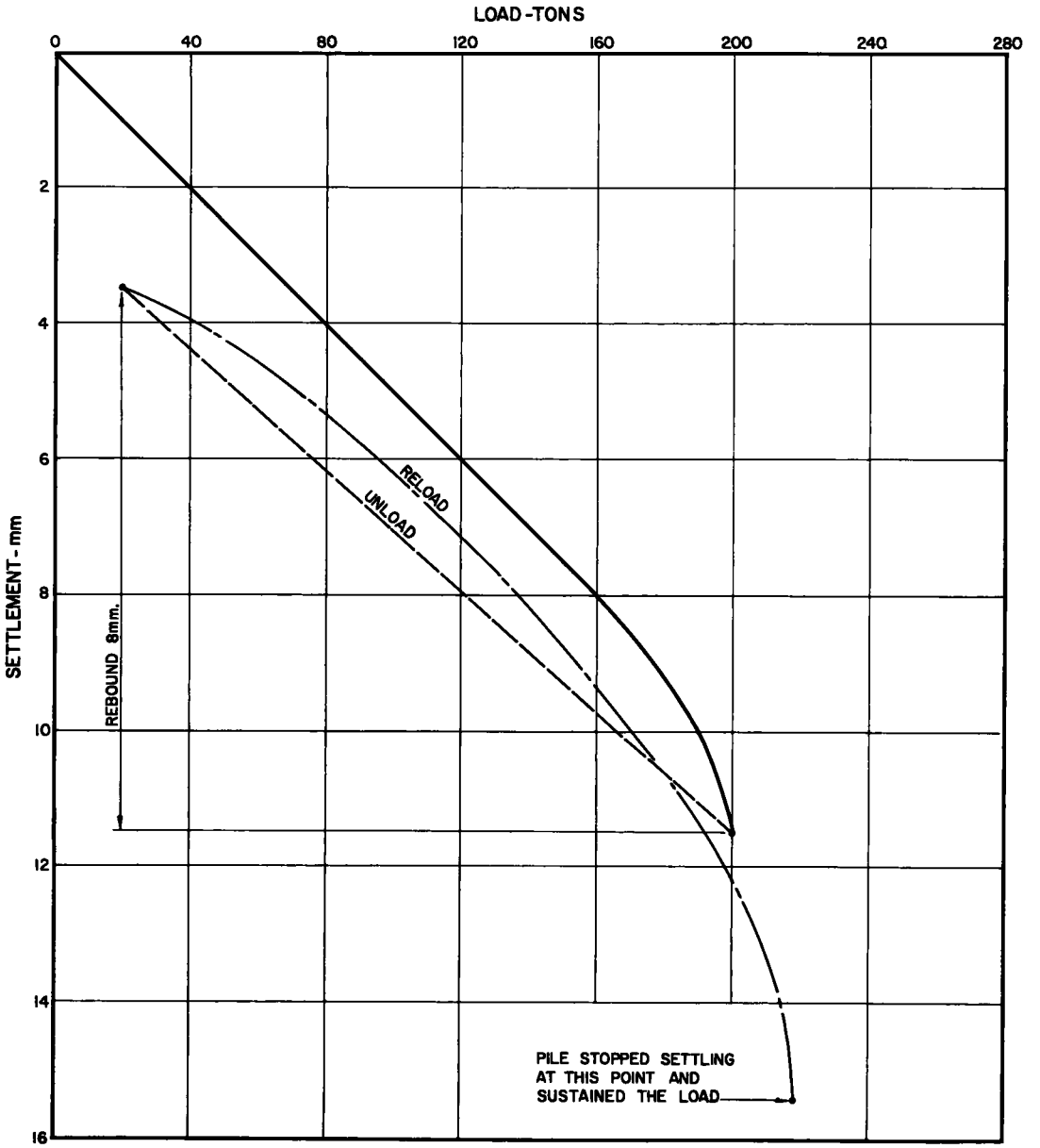

Figure 10. Saigon River—north bank 18-in. tapered, fluted pile.

blows to drive the pile was good. Very good correlation occurred for the Rach Chue pile. This was also true to a lesser extent for both the other two 20-in. tubular piles. The correlation was not as good for the fluted-taper piles. It is noted that the location of high blow count for both piles at the north bank of the Saigon River occurred at somewhat higher elevations than where the high blow count for the sampler occurred. This was also true for the 20-in. pile on the south bank. This could be due to the soil strata being actually a bit higher than as shown. The piles were some distance from the hole locations. Holes were bored at the final pier locations and test piles had to be moved a sufficient distance in order not to interfere with pier construction. Removal of the test piles is not contemplated before completion of the structure. In this type of delta deposit, it is not likely that the soil strata will have any appreciable slope. Results of the blow counts of the sampler give a basis for predicting penetrations of large displacement type of piles.

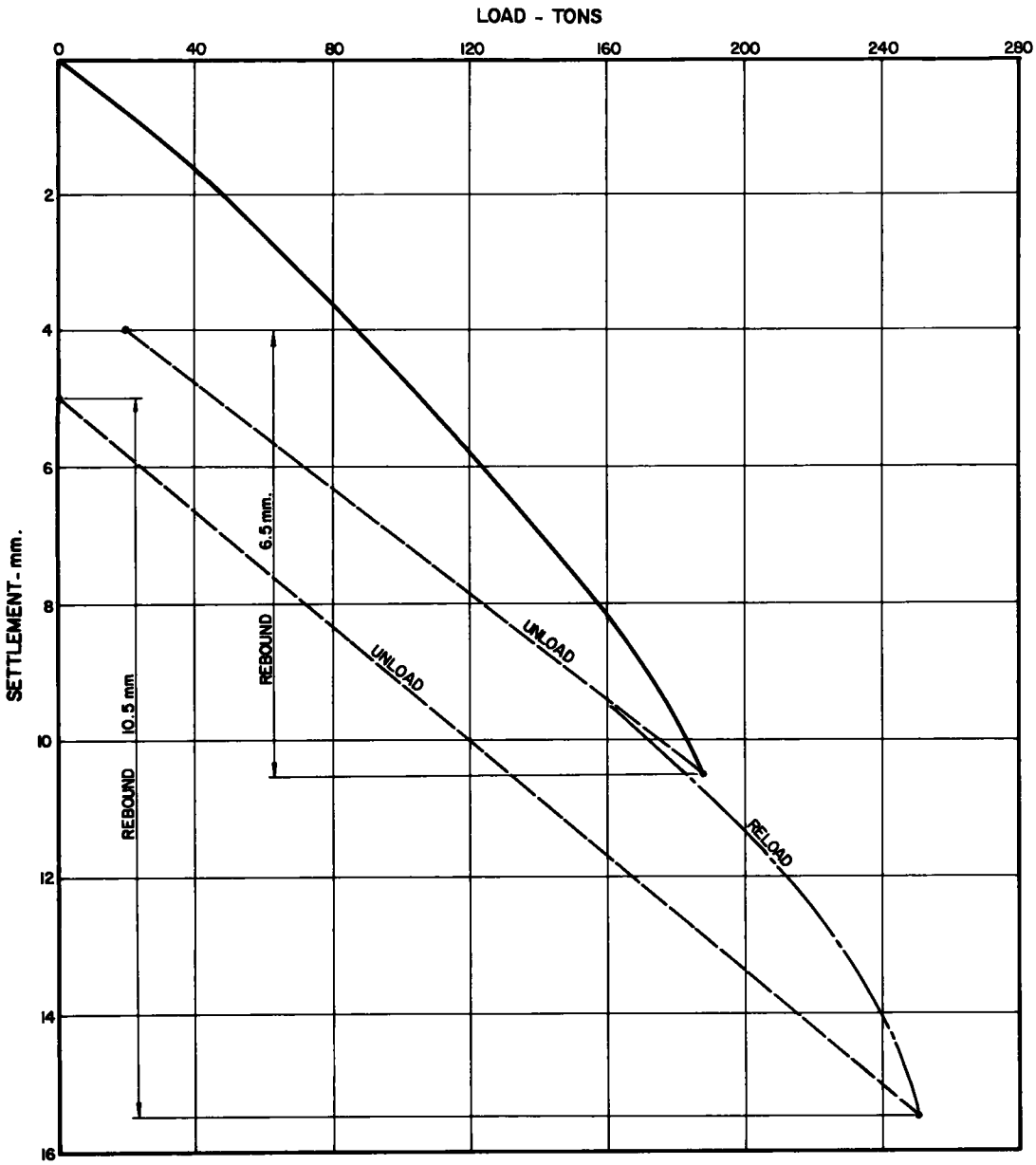

Figure 11. Saigon River– north bank 20-in. tubular pile.

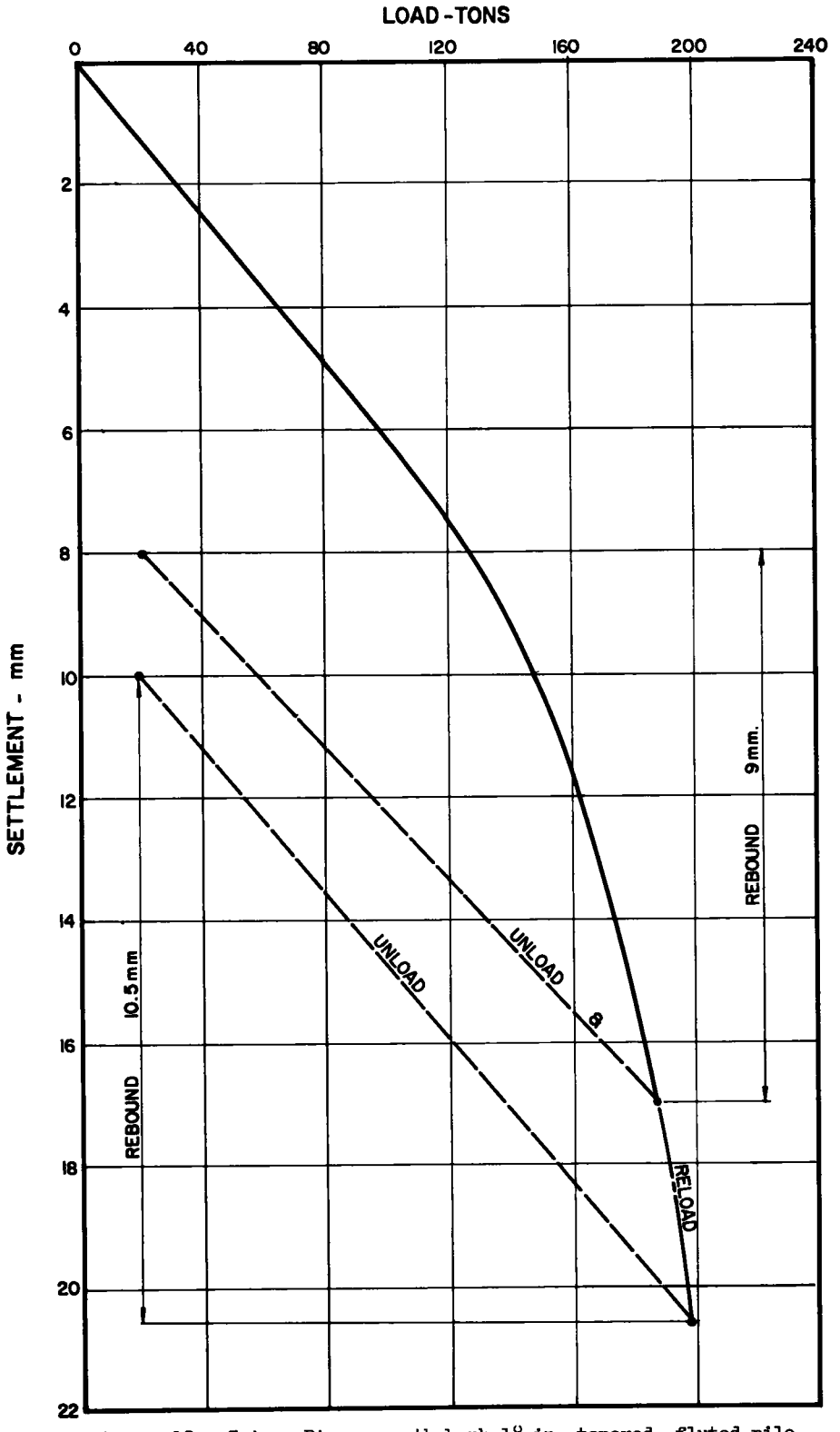

Figure 12. Saigon River— south bank 18-in. tapered, fluted pile.

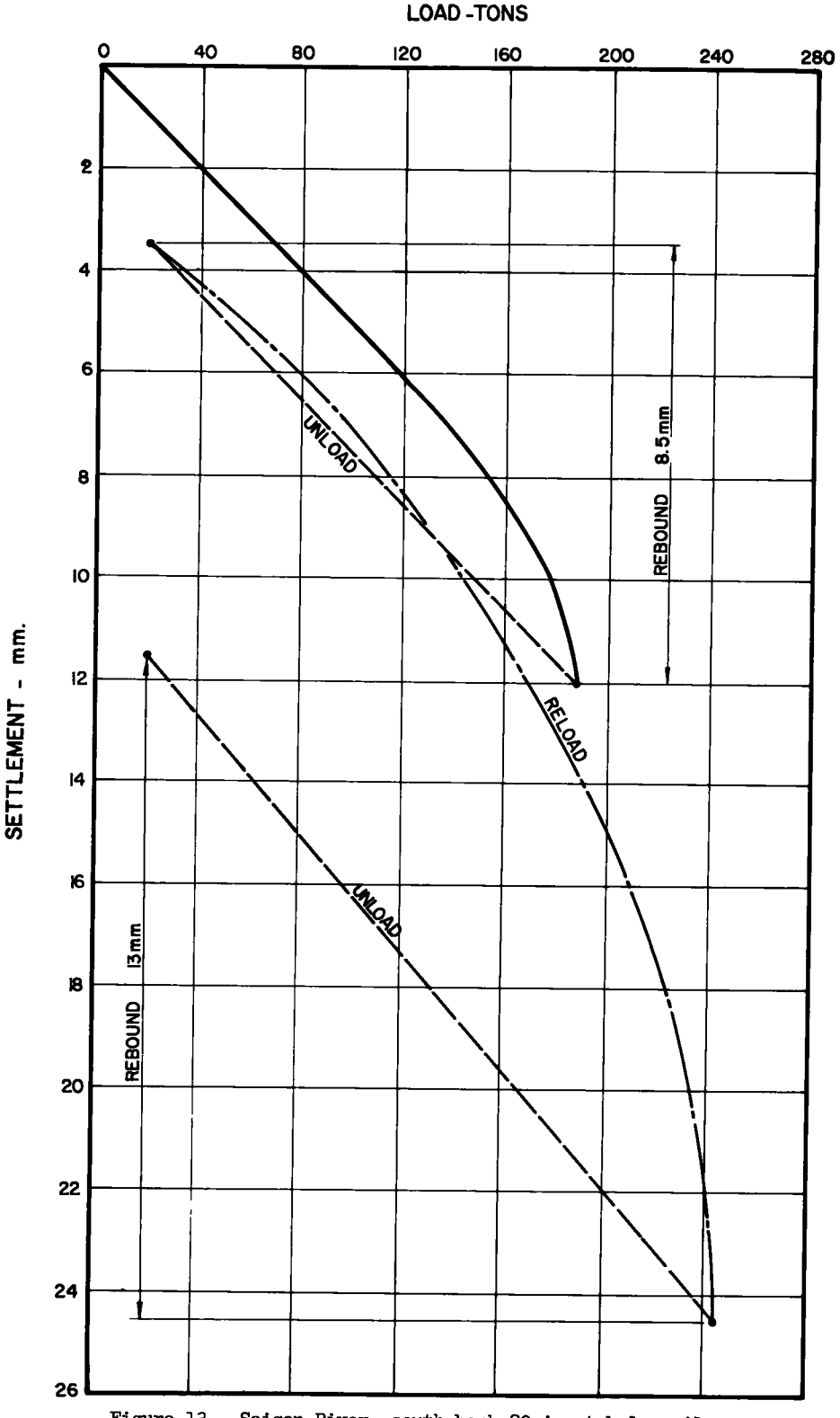

Figure 13. Saigon River— south bank 20-in. tubular pile.

Penetrations

On the north bank, the two types of piles penetrated to nearly the same depth with the 20-in. tubular pile showing a slightly greater blow count. At the south bank, the fluted pile drove 29 ft deeper to obtain nearly the same blow count. The large 20-in. tip could not penetrate any appreciable distance into the layer of dense fine sand that started at about the 60-ft depth. The smaller 8-in. tip of the fluted pile provided no such strong resistance. This is verified by the blow count graph. The 20-in. pile showed a very sudden build-up in blow count while the 18-in. fluted pile showed a gradual build-up.

Comparison With Pile Formulas

A comparison of the loads carried by these five piles, with the dynamic pile formula of

$$Ru = \frac{12\ Ef\ En}{S + \frac{1}{2}(C_1+C_2+C_3)} \times \frac{Wr + e^2Wp}{Wr + Wp}$$

showed a considerable increase in load carried over the predicted capacity as obtained from the formula.

Ru = Ultimate carrying capacity of pile in pounds
En = rated energy of the hammer per blow in ft - lb
Ef = efficiency of the hammer
S = set of pile in inches per blow
C_1 = temporary compression allowance for pile head and cap in inches
C_2 = temporary compression of pile in inches
C_3 = temporary compression allowance for ground in inches
Wr = weight of ram - lb
Wp = weight of pile - lb
e = coefficient of restitution

The values of Ru from the dynamic formula were as follows:

Pile No. 1—Rach Chue, Ru = 280 kips
Pile No. 2—Fluted—north bank Saigon = 270 kips
Pile No. 3—20-in. tubular—north bank Saigon = 270 kips
Pile No. 4—Fluted—south bank Saigon = 270 kips
Pile No. 5—20-in. tubular—south bank Saigon = 336 kips

For all these piles, the constants C_2 and C_3 were so much greater in value than the set (S) that even an increase in S of double the value obtained would give practically the same value from the formula. The lesser weight of Pile No. 5 was responsible for the larger value of Ru as obtained by the formula.

The Modified Engineering News-Record formula gave values as follows:

Pile No. 1 = 252 kips
Pile No. 2 = 254 kips
Pile No. 3 = 215 kips
Pile No. 4 = 286 kips
Pile No. 5 = 302 kips

The actual factor of safety by using this formula would vary from a low of 1.26 for Pile No. 4 to a high of 2.3+ for Pile No. 3.

Because of the amount of sand through which the piles penetrated, a prediction of skin friction based on the shearing strength of the soil resulted in considerably smaller predicted loads than was actually obtained.

CONCLUSIONS

The following general conclusions can be drawn from these tests:

1. Large load capacity can be obtained from large diameter steel pipe piles driven deeply into sedimentary deposits of clay and sand.
2. The predicted capacity from the dynamic formula was quite low as compared to the actual load test.
3. The Modified Engineering News-Record formula will give too small a factor of safety for small penetrations of piles of this size.
4. Load tests should always be conducted when using piles of this size driven into clay and sand deposits.

Discussion

RALPH B. PECK, Professor of Foundation Engineering, University of Illinois—This paper presents the results of pile tests admirably suited for the design of the specific structures with which the author was concerned. Such tests may also provide valuable data for the general fund of knowledge concerning pile foundations. They represent a substantial financial investment and, with very little extra expenditure, could serve a broader purpose

In connection with the correlations among pile tests, the principal shortcoming of most records lies in the description of the properties of the soils surrounding the piles. The load-test procedures as such are usually satisfactory: the ASTM tentative standard method of test for "Load-Settlement Relationship for Individual Piles Under Vertical Axial Load" (D1143-57T) is quite suitable in all respects except that the procedure calls for no more than "a description of soil conditions at the location of the test pile."

The author presents the results of verbal descriptions and standard penetration tests. This is certainly a step in the right direction. It is suggested however, that more detail would be helpful. Unfortunately, the appropriate procedures differ for different soil conditions and hard-and-fast rules cannot be laid down. Nevertheless, the following would seem to be the minimum requirements:

For clays: verbal descriptions, natural water contents, liquid and plastic limits on representative samples, unconfined compressive strengths or equivalent measure of shear strength (as vane tests). Standard penetration tests provide useful supplementary data but are not in themselves adequate.

For silts: verbal, descriptions, standard penetration tests. Drained shear tests, if possible. Present knowledge regarding the properties of silts is very inadequate and no really satisfactory recommendations can be made.

For sands: verbal descriptions including estimates of size and grading, standard penetration tests on several borings near the test pile.

The records of pile load tests are often either too brief, or more elaborate than necessary. A form found suitable in studying the numerous tests included in the survey of friction piles for the Highway Research Board is that shown in HRB Special Report 36. A single page was found adequate for most records.

D. ALLAN FIRMAGE, Closure — Peck has pointed out a major difficulty in correlations among pile tests. That is, the desired quantity of soil information is in most cases somewhat lacking. This is true because most load tests have the primary objective of determining pile capacity for use in a specific design and the gathering of information on a research basis is only incidental to the work. This was the case with regard to the pile load tests in Vietnam. The main objective was to determine pile capacities for the foundation of bridges in the specific locations.

Soil borings had been taken at the proposed pier locations and laboratory tests conducted on the samples. As the test piles could not be incorporated in the final structure or easily removed, the test piles were driven some distance away from the pier locations. Because of the nature of the geology in this region, it was considered that prediction of pile capacity in the actual structure could quite accurately be obtained from the test piles. Figures 2 and 3 of the paper showed that the test piles on the south bank of the Saigon River were 37 ft and 82 ft from the soil boring and on the north bank

TABLE 1

LOCATION: SAIGON RIVER—SOUTH BANK

Depth-Meters From	To	Class-ification	Un. Comp. Str. Kg/M^2	Dry Density Kg/L	Moisture Content (%)
0	3.60		No sample—muck		
3.60	5.12	Clay	1,200	0.794	86.1
5.12	6.64	Clay	2,650	0.833	80.9
6.64	8.17	Clay	3,610	0.884	73.1
8.17	9.70	Clay	2,650	0.836	81.0
9.70	11.22	Clay	2,970	0.872	68.8
11.22	12.74	Sandy clay	4,250	0.853	75.1
12.74	14.26	Clay	5,540	0.877	68.6
14.26	15.79	Clay	3,290	0.865	74.6
15.79	17.31	Sandy clay	2,490	1.174	45.5
17.31	18.84	Sandy clay	3,610	1.088	54.6
18.84	20.36	Sand	1,363	1.808	15.6
20.36	21.88	Sand	3,370	1.792	18.3
21.88	23.41	Sand	2,810	1.735	20.4
23.41	24.93	Sand	3,450	1.744	19.4
24.93	26.46	Sand	2,490	1.770	22.9
26.46	27.98	Sand	3,610	1.750	18.8
27.98	29.50	Clay	8,587	1.131	52.0
29.50	31.03	Clay	8,427	1.141	51.8
31.03	32.55	Clay	10,433	1.157	50.0

TABLE 2

LOCATION: SAIGON RIVER—NORTH BANK

Depth-Meters From	To	Class-ification	Un. Comp. Str. Kg/M^2	Dry Density Kg/L	Moisture Content (%)
0	6.89	Soft muck—no sample			
6.89	8.42	Clay	3,300	0.789	90.3
8.42	9.94	Clay			
9.94	11.47	Clay	1,440	0.822	81.9
11.47	12.99	Silty clay	5,300	0.837	80.7
12.99	14.51	Sand	2,650	0.903	74.6
14.51	16.04	Sand	13,240	1.478	29.5
16.04	17.56	Sand	6,020	1.880	14.4
17.56	19.09	Sand			
19.09	20.61	Sand		1.770	19.3
20.61	22.13	Sand			
22.13	24.65	Silty sand			
24.65	25.18	Sand	1,565	1.715	21.4
25.18	26.71	Clay	6,020	1.256	40.4
26.71	28.23	Sandy clay	26,900	1.616	26.0
28.23	29.75	Sandy clay	2,650	1.814	16.5
29.75	31.28	Sand	1,850	1.891	13.9
31.28	32.80	Clay	6,980	1.895	15.2
32.80	34.32	Clay	5,580	1.894	15.0

44 ft and 121 ft from the nearest boring. The results of laboratory analysis of samples from these two borings is given as part of this discussion (Table 1 and 2) .

It would have been desirable to have made additional borings near the test piles but because of a limited number of drill rigs in proportion to the quantity of drilling necessary for the over-all program additional borings at these locations could not be justified.

Peck's outline of information requirements in pile load tests should be followed wherever practical. This outline should be an aid to those conducting future pile tests.

A Rational Method for Determining Safe Foundation Pressures and Embankment Stability

S. LIFSITZ, Chief Engineer, Wayne County Road Commission, Detroit, Michigan

The purpose of this paper is to describe the application by the Wayne County Road Commission of Housel's[1] method for determining safe foundation pressures and stability of sloping embankments in cohesive soils. The county had been using his method in designing foundations for highway and railroad grade separation structures since the late twenties with satisfactory results.

However, at the conclusion of World War II, the county had undertaken an extensive program of expressway construction necessitating a fivefold increase in the engineering staff. The young engineers available at that time had little or no experience in the art of soil mechanics, and a bottleneck was created whenever they had to determine the allowable foundation bearing pressures for the structures they were designing. To obtain uniform and safe design computations, the writer had undertaken to standardize and simplify the design procedure. Thus, once the laboratory had furnished the shear values of the various soil strata in the test borings, the designer would arrive at the correct answer without having to rely on his own judgment. This does not mean, of course, that inexperienced designers were relied on to make major decisions on the type of design to be used. This did, however, provide the squad leader or chief designer a basis on which to exercise his judgment.

The writer will readily concede that a number of simplifications have been made to avoid the complexity of more theoretical treatments and that some of the assumptions may be difficult to prove. However, in the 12 years that this procedure has been used, it has amply demonstrated its reliability. It has afforded a simple and rational method of evaluating the benefits of struts, subbases, ties and permanent steel sheet pile cofferdams around footings in the design of highway and railroad structures; it has eliminated the need for costly piles under foundations, where piles have previously been used; and it has enabled safe embankment slopes to be determined, by a few simple calculations. On a few occasions, soil samples have been taken, adjacent to old structures designed without the benefit of Housel's theory and it was found that where his formulas indicated safe bearing pressures lower than the actual, the structure has actually undergone some progressive settlement.

Before proceeding with the description of the procedure and with some typical examples of actual designs, a brief description of Housel's basic equations will be given.

●ALL THE factors of resistance determining the ultimate bearing capacity of a strip footing in cohesive soil are shown in Figure 1. These are composed of the developed pressure in the compression block immediately below the bearing area ($4S$); the lateral distribution below the bearing area ($2S$); the resistance to upheaval ($2S\frac{h_0}{b}$); the perimeter shear resistance ($2S\frac{h_0}{b}$), and the static head (wh_0). For square or round footings the lateral distribution and the perimeter shear resistance is doubled ($4S$ and $4S\frac{h_0}{b}$).

[1] Professor of Civil Engineering, University of Michigan, Research Consultant, Michigan State Highway Department.

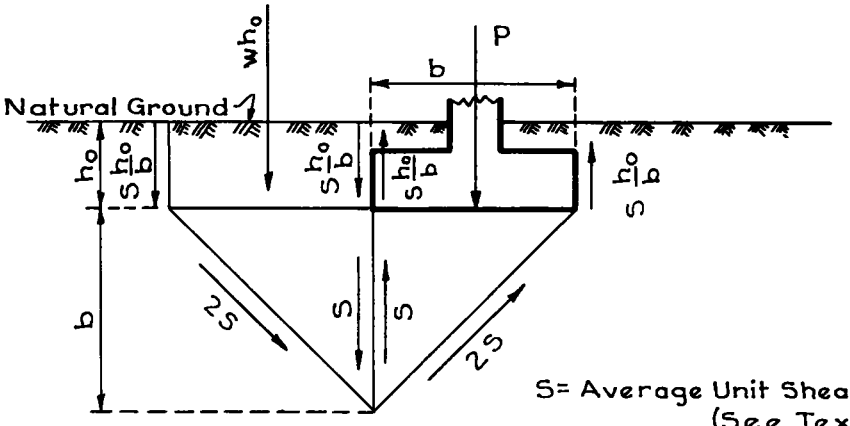

For strip footings,

$$\frac{P}{A} = wh_o + 6S + 4S\frac{h_o}{b} \qquad (1)$$

For square or round footings,

$$\frac{P}{A} = wh_o + 8S + 6S\frac{h_o}{b} \qquad (1a)$$

Figure 1. Basic equations for bearing capacity.

The unit shear resistance S is obtained by means of a transverse or ring shear test as developed by the University of Michigan Soil Mechanics Laboratory. It is a measure of the shear stress greater than which the soil will suffer progressive deformation and is approximately equal to one-quarter the shear resistance value obtained by the unconfined compression test.

Basic Equations for Stability of a Sloping Embankment

Figure 2 shows the pressure intensities at a depth h_o, acting on the principal planes of an elementary cube of cohesive soil of unit dimensions. The shear on the maximum shear plane is upward if P_v is greater than P_h, and downward if P_v is less than P_h. From mechanics of materials,

$$P_h = P_v - 2S = wh_o - 2S, \quad \text{when } P_v > P_h \qquad (2)$$

and

$$P_h = P_v + 2S = wh_o + 2S, \quad \text{when } P_v < P_h. \qquad (2a)$$

Eq. 2 represents the intensity of the active earth pressure at any point on a vertical plane through the top of slope. Eq. 2a represents the intensity of passive earth pressure offered at any point on a vertical plane through the toe of slope. The total active pressure above plane B (at a depth d below the bottom of slope plane A) is resisted by the total passive pressure between planes A and B, plus the resistance to sliding mobilized on plane B for a length of L + 2d. Referring to Figure 3, L is the horizontal width of the slope, while 2d represents an additional length on plane B assumed to be effective in resistance to sliding and is due to the lateral distribution of the vertical load. This lateral distribu-

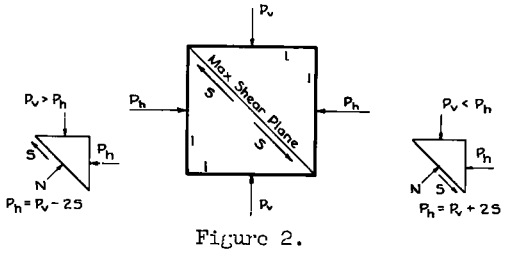

Figure 2.

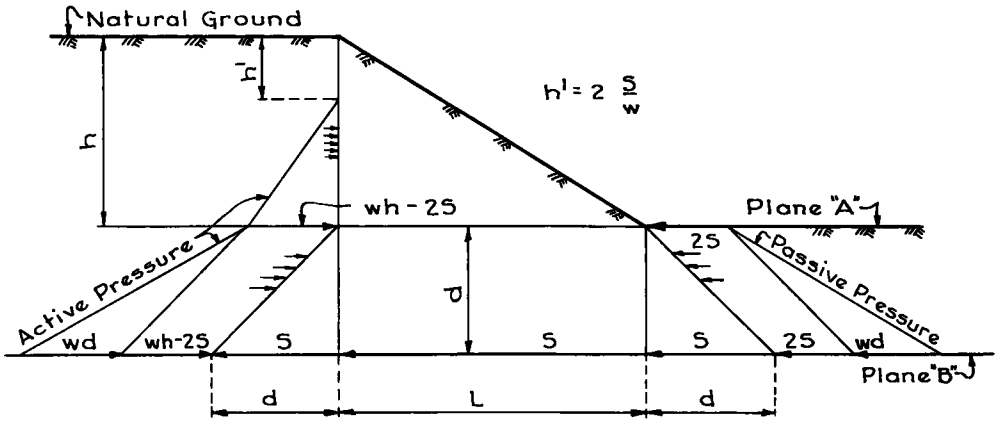

$$\text{Active Pressure} = \frac{w}{2}\left(h - 2\frac{S}{w}\right)^2 + (wh - 2S)\,d + \frac{wd^2}{2}$$

$$\text{Passive Pressure} = 2Sd + \frac{wd^2}{2}$$

$$\text{Shear Resistance} = (L + 2d)S$$

The minimum length required for a stable embankment is determined by equating the active pressure to the passive pressure plus the shear resistance and then solving for "L"

$$\frac{w}{2}\left(h - 2\frac{S}{w}\right)^2 + (wh - 2S)d + w\frac{d^2}{2} = 2Sd + w\frac{d^2}{2} + (L + 2d)S$$

$$L = \frac{\frac{w}{2}\left(h - 2\frac{S}{w}\right)^2 + (wh - 6S)d}{S} \qquad (3)$$

Figure 3. Stability of a sloping embankment (based on Housel's method).

tion is assumed to take place below plane A on a 1 : 1 slope, and the horizontal pressures shown in Figure 3 are, therefore, applied on 45 deg planes instead of the vertical planes mentioned before.

The equations derived from Figure 3 are based on Housel's original method of analyzing the stability of sloping embankments. The resistance due to lateral distribution below plane A has also been derived by the so-called element method following the procedure used in derivation of the bearing capacity of spread footings (2). The mass stability analysis of embankments has also been modified by Housel to include the additional vertical shear resistance mobilized along the vertical plane of a potential failure surface (3, 4). However, it is sufficient to use Figure 3 in its original form and obtain the basic equations for slope stability therefrom. For a later and more detailed description, see references at the end of the text.

Overload Ratio vs Safety Factor

The shearing resistance in unconfined compression tests is taken as one-half the unconfined compressive strength, and a safety factor of four is used to determine the safe shearing resistance. Since the unit shear resistance obtained from ring shear tests has a value of one-quarter of the above, a safety factor of four is inherent in the term S in the Housel equations.

The relationship between the desired safety factor of four, based on the allowable shear values, to the actual safety factor resulting when higher than allowable shear

values are used is termed the Overload Ratio. Thus,

$$\text{Overload Ratio} = \frac{4}{\text{Factor of Safety}} = R$$

The Overload Ratio, R, is applied as a coefficient of S in all the preceding equations.

Table 1 gives the overload ratios as recommended by Housel and corresponding factors of safety recommended by Terzaghi and Peck (5) with reference to the ultimate shearing resistance from the rapid unconfined compression test.

TABLE 1

HOUSEL'S RECOMMENDED OVERLOAD RATIOS

Description	Overload Ratio (R)	Factor of Safety (F S)
Permanent structures	1.00	4.00
	1.33	3.00
Temporary structures	2.00	2.00
	2.50	1.60
Failure condition	4.00	1.00

PROCEDURE FOR DETERMINING ALLOWABLE FOUNDATION PRESSURES

In determining the allowable foundation pressures on strip footings, the values of the perimeter shear resistance and the resistance to upheavel have been arbitrarily reduced by 50 percent, since the excavated area is frequently larger than the footing area, and the backfill material cannot be relied upon to offer appreciable shear resistance (see Fig. 4). Two values have also been established for the Overload Ratio, R, to be used in the equations: a value of R = 1 for pressures resulting from dead load plus overturning, and a value of R = 1.5 for pressures resulting from a combination of dead load plus overturning plus live load. This results in a safety factor of 4 and 2.67, respectively.

If, as sometimes happens, the shear values in the soil strata at 5 or 10 ft below the bottom of footing permit higher pressures, steel sheet piling is driven to that depth and the bottom of the piling is considered as the bottom of the footing plane. The sheet

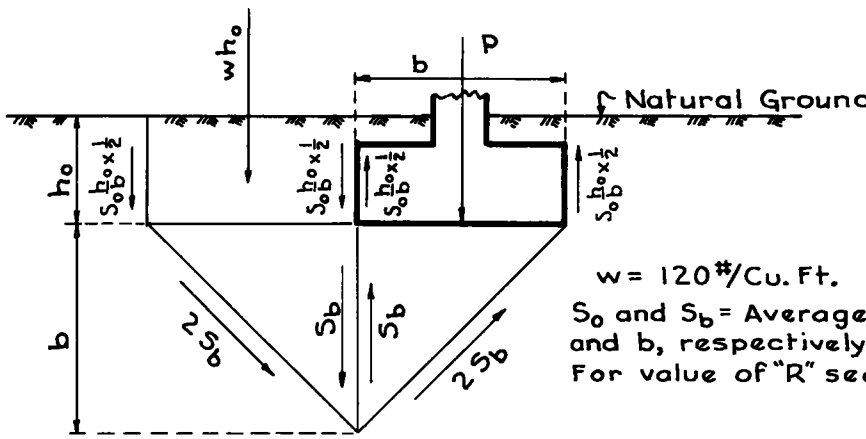

For strip footings,

$$\frac{P}{A} = 120\,h_0 + 6S_bR + 2S_0R\frac{h_0}{b} \qquad (4)$$

Figure 4.

piling is anchored to the footing and sheet pile diaphragms placed at intervals equal to the width of the footing. Figure 4 shows the Housel method as modified by the county.

EFFECT OF A CONCRETE SUBBASE ON FOUNDATION PRESSURES

A reinforced concrete strut placed between two abutment footings serves to resist the active soil pressures on the abutments. If, instead of a strut, a reinforced concrete subbase is used, the subbase acts as an auxiliary footing as well as a strut. Figures 5 and 6 show the assumed pressure distribution on abutment and pier footings with and without subbases. The assumed pressure distribution on the subbase is admittedly an approximation but is considered sufficiently accurate for design purposes in determining

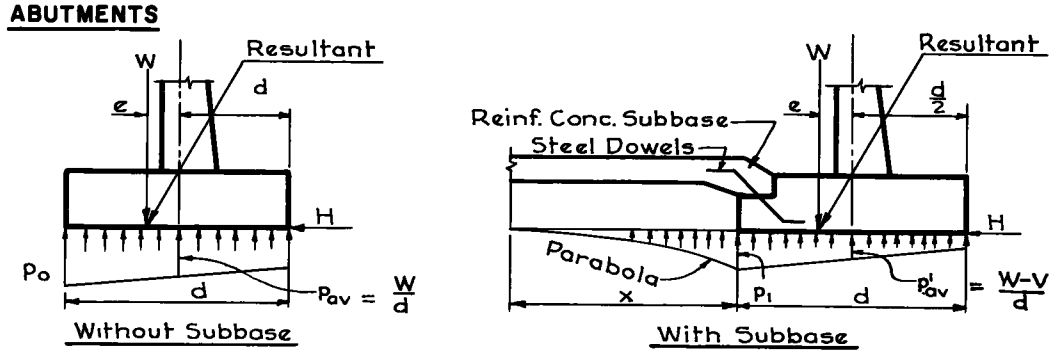

p_o = Computed max. toe pressure without subbase

p_1 = Computed max. toe pressure with subbase

$V = \frac{1}{3} p_1 x$ = Total pressure taken by subbase = Load on dowels

$x = \begin{cases} \frac{d}{2} & \text{for 12" to 18" thick subbase} \\ d & \text{for 24" thick subbase.} \end{cases}$

Figure 5. Effect of concrete subbase on foundation pressures.

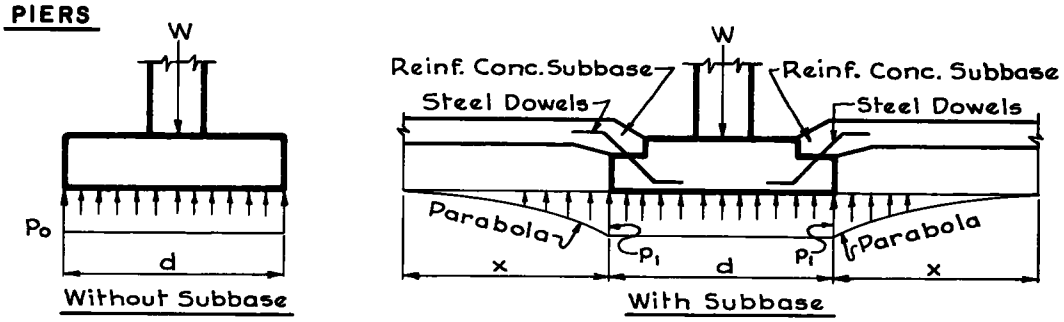

$p_o = \frac{W}{d}$

$V = \frac{1}{3} p_1 x$

$p_1 = \frac{W-2V}{d}$

$x = \begin{cases} \frac{d}{2} & \text{for 12" to 18" thick subbase} \\ d & \text{for 24" thick subbase.} \end{cases}$

Figure 6.

the reduced footing pressures resulting from subbase action.

The conventional straight line pressure distribution is assigned to the footing, while a parabolic pressure distribution is assumed acting on a portion of the subbase. This portion was arbitrarily assumed to be one-half the width of the footings for a subbase 12 to 18 in. thick and the width of the footing for a subbase 24 in. thick.

Referring to Figure 5:

$$P_o = \frac{W}{d} + \frac{6We}{d^2}$$

$$p_1 = \frac{(W-V)}{d} + \left(We - \frac{Vd}{2}\right) \times \frac{6}{d^2} = p_o - 4\,\frac{V}{d} = p_o - \frac{4}{3}\,p_1 X$$

$$p_1 = \frac{3}{5}\,p_o \text{ for } X = \frac{d}{2} \qquad (5)$$

$$p_1 = \frac{3}{7}\,p_o \text{ for } X = d \qquad (5a)$$

Referring to Figure 6:

$$W = p_o d = p_1 d + 2V = p_1 d + 2p_1 \times \frac{X}{3}$$

$$p_1 = \frac{3}{4}\,p_o \text{ for } x = \frac{d}{2} \qquad (6)$$

$$p_1 = \frac{3}{5}\,p_o \text{ for } x = d \qquad (6a)$$

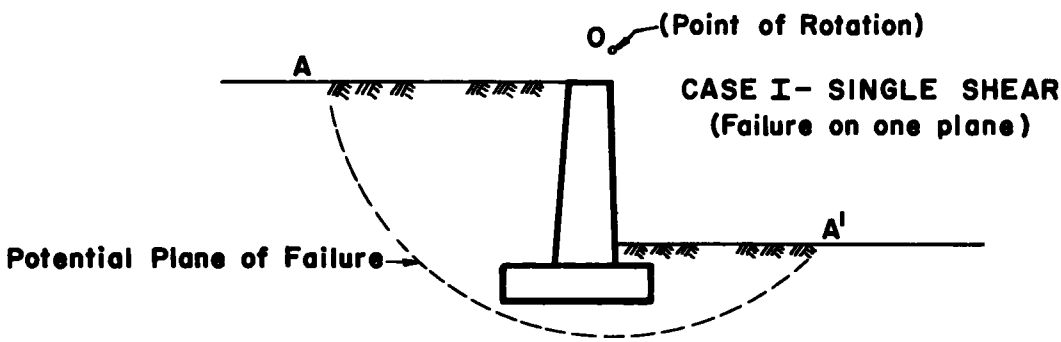

Figure 7. Showing bank supported by wall without struts.

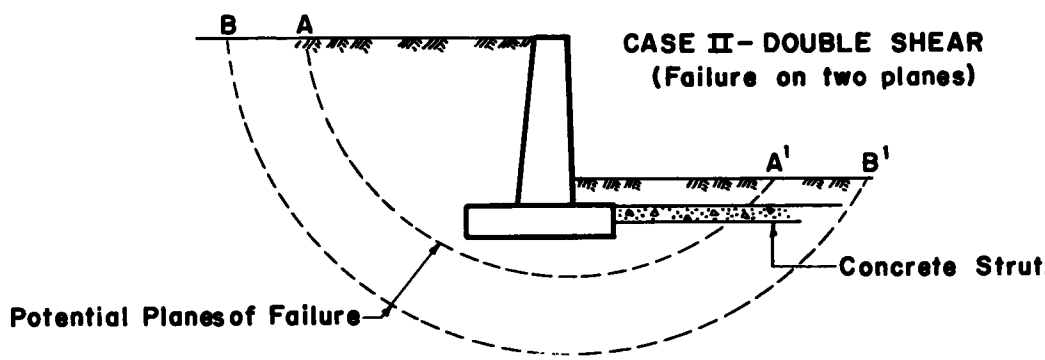

Figure 8. Showing bank supported by wall with struts.

STABILITY OF AN EMBANKMENT SUPPORTED BY A WALL

Figure 7 shows a wall retaining a high bank of earth. If the soil conditions are such as to make the bank unstable, there will be a tendency of the unstable mass to rotate on the potential failure surface AA' about some point 0. If, however, the rotation of the wall is prevented by means of a concrete strut between footings on the opposite banks, failure of the bank on a single surface is no longer possible. As shown in Figure 8, failure of the bank can now occur only by a movement of a portion of the retained mass along two sliding surfaces AA' and BB'—one at or near the back of the wall and the other at some finite distance farther back. As a result, shear resistance against sliding is now mobilized on the two surfaces, thus materially increasing the factor of safety.

The county has recently constructed an earth-filled exit ramp near the terminus of the John C. Lodge Expressway in the City of Detroit. The terminus is located near the Detroit River, and the soil conditions at this location are the worst so far encountered along the entire Expressway. The fill is retained by a wall on each side, with reinforced concrete ties placed at intervals between the walls. The walls are supported on cast-in-place concrete piles extending to hardpan (the only area on the Expressway where piles were used). The main function of the ties is similar to that described for struts; namely, to prevent movement or rotation of the walls. However, since the ties are anchored to the walls above the footings, they also reduce the moments on the stems from horizontal earth pressures. See Figure 9 for a typical cross-section of the ramp.

A reinforced concrete subbase is an extension of the strut to make a continuous slab between footings. While acting as a strut between footings on the opposite banks, it will, if properly reinforced, provide additional passive resistance against upheavel. An approximate method of evaluating this resistance will be discussed later.

PROCEDURE FOR COMPUTING THE STABILITY OF AN EMBANKMENT

As previously stated, the county's procedure differs somewhat from Housel's method (3 and 6). It has also been the practice to carry the investigation to not more than 50 ft from the top of the natural ground or to not more than 30 ft from the bottom of the slope. If the computed overload ratio, R, does not exceed 1.5 on any plane in the above depths, the embankment is considered safe.

In Figure 10 the values of S', S_1, S_2 and S_4 are the average shear values in the respective strata, while S_3 and S_5 are the smallest shear values in the immediately

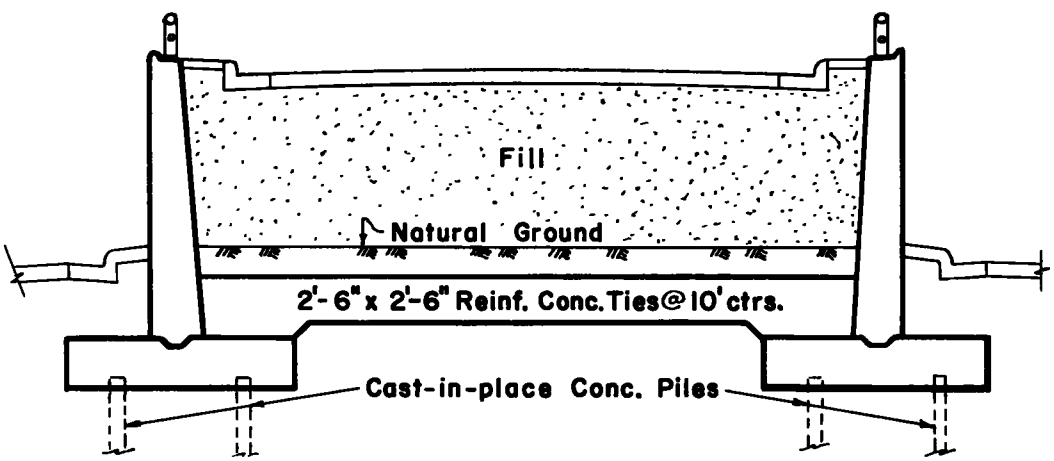

Figure 9. Showing fill supported by walls with ties.

adjacent planes. To simplify the computations, a value of R equal to one is used for determining h'.

Figure 10 is shown as applying either to an abutment, a retaining wall or to a sloping embankment. In the case of a sloping embankment, all terms containing d' are omitted from the equation, since d' is equal to zero. The shear resistance, S_5RL, at the bottom of the footing plane is utilized only if struts are used. The triangle of active pressure above the footing plane is neglected if struts are used. The vertical shear resistance, S_1Rh, is fully utilized in the case of abutments and walls with struts. However, for sloping embankments and for abutments or walls without struts, it may be utilized only when investigating the overload ratios on planes when d exceeds $\frac{h}{2}$.

PREVENTING UPHEAVAL BY MEANS OF A CONCRETE SUBBASE

As was mentioned before, the county considers an overload ratio of 1.5 to be satisfactory. This is equivalent to a factor of safety of 2.67. It is assumed that no displacement takes place as long as this overload ratio is not exceeded, but once exceeded, a progressive displacement of the soil will take place unless prevented by some positive

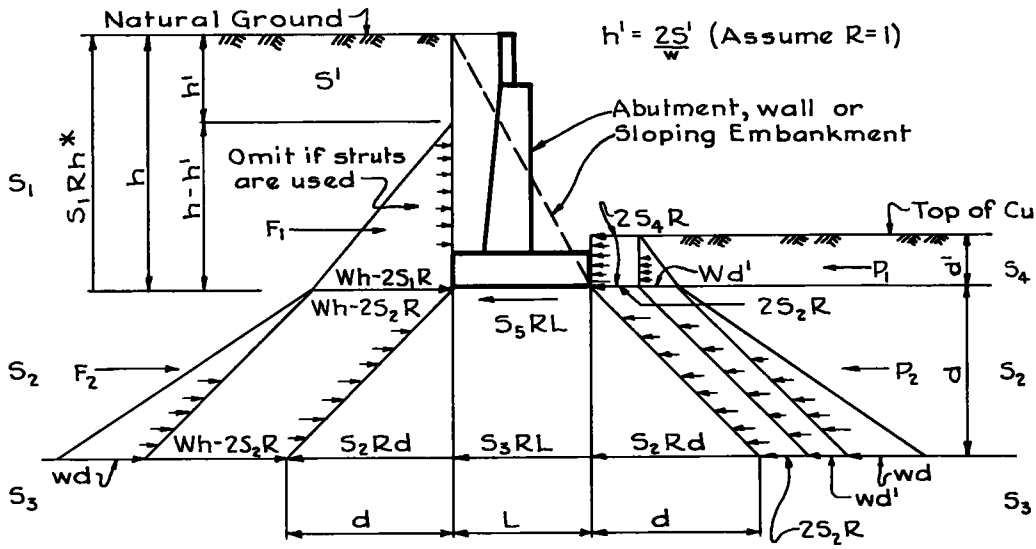

* To be included only if struts are used. If no struts are used, it may be included only when "d" is greater than "$\frac{h}{2}$"

$F_1 = (Wh - 2S_1R)\frac{(h-h')}{2}$

$F_2 = (Wh - 2S_2R)\,d + \frac{wd^2}{2}$

$P_1 = 2S_4Rd' + w\frac{(d')^2}{2}$

$P_2 = 2S_2Rd + wd'd + \frac{wd^2}{2}$

Bottom of Footing Plane (d=o) — No Struts used:-

$$F_1 = P_1 + S_5RL \qquad (7)$$

Planes below bottom of Footing — No Struts used:-

$$F_1 + F_2 = P_1 + P_2 + S_3RL + 2S_2Rd + S_1Rh\,* \qquad (8)$$

Planes below bottom of Footing — Struts used:-

$$F_2 = P_1 + P_2 + S_5RL + S_3RL + 2S_2Rd + S_1Rh \qquad (9)$$

Figure 10. Procedure for computing the stability of an embankment.

means. A reinforced concrete subbase, anchored securely at each end to the abutment, pier or wall footings, may be designed to contain the upward pressure imposed on it by an incipient displacement and, thus, prevent the displacement.

Inasmuch as an exact determination of the magnitude of the pressures exerted on the subbase is rather involved, an approximate method for evaluating these pressures with the use of Housel's equations has been developed. This method, although lacking in elegance, appears to be rational enough to yield results on which the subbase may be safely designed.

Briefly, the method is based on the assumption that no pressure is exerted on the subbase as long as the overload ratio does not exceed 1.5. When the overload ratio exceeds this figure, the upward pressure on the subbase is equal to the amount of overburden which would have to be placed on the bottom of the cut in order to reduce the overload ratio to 1.5. The weight of this overburden, p_s, when converted to passive pressure may be determined by considering it as a uniform passive pressure applied horizontally on depth d as shown in Figure 11. A value of 1.5 is then assigned to all terms containing the factor r and p_s is computed from Eq. 11. Note that the active pressure above the bottom of footing is neglected in the computations, since the subbase also acts as a strut.

SUMMARY

The procedure for determining safe foundation pressures, the stability of sloping embankments, the value of reinforced concrete struts and the effect of a reinforced concrete subbase in reducing foundation pressures and preventing upheaval has been

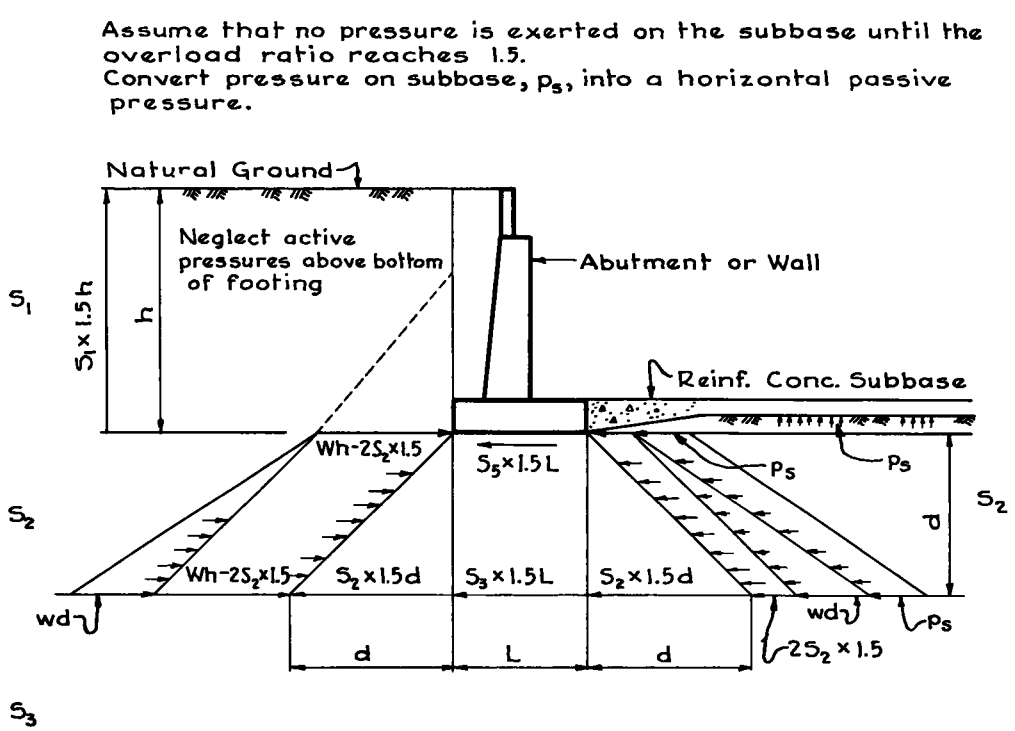

$$(wh-2S_2 \times 1.5)d+\frac{wd^2}{2} = 2S_2 \times 1.5d+\frac{wd^2}{2}+p_s d+S_5 \times 1.5L+S_3 \times 1.5L+2S_2 \times 1.5d+S_1 \times 1.5h \quad (10)$$

$$P_s = \frac{whd-(9S_2 d+1.5S_5 L+1.5S_3 L+1.5S_1 h)}{d} \quad (11)$$

Figure 11. Effect of concrete subbase in preventing upheaval.

described. The methods used for determining this procedure are rational and practical. It has time and again proven its value in comparing test boring data obtained in one location with test boring data obtained in other locations, and thus enabling the exercize of judgment with a certain degree of confidence.

Because of the simplicity of the procedure, little experience is necessary for performing the calculations. Where the computed overload ratios fall below the allowable, the designer may be allowed to proceed on his own; where the overload ratios exceed the allowable, the Chief Designer may then exercise his judgment in selecting the method best suited to insure a safe design.

REFERENCES

1. "Design Memorandum on Bearing Capacity of Spread Footings on Cohesive Soil." Department of Civil Engineering, University of Michigan, (June 1952) Published by Edward Brothers, Ann Arbor, Michigan.
2. "Notes on Stability of Embankments." Soil Mechanics Research Laboratory, Michigan State Highway Department, Ann Arbor, (June 1952).
3. "Design Memorandum on Embankment Stability—Lateral Distribution or Weight Transfer above the Loading Plane." Soil Mechanics Laboratory, University of Michigan, (April 1952).
4. "Embankment Stability as a Factor in Adequate Sheeting and Bracing." Journal, American Waterworks Association, Volume 50, No. 2, (February 1958)
5. Tschebotarioff, G.P., "Soil Mechanics, Foundations and Earth Structures." McGraw-Hill (1951).
6. Kerkhoff, G.O. and Housel, W.S., "Uplift Soil Pressure on Bridge Foundations as Revealed by Shear Tests." Proceedings, American Society for Testing Materials, Volume 47 (1947).

Appendix A

SHOWING TYPICAL LABORATORY TEST RESULTS OF SOIL SAMPLES

TEST RESULTS

	Laboratory Numbers 558-			314		317		321	
	A.A.S.H.O. Soils Classification	Sieve Size	Sieve Opening mm.	Cumulative Per cent Passing	Per cent Retained	Cumulative Per cent Passing	Per cent Retained	Cumulative Per cent Passing	Per cent Retained
Sieve Analysis	Gravel	¾ inch	19.10						
		½ inch	12.70						
		⅜ inch	9.52						
		No. 4	4.76						
		No. 10	2.00	100		100		100	
	Coarse Sand	No. 18	1.00	98		99		99	
		No. 20	0.84	97		98		99	
		No. 35	0.50	95		96		97	
		No. 40	0.42	94	6	95	5	97	3
	Fine Sand	No. 60	0.25	90		89		94	
		No. 140	0.105	80		65		83	
		No. 200	0.074	76	18	56	39	78	19
Hydrometer	Silt		0.030 0.003	70 29	47	49 21	35	67 24	54
	Clay		0.001		29		21		24
	Colloids								
Soil Constants	Liquid limit			34		17		19	
	Plasticity index			17		6		7	
	Specific gravity			2.73		2.67		2.68	
	Shrinkage limit, per cent by weight			14.1		10.6		11.4	
	Shrinkage ratio			1.92		2.04		2.04	
	Organic content, per cent by weight								
	Loss on ignition, per cent by weight								
	Shear stress, psf.			1,008		No Test		274	
	One-half compressive strength, psf.			2,688		1,152		1,008	
	Natural moisture, per cent by weight			18.9		12.2		17.6	
	Dry density, lb. per cu. ft.			110.4		122.9		114.2	

REMARKS: 558-314 Sample No. 1 Sample Depth 5' Elevation 604.0'
558-317 Sample No. 4 Sample Depth 20' Elevation 589.0'
558-321 Sample No. 8 Sample Depth 40' Elevation 569.0'

Appendix B

SHOWING TYPICAL SOIL ANALYSIS DATA SHEET

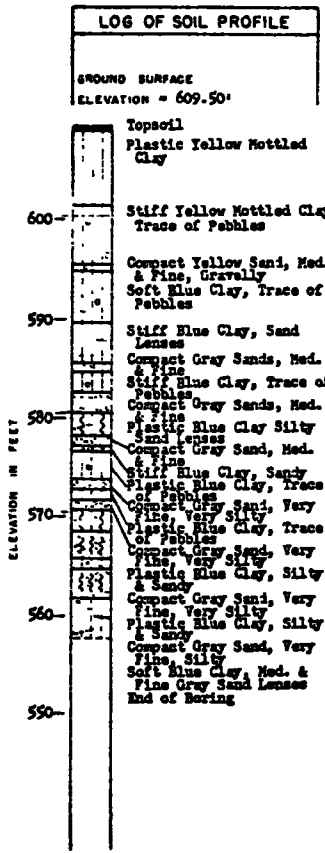

SOIL SAMPLE

	FIELD DATA				LABORATORY DATA		
SA. NO	ELEV.	PENETRATION NO OF BLOWS	PENETRATION DRIVE IN INCHES	CONSISTENCY	CONSISTENCY	MOISTURE PER CENT DRY WT.	DRY WT LB. PER CU. FT.
1	604.0	7	12	Plastic	Plastic	18.9	110.4
2	599.0	13	12	Stiff	Stiff	18.1	113.6
3	594.0	Sampler Pushed		Soft	Soft	24.9	101.4
4	589.0	"	"	Sand & Stiff Clay	Compact Sand & Firm Clay	12.2	122.9
5	584.0	13	12	Stiff	Stiff	13.6	126.0
6	579.0	Sampler Pushed		Plastic	Soft	11.5	127.9
7	574.0	"	"	Plastic	Plastic	19.0	109.8
8	569.0	"	"	Plastic	Plastic	17.6	114.2

PENETRATION NOTE NUMBER OF BLOWS REQUIRED TO DRIVE CORE SAMPLER 12 INCHES GIVEN, USING 140 POUND WEIGHT FALLING 30 INCHES

GENERAL NOTE FIELD CONSISTENCY DETERMINED BY INSPECTION OF SAMPLES AND SUBSTANTIATED BY RESISTANCE TO PIPE CASING AND JET ROD. BELOW DEPTH OF SAMPLING, CONSISTENCY DETERMINED BY SOIL RESISTANCE TO JET ROD.

BORING DATA

NUMBER 43

LOCATION Centerline of Southfield R.O.W., 370' north of centerline of Ford Rd. R.O.W.

DATE OF BORING February, 1955

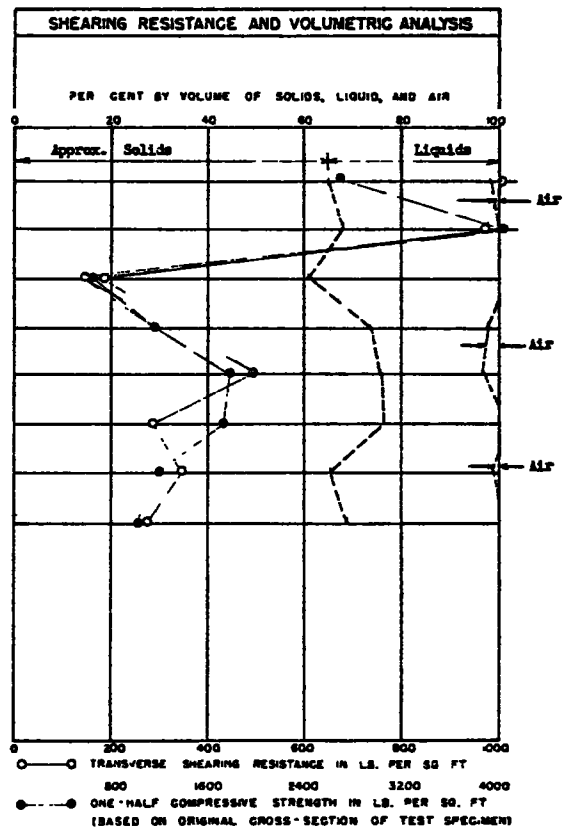

Appendix C

TYPICAL EXAMPLE

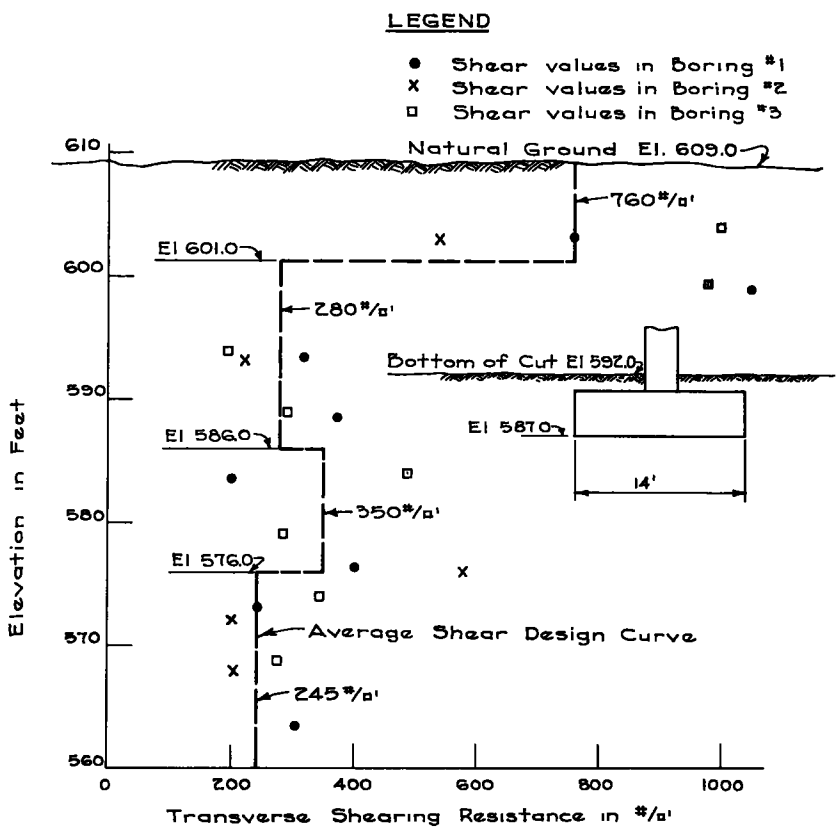

Figure 12. Typical shearing resistance curve.

ALLOWABLE FOUNDATION PRESSURES

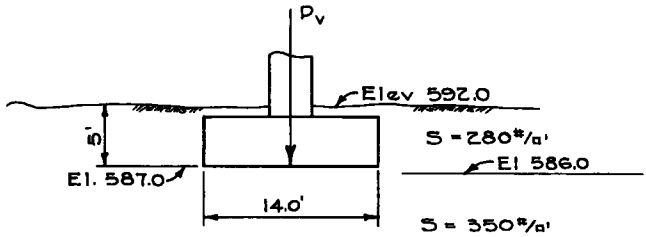

Refer to Equation 4

At Elev 587.0

$$\text{Allowable } \frac{P}{A} = 120 \times 5.0 + 6\left(\frac{1 \times 280 + 10 \times 350 + 3 \times 245}{14.0}\right) R + 2 \times 280 \times \frac{50}{14.0} \times R$$

$$= 600 + 1935R + 200R = 600 + 2135R$$

For $R = 1.0$ $\frac{P}{A} = 2735$ #/□'

For $R = 1.5$ $\frac{P}{A} = 3800$ #/□'

STABILITY OF EMBANKMENT AT ABUTMENT

Refer to Figures 10 & 11

To simplify computations, assume $h' = 8.0'$

Then $h - h_1 = 22.0 - 8.0 = 14.0'$, $d' = 5.0'$, $L = 14.0'$

$$F_1 = (120 \times 22.0 - 2 \times 280R) \times \frac{14.0}{2} = 18480 - 3920R$$

$$P_1 = 2 \times 280R \times 5.0' + 120 \times \frac{\overline{5.0}^2}{2} = 2800R + 1500$$

At Elev. 587.0 (Bottom of Footing Plane)

$F_1 = P_1 + S_5 R \times L$, or

$$18480 - 3920R = 2800R + 1500 + 280R \times 14.0$$

$$R = \frac{16980}{10640} = 1.60 > 1.5 \qquad \therefore \text{ use struts}$$

At Elev. 560.0 $\quad d = 27.0' \quad d' = 5'$

$$S_1 = (760 \times 8 + 280 \times 14) \times \frac{1}{22} = 454\ \#/\text{o}'$$

$$S_2 = (280 \times 1.0 + 350 \times 10 + 245 \times 16) \times \frac{1}{27} = 285\ \#/\text{o}'$$

$S_3 = 245\ \#/\text{o}' \quad S_3 = 280\ \#/\text{o}'$

$$F_2 = (120 \times 22.0 - 2 \times 285R) \times 27.0 + 120 \times \frac{\overline{27}^2}{2} = 115{,}020 - 15390R$$

$$P_2 = 2 \times 285R \times 27 + 120 \times 5 \times 27 + 120 \times \frac{\overline{27}^2}{2} = 15390R + 59940$$

Using Equation 9, we get

$$115{,}020 - 15390R = (2800R + 1500) + (15390R + 59940) + (280R \times 14.0) + (245R \times 14.0) + (2 \times 285R \times 27.0) + (454R \times 22.0)$$

$$R = \frac{53{,}580}{66{,}300} = 0.81 < 1.5$$

$\therefore$ struts are sufficient

Use of Backwater in Designing Bridge Waterways

JOSEPH N. BRADLEY, Hydraulic Research Engineer, Bureau of Public Roads

How is the length of a bridge over a stream determined? This question has many answers since bridge engineers, responsible for such decisions, have had to rely principally on personal observation and experience for the answers. In short, no generally accepted method for bridge waterway design has existed. A comparison of the small number of bridge failures to the total number of bridges throughout the country attest to the commendable job bridge designers have performed with the limited design tools available. Their record is most certainly impressive.

What proportion of existing bridges are under-designed and what proportion are over-designed from the standpoint of length and clearance? With many new bridges scheduled to be constructed under the accelerated highway program, the above question deserves serious thought from the standpoint of safety and economy. Under-designed bridges usually speak for themselves, given sufficient time. In the case of over-design, no reliable standards exist at the present time by which these structures can be judged impartially.

CURRENT RESEARCH

●AS A STEP aimed at placing bridge waterway design on a sounder footing, a cooperative research project was initiated in 1954 by the Bureau of Public Roads at Colorado State University. The project has been active since that time. To date the investigations have centered on the determination of backwater produced by bridges (1, 2), scour at bridge abutments, scour around piers, and methods for alleviating such scour. Two other research projects at the University of Iowa, sponsored by the Iowa State Highway Commission and the Bureau of Public Roads, have also contributed much needed information on scour at bridge piers (3) and scour at bridge abutments (4).

Bridge waterway problems are diversified and complex, which accounts to some extent for the limited headway made in understanding and resolving this phase of design in the past. Because of the many variables involved, hydraulic models were called upon to serve as the principal research tool in all the work mentioned above. It is possible with models to hold a certain number of variables constant while investigating the effect of others; then by systematically rotating the combination of variables in the test program, holding some constant and allowing others to vary, to isolate the part that certain principal variables play in the final result. In addition to aiding in a better understanding of the theory and mechanics involved, the models are indispensable since experimental coefficients are required, which can be obtained in no other way.

The waterway problem is much too extensive for even a condensed treatment here; the context of this paper will thus be confined principally to a discussion of the bridge backwater phase. It contains a brief account of the problem, the research results, the design information derived therefrom, and the application of bridge backwater to waterway design.

EXPERIMENTAL BACKWATER STUDIES

A comprehensive record of the experimental data, test procedures, and analysis of results on bridge backwater appears in a report issued by Colorado State University (1). For those interested only in the design application, a booklet titled "Computation of Backwater Caused by Bridges" is available (2). The latter contains design charts,

an explanation of design procedures, and five practical examples. Since the above information is available in printed form, it will be necessary to draw from it only sufficiently to understand the contents of this paper.

The manner in which flow is contracted in passing through a channel constricted by bridge embankments is illustrated in Figure 1. The flow bounded by each pair of

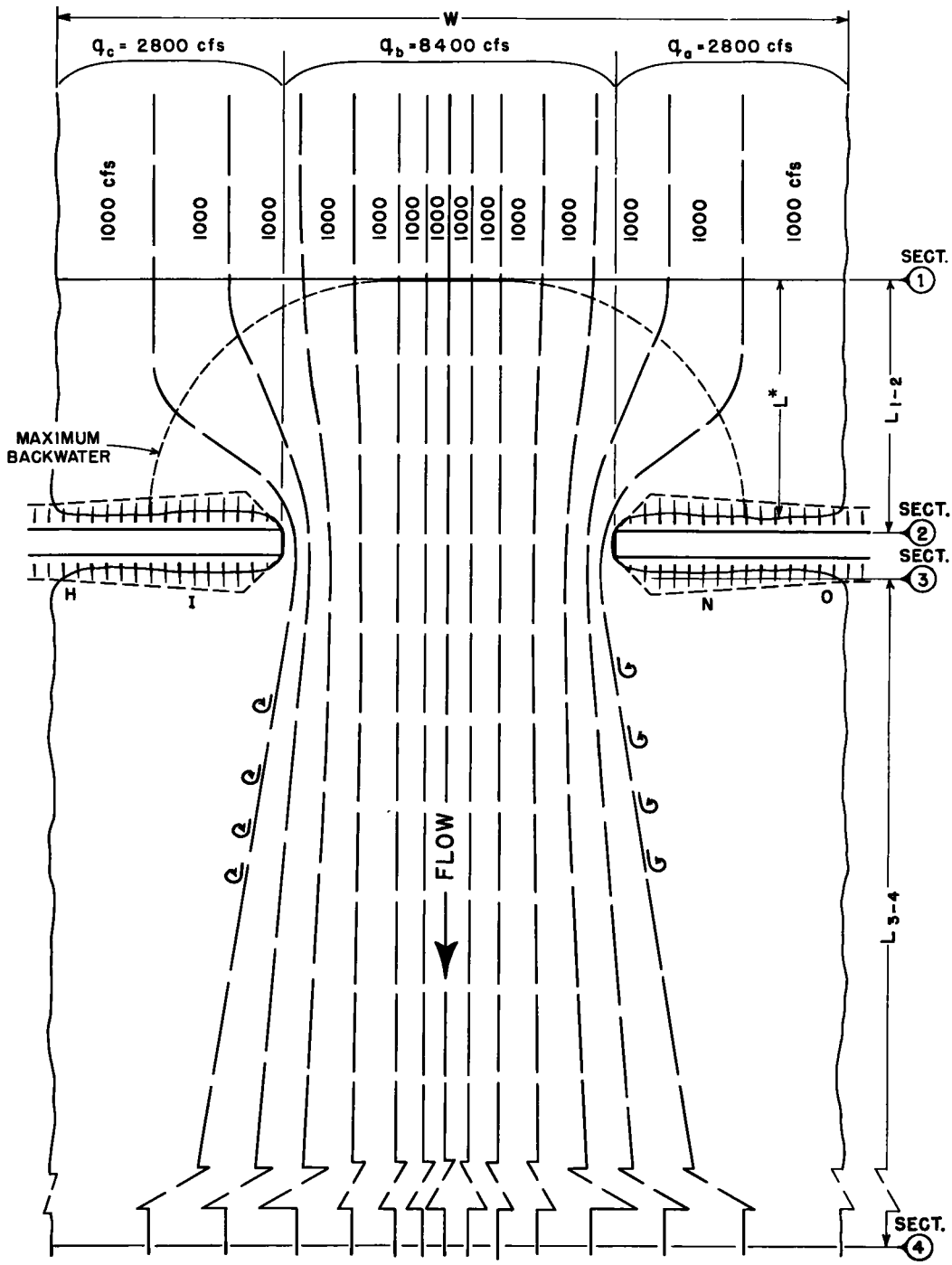

Figure 1. Flow lines– typical normal crossing.

streamlines represents 1,000 cfs. Note that channel constriction appears to produce very little alteration in the shape of the streamlines near the center of the channel, while a marked change is evident near the abutments where flow from the flood plains enter the constriction. As the discontinuity is greatest in this region, it is not difficult to visualize that areas adjacent to the abutments are most vulnerable to attack by scour during floods. Upon leaving the constriction the flow, which is now concentrated in the central portion of the channel, expands at an angle of 5 to 7 deg on a side until normal conditions are again re-established downstream, which may involve a considerable reach of the river.

Constricting the flow of a stream, of course, produces a loss of energy, the greater portion of this occurring in the re-expansion process downstream from the constriction. This loss of energy is reflected in a rise in both the water surface and the energy gradient upstream from the bridge, as demonstrated by a profile of this same crossing taken along the centerline of the stream (Fig. 2). The normal stage or water surface existing for a given flood, prior to construction of the bridge, is represented by a straight dash line labeled "normal stage." The water surface for the same flood, with constricting bridge embankments, is denoted by the solid line labeled "water surface on centerline." The water surface is now above normal stage at section 1, passes through normal stage in the vicinity of section 2, reaches minimum depth near section 3, and returns to normal stage a considerable distance downstream at section 4 where the original regime of the river has not been disturbed. The energy at section 4 is thus the same with or without the bridge. The energy at section 1, on the other hand, must increase to provide head to overcome the loss introduced by the constriction. The major portion of this energy is reflected in the backwater, which is the rise in water surface at section 1 (denoted by the symbol h_1^*) on Figure 2.

Note that the drop in water surface measured across the roadway embankment is not the backwater as is so often presupposed to be the case. The water surface as indicated in the central part of the channel at section 3, which is essentially the water surface along the downstream side of the embankments, is invariably lower than normal stage, so the difference in level across the embankments Δh, is always larger than the backwater h_1^*.

It was found that the backwater to be expected at a bridge for a given discharge is dependent on a number of factors, the more prominent of which are:

1. The degree of constriction of the channel;
2. The number, size, shape and orientation of piers in the constriction;
3. Eccentricity of the bridge with the low-water channel or flood plain;
4. The angle or skew of the bridge with the stream;

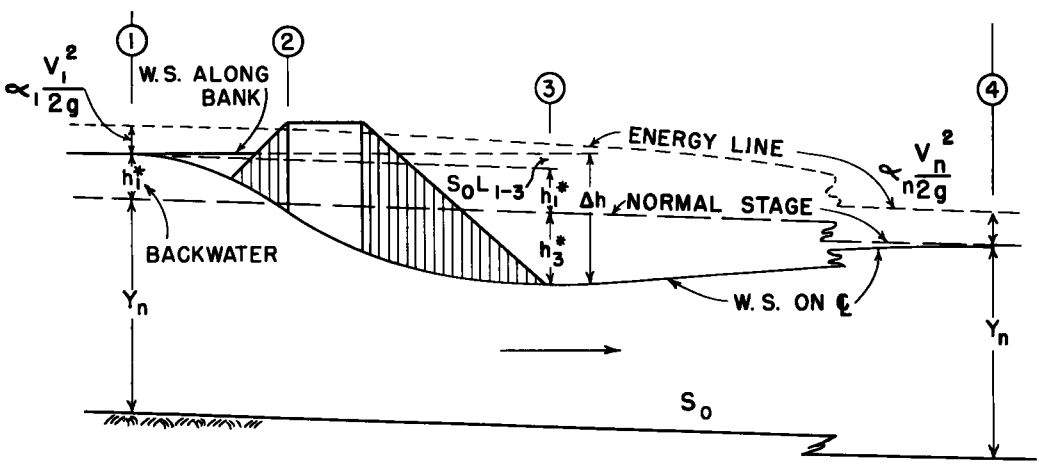

Figure 2. Profile on centerline of stream.

5. The type and slope of bridge abutments (important only for the shorter bridges);
6. The amount of scour experienced in the constriction; and
7. Whether the crossing consists of a single bridge or two or more parallel bridges on a divided highway.

Contrary to expectations, the width of the abutment or fill had no significant effect on the backwater.

It should be quite evident at this point that a backwater study can have but limited value without a reliable stage-discharge curve for the bridge site. Also a knowledge of the flood frequency and magnitude are required to intelligently determine the design discharge for a bridge and the necessary clearance (2).

In spite of the number of principal variables enumerated above, the backwater expression and the procedure for computing backwater, as developed from the experimental studies, are very much down to earth. A man with some training in hydraulics should have no particular difficulty in mastering this phase of waterway design.

An abbreviated form of the expression for computing bridge backwater is given here:

$$h_1^* = K^* \frac{V_{n2}^2}{2g} + (\ldots . \qquad (1)$$

in which K^* consists of a combination of experimental backwater coefficients multiplied by a velocity head. The coefficient K^* varies with the seven geometric factors mentioned above while the velocity is computed with respect to the average water cross-section under the bridge relative to normal stage. The remainder of the expression, which has been omitted for the sake of simplicity, consists of the change in kinetic energy between sections 1 and 4 (Fig. 2) produced by alteration of the stream by the bridge. In the majority of cases, this factor represents a small portion of the total backwater, but this is not always the case. Guides are provided whereby the importance of this factor can be readily recognized and omitted from the computations where permissible (2).

To give a general idea of the manner in which Eq. 1 operates, the backwater coefficient for a symmetrical normal stream crossing, having wing-wall abutments, but without piers or other complicating features, would be obtained directly from Figure 3. The coefficient K_b (known as the base curve value) varies with the degree of constriction of the channel M, and the type of abutment. The parameter M is the ratio of the quantity of flow which can pass through the constriction unimpeded to the total discharge of the river. For M = 1, there is no constriction of the stream, and the coefficient is zero. As the degree of constriction increases, M becomes smaller and the coefficient K_b increases in value. To illustrate, the contraction ratio for the condition shown on Figure 1 would be

$$M = \frac{8,400}{14,000} = 0.60.$$

Should piers, eccentricity, or skew be involved, the effect of these factors are accounted for by adding incremental coefficients to the value obtained from the base curve (Fig. 3), thus the over-all coefficient

$$K^* = K_{b\,(\text{base})} + \Delta K_{p\,(\text{piers})} + \Delta K_{e\,(\text{eccentricity})} + \Delta K_{s\,(\text{skew})}.$$

The value of the incremental coefficients for the effect of piers, eccentricity, skew, etc., are obtained from charts prepared for that purpose. For a detailed description of the procedure and the charts see (2). A general idea as to the magnitude of the individual coefficients can be gleaned from an inspection of the first eight columns of Table 2.

RELIABILITY OF MODEL RESULTS

A tremendous difference can exist between a model and a field structure insofar as bridges are concerned. Because of the model limitations, it was imperative that some

means be devised to verify or disprove the validity of the experimental information. This was accomplished by applying the computational procedure, developed from the model studies, to existing bridges on which the Geological Survey had furnished field measurements obtained during floods. Reliable measurements on bridge backwater are extremely difficult to make in the field, but the drop in water surface across embankments Δh, is readily measurable (Fig. 2). Model results showed a very definite relation to exist between the drop in water surface across the embankments Δh, and the backwater h_i^*, so model computations and prototype measurements are compared on the basis of Δh. A comparison of measured and computed values for several bridges varying from 20 to 340 ft in length is presented in Table 1. Columns 2 through 6 give the bridge length, flood discharge, average velocity under the bridge, the contraction ratio, and the computed backwater, respectively. The computed and measured values of Δh are shown in Columns 7 and 8, respectively, while the percentage difference in each case is shown in Column 9. The differences range from -8.5 to +13 percent, the deviation being positive in six instances and negative for six; the average deviation is +2 percent. The deviation in the majority of the cases is well within the error of field measurement. The experimental error of the model experiments is estimated as comparable to the average deviation. Thus, the comparison affords satisfactory verification to date. Field measurements on longer bridges are needed but these have not been forthcoming as yet.

APPLICATION OF BACKWATER TO DESIGN

Now that it is possible to compute bridge backwater with a fair degree of confidence, to what practical purpose can this information be used in design?

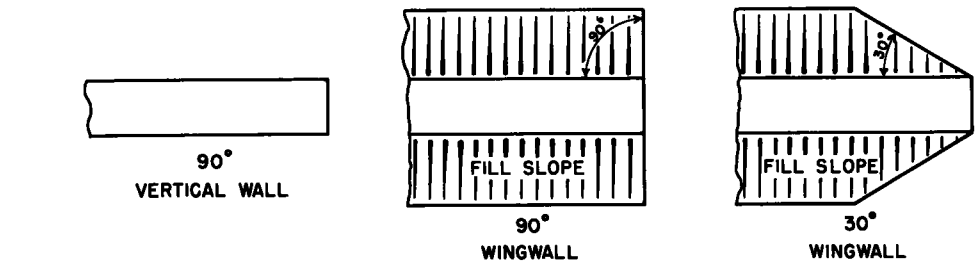

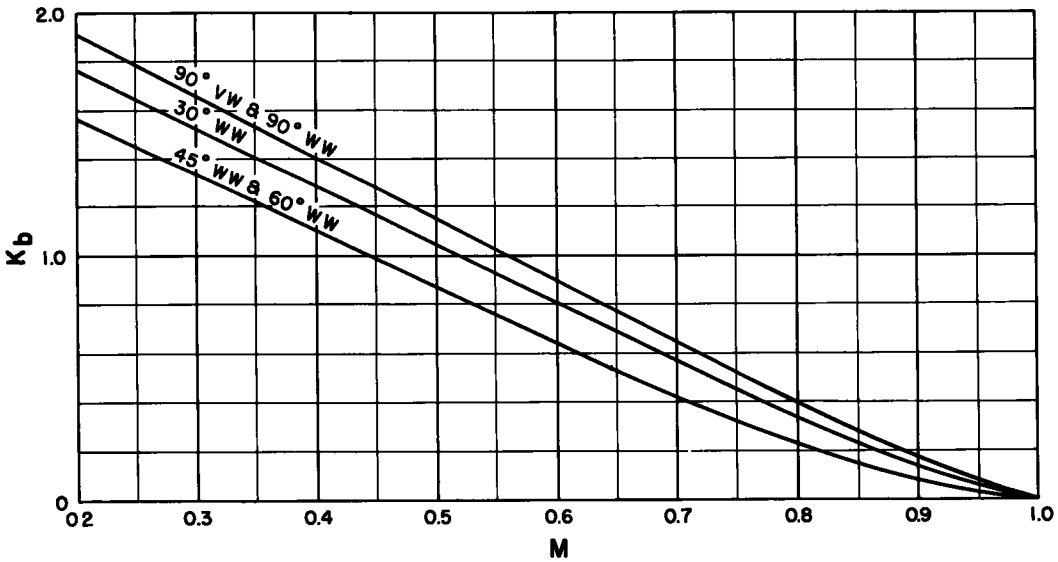

Figure 3. Backwater coefficient K_b for wing-wall abutments (base curve).

1. It makes it possible to proportion bridges to operate during flood flows at a limited specified backwater.
2. It offers a fair means of settling claims involved in backwater damage suits instigated by upstream property owners.
3. It makes it possible to understand and compute the hydraulics involved in cases where approach roadways can be overtopped during infrequent floods.
4. It provides a large share of the necessary hydraulic information for a proposed economic analysis to determine the optimum design discharge and the most economical length of bridge.

In the case of item 2, no reliable method has existed for computing backwater produced by bridges. Backwater based on field measurements made by the novice were also justifiably questionable. Thus, damage suits of this nature have resulted in indefinite delays or settlements have been made on considerations other than fact.

TABLE 1

COMPARISON OF COMPUTED Δh VALUES WITH FIELD MEASUREMENTS

Bridge No.	Length (ft)	Discharge (cfs)	Velocity Under Bridge (fps)	Contraction Ratio, M	Computed Backwater, h_i^* (ft)	Drop Across Embankments, Δh (ft)		% Diff. Δh
						Computed	Measured	
(1)	(2)	(3)	(4)	(5)	(6)	(7)	(8)	(9)
1	20	1,370	9.1	0.57	1.07	1.90	1.99	- 4.5
2	84	4,340	6.8	0.85	0.21	0.65	0.70	- 7.2
3	220	27,500	7.5	0.90	0.28	0.76	0.83	- 8.5
4	83	5,240	8.6	0.60	1.03	1.81	1.60	+13
5	72	12,000	10.2	0.83	0.57	1.94	1.95	- 0.5
6	58	3,400	7.1	0.82	0.18	0.61	0.55	+10.9
7a	44	2,620	7.8	0.66	0.63	1.23	1.15	+ 6.9
7b	44	1,450	5.4	0.70	0.30	0.66	0.69	- 4.4
8	112	9,640	9.0	0.33	1.80	2.53	2.24	+12.9
9	340	70,000	10.5	0.90	0.77	2.57	2.70	- 5.0
10	68	7,230	Deck girder immersed			1.53	1.48	+ 3.4
11	120	2,600	Deck girder immersed			1.70	1.61	+ 5.6

TABLE 2

COMPARISON OF LENGTH AND COST OF SKEW BRIDGES WITH NORMAL CROSSINGS

Bridge	Skew Angle (deg)	Contraction Ratio, M	Backwater Coefficients					$\frac{V_{n2}^2}{2g}$ (ft)	Back-water h_i^* (ft)	Projected Bridge Length	$\frac{L_s \cos\phi}{L_n}$	$\frac{L_s}{L_n}$	$\frac{C_s}{C_n}$
			Base K_b	Piers ΔK_p	Ecc. ΔK_e	Skew ΔK_s	Total K^*						
(1)	(2)	(3)	(4)	(5)	(6)	(7)	(8)	(9)	(10)	(11)	(12)	(13)	(14)
A	0	0.90	0.12	0.09	0.07	0	0.28	1.70	0.76	340	1.0	1.0	1.0
	30	0.90	0 12	0.09	0.07	-0.02	0.26	1.84	0.76	335	0.98	1.14	1.22
	45	0.90	0.12	0.09	0.07	-0.03	0.25	1.89	0.76	330	0.97	1.37	1.54
B	0	0.67	0.48	0.04	0.15	0	0.67	1.22	0.89	2,000	1.0	1.0	1.0
	30	0.665	0.50	0.05	0.15	-0.05	0.65	1.26	0.89	1,925	0.96	1.12	1.18
	45	0.66	0.51	0.06	0.15	-0.08	0.64	1.30	0.89	1,900	0.95	1.34	1.50
C	0	0.64	0.55	0.19		0	0.74	2.66	2.18	87	1.0	1.0	1.0
	30	0.635	0.55	0.19		-0.06	0.68	2.84	2.18	84	0.96	1.12	1.22
	45	0.63	0.56	0.19		-0.09	0.66	2.90	2.18	80	0.92	1.30	1.50
D	0	0.62	0.60	0.03	0.16	0	0.79	1.65	1.41	1,100	1.0	1.0	1.0
	30	0.62	0.60	0.04	0.16	-0.07	0.73	1.79	1.41	1,025	0.93	1.08	1.15
	45	0.61	0.62	0.05	0.16	-0.11	0.72	1.82	1.41	1,010	0.92	1.30	1.45
E	0	0.53	0.92	0.08		0	1.00	1.11	1.19	630	1.0	1.0	1.0
	30	0.52	0.96	0.09		-0.19	0.86	1.27	1.19	600	0.96	1.10	1.16
	45	0.51	1.00	0.12		-0.37	0.75	1.46	1.19	575	0.91	1.29	1.42
F	0	0.46	1.13	0.15	0.04	0	1.32	0.67	0.93	1,075	1.0	1.0	1.0
	30	0.43	1.16	0 16	0.04	-0.26	1.10	0.82	0.93	990	0.92	1.06	1.08
	45	0.42	1.21	0.19	0.04	-0.49	0.95	0.90	0.93	925	0.86	1.22	1.31
G	0	0.46	1.06	0.06		0	1.12	0.90	1.05	75	1.0	1.0	1.0
	30	0.44	1.08	0.08		-0.25	0.91	1.09	1.05	69	0.92	1.06	1.12
	45	0.42	1.14	0.09		-0.48	0.75	1.35	1.05	64	0.86	1.20	1.34

The attainment of a sound method of procedure for determination of the optimum design discharge and the most economical length of bridge (item 4) constitutes the ultimate goal in the present research program.

APPLICATION OF BACKWATER TO LENGTH OF SKEW CROSSING

A practical application to which the bridge backwater information may be used to advantage can be demonstrated in comparing the length and cost of skew bridges with the length and cost of equivalent normal crossings, on the basis of backwater. The procedure consists of first choosing an existing normal stream crossing and computing the backwater which the bridge will produce for a given flood condition; then, holding stream conditions the same, computing the length of equivalent skew bridges which have the same effective waterway, or in other words, produce the same backwater. This course of computation was followed through for seven existing crossings and the results are given in Table 2. The normal length of these bridges varied from 75 to 2,000 ft and included both wing-wall and spill-through type abutments. The faces of the abutments under the bridge were oriented parallel with the flow, as shown in the sketch in Figure 4. This is the most efficient skew abutment shape. Types with faces at an angle to the flow require more length of bridge.

The ordinate in Figure 4 is the ratio of skew length to normal length of crossing in percent, which is plotted with respect to the skew angle as abscissa and the contraction ratio M as a third variable. In the case of M = 1.0 (no constriction of the stream) the skew length is simply $L_n/\cos\phi$. With constriction of the stream, the ratio L_s/L_n reduces with the value of M.

What is occurring can be better understood by referring to Figure 5. On this chart the ordinate is the ratio of the projected skew length to the normal length (see sketch) while the other two parameters remained unchanged. For M = 1.0, no constriction, the ordinate is 1.0 for all angles of skew. With constriction of the stream, the projected skew length, required to produce the same amount of backwater, is shorted than the normal bridge length. This characteristic is to be expected but the actual relationship has been until now entirely a matter of conjecture. The curves in Figures 4 and 5 offer actual values which may prove useful in design.

A plot relating the cost ratio in percent of skew to normal crossings for the same

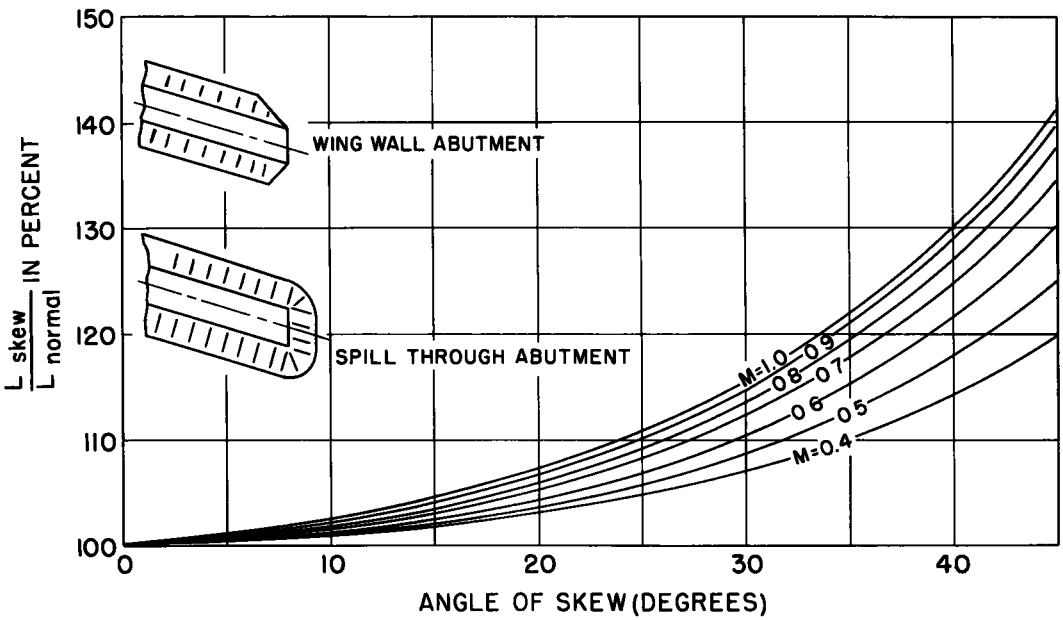

Figure 4. Length ratio of skew to normal crossing for equivalent backwater.

bridges, is presented in Figure 6. Again the parameters are the same except for the ordinate. The consistency is not of the same order found in the length curves since it was necessary to adjust span lengths and provide additional piers for the skew bridges.

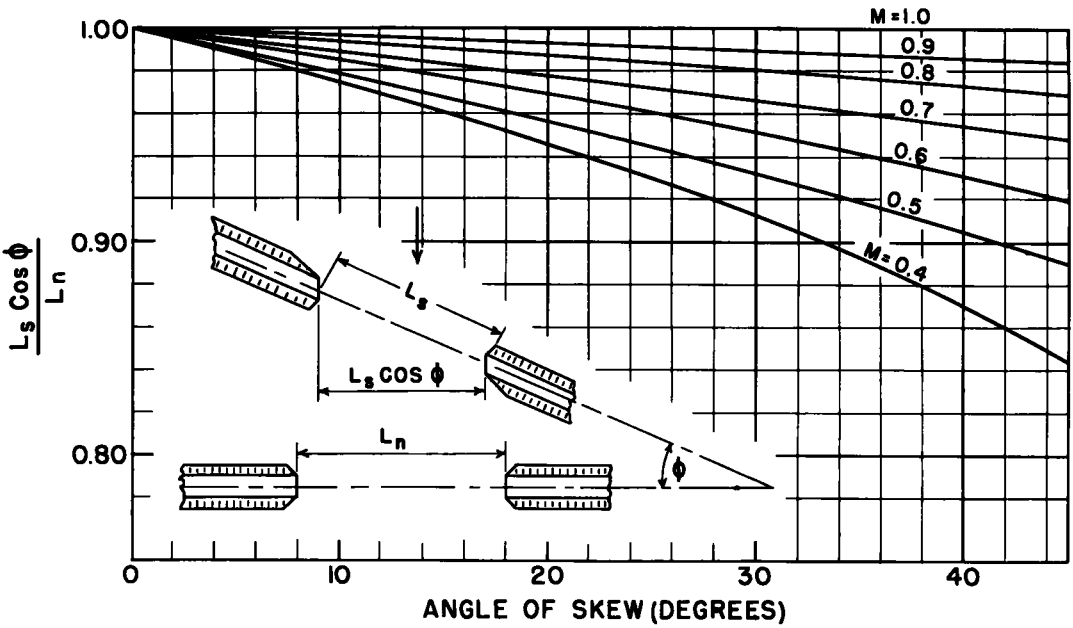

Figure 5. Ratio of projected skew length to normal bridge length for equivalent backwater.

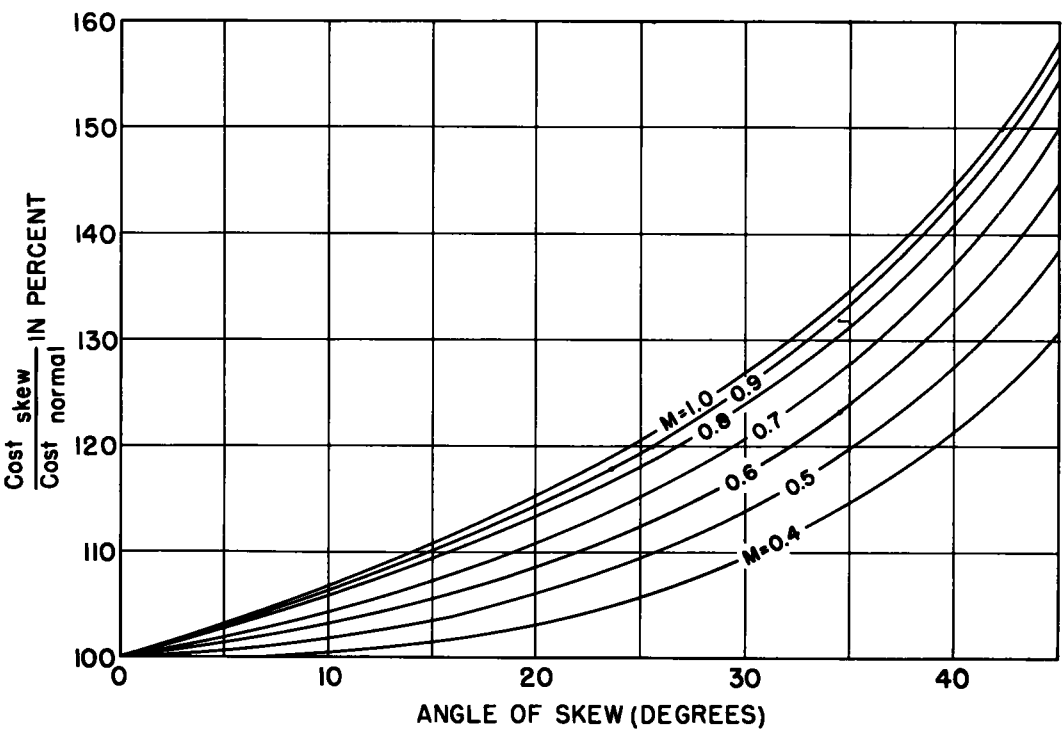

Figure 6. Cost ratio of skew to normal crossing for equivalent backwater.

Also the higher unit cost of skew construction and the increased length of embankments were considered. The cost was affected to a greater extent than the length by these factors. The criterion for determining span lengths for the skew crossing consisted of balancing the cost of superstructure against the cost of piers on an equal basis. The increase in cost of superstructure per square foot was assumed at 5 percent for the 30-deg skew and 10 percent for the 45-deg skew.

For the purpose of comparison, the length varies from 107 to 115 percent or normal for the 30-deg skew while the cost varies from 110 to 127 percent for the same range of contraction ratios. In the case of the 45-deg skew, the length varies from 120 to 141 percent of normal compared with a cost variation of 130 to 158 percent for the same values of M.

As can be observed, skew angles up to approximately 20 deg produce only a small increase in both length and cost over the normal crossing. As the angle increases above this value, the curves steepen and the length and cost rise rapidly. In this same connection, it was observed in the course of the model studies that the hydraulic flow problems encountered with skew crossings, for angles up to approximately 20 deg, were little different than for normal crossings. As the angle exceeds this value, the flow and scour problems increase in complexity.

LIMITATION OF BACKWATER AND ACCOMMODATION OF SUPER FLOODS

Another application in which the backwater design information can be used to advantage is for the case where approach roadways can be depressed to protect the bridge during floods of extreme proportions. Although it is seldom economically feasible to construct a bridge sufficiently long to accommodate the super type of flood, it is possible in many cases to design for a 35- or 50-yr flood but make provision to pass flows of much greater magnitude with little or no damage to the bridge proper and, at the same time, keep the backwater within specified limits. The most effective way to present this case is by an actual illustration.

The stream at a proposed crossing has a low-water channel about 700 ft across while in flood the stream may be a mile wide. Records show that within the past 50 yr, two floods approximating frequencies of 100 yr have occurred on this stream, the last one destroying a bridge at the site. This is on a state route carrying a fairly heavy volume of traffic which will increase with time. A considerable amount of residential and business development, occupying portions of the flood plain, have sprung up within the last decade. It is therefore important from the traffic viewpoint that the bridge proper not fail or be out of service for an extended length of time during its expected life; and from the standpoint of life and property damage, it is desirable that the bridge backwater be limited to a definite figure for all flows. For the purpose of illustration, the bridge will be reconstructed to satisfy the above requirements and limit the backwater to 0.5 ft for any discharge likely to occur during the life of the bridge.

There is a choice here of designing a long bridge to take the full flow of the river for, say, a 100-yr frequency flood, keeping the embankments above high water at all times, or the alternative of choosing a shorter bridge and using the ½ to ¾ mile of roadway transversing the flood plain as a spillway during high water. In either case the superstructure will be located above extreme high water at all times.

The case where the embankments are located above high water and the bridge is required to accommodate the entire flow will be first investigated. The chart on Figure 7 shows the backwater relative to length of bridge and discharge for this type of operation. In addition, scales have been superimposed showing flow recurrence interval at top and cost of bridge at right. Were there no restriction on backwater, a bridge 1,500 ft long, producing 1.5 ft of backwater, might be a reasonable choice. But with backwater limited to 0.5 ft, it can be observed that the bridge should be 2,250 ft long for a 50-yr flood or 2,600 ft long for a 100-yr flood. From the scale on the right, the cost involved in reducing the backwater from 1.5 to 0.5 ft approximates $400,000 in this case or about 40 percent of the initial cost. This comparison demonstrates how limitation of backwater can increase the initial cost.

How can limitation of backwater be accomplished less painfully? The alternative,

the depressed roadway, will now be examined. Figure 8 demonstrates a very extreme case; the bridge has been shortened to 800 ft with approximately 3,500 ft of depressed roadway. The lower broken line labeled "normal stage" represents the stage-discharge

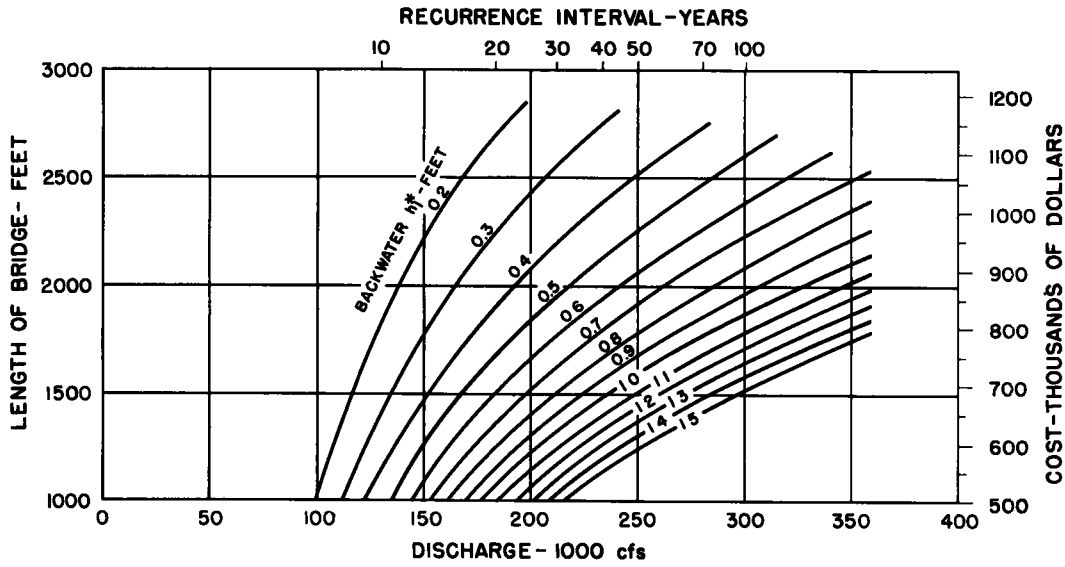

Figure 7. Variation of backwater with length of bridge and discharge.

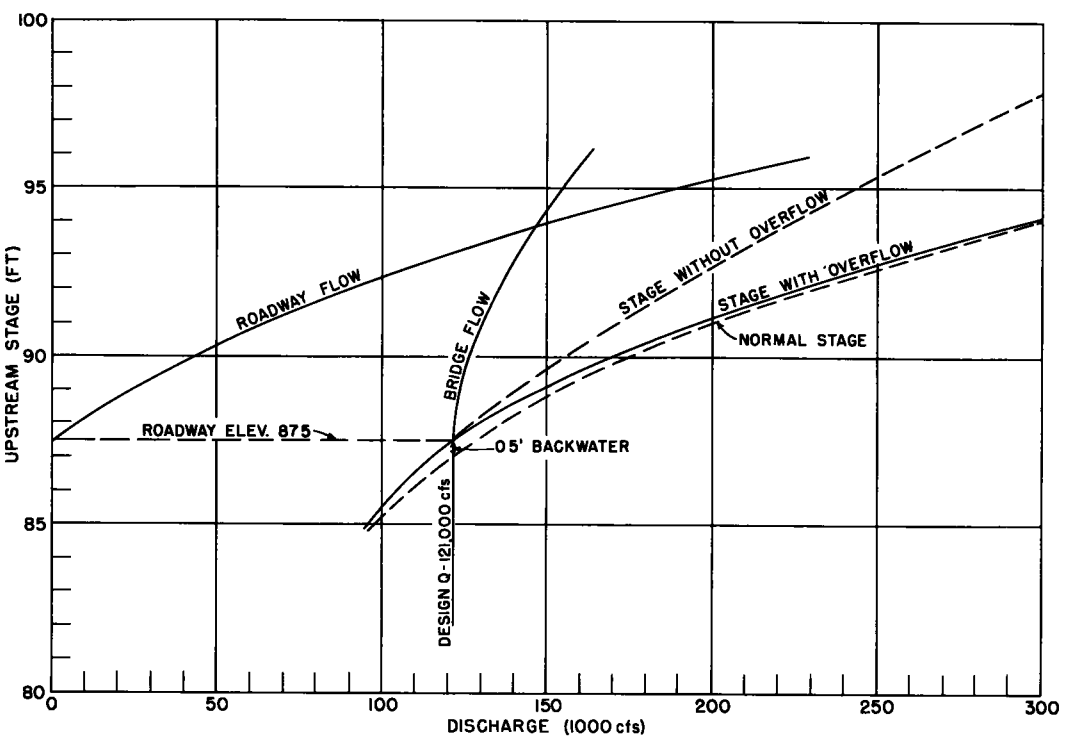

Figure 8. Operation with depressed roadway and 800-ft bridge-backwater limited to 0.5 ft.

curve for the river prior to construction of the bridge. The upper dotted line labeled "stage without overflow" represents the stage discharge to be expected upstream from the 800-ft bridge without overflow. The difference between the two curves represents the backwater. Note that for a discharge of 250,000 cfs (50-yr flood) the backwater is 2.5 ft and for 300,000 cfs (100-yr frequency flood) the backwater approximates 4 ft. The limitation of 0.5 ft for backwater is reached at a discharge of 121,000 cfs. If the approach embankment is placed at elevation 87.5 so water will spill over the roadway for flows greater than 121,000 cfs, the backwater will decrease with further increase in discharge, falling off to about 0.1 ft for a discharge of 300,000 cfs. The backwater with overflow is represented by the difference between the lines labeled "normal stage" and "stage with overflow." The flow under the bridge and flow over the roadway are indicated by the lines so labeled. Note that as the roadway overflows, the discharge under the bridge now increases slowly with upstream stage, while flow over the roadway increases rapidly with stage. At stage 93.8, the roadway is carrying as much flow as the bridge.

As the roadway is elevated, the backwater and flow characteristics remain similar to those shown on Figure 8 but the bridge length must be increased if the backwater is to be limited to 0.5 ft for upstream stage level with the new roadway. Figure 9 demon-

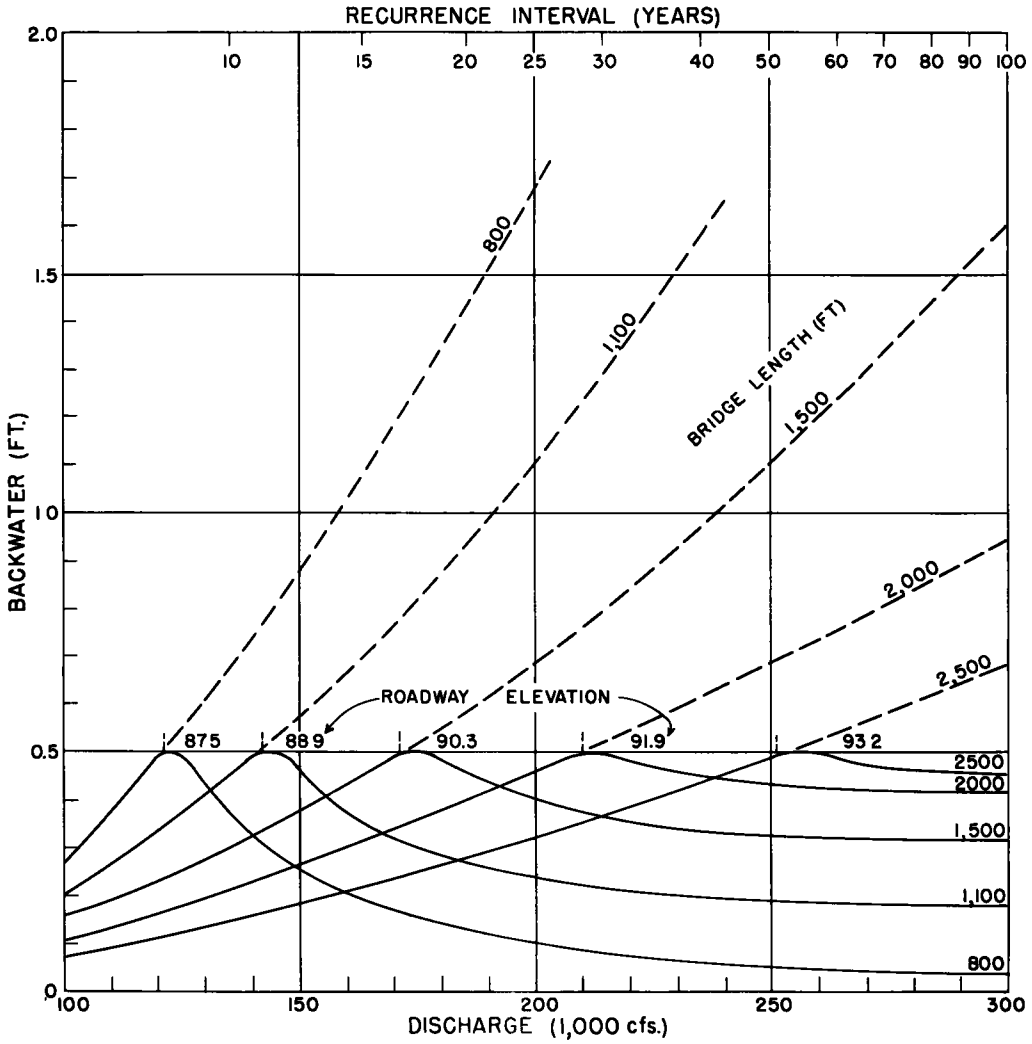

Figure 9. Operation with depressed roadway for several lengths of bridge—backwater limited to 0.5 ft.

strates how the backwater varies with roadway elevation and length of bridge. The dash lines denote the backwater which could be expected for several bridge lengths were flow over the road not permitted. The solid lines demonstrate how flow over the roadway limits the backwater to a maximum of 0.5 ft regardless of the discharge.

The depressed roadway not only serves to hold the backwater within limits but offers a means of accommodating the superflood without undue overloading of the bridge proper. It is true that the higher the approaches and the shorter the length of embankment, the longer the bridge must be for a given amount of backwater; nevertheless, it is usually possible to set embankments for the 50-yr flood stage and still retain the safety valve feature.

CONCLUSIONS

The above illustrations represent only a few ways in which the recently acquired bridge backwater information can be applied to waterway design. Gaps still remain which eventually will be plugged as reliable field data become available.

An equally important, or second phase, involving the hydraulics of waterways is the reasonable prediction of maximum scour depths at abutments and piers. Some information is already available for streams with alluvial beds (3, 4) and additional information will be forthcoming.

It will be found that the hydraulic analysis offers many variations of supposedly equally good waterway proportions. How, then, is an unbiased choice to be made? It is believed that this can best be accomplished through development of a generally acceptable type of economic analysis, which at the present does not exist, taking into account all tangible and certain intangible costs which may be incurred by the highway agencies in building and maintaining a bridge and by the highway users who travel over the bridge. In this way, a fair monetary value can be assigned to each design, whereby comparisons can be made on a basis familiar to all parties concerned. Determination of the fundamental concepts on which such an economic analysis should be founded constitutes the third major phase of this research program, which is now under consideration.

REFERENCES

1. Liu, H.K., Bradley, J.N., and Plate, E.J., "Backwater Effects of Piers and Abutments." CER 57 HKL10, Colorado State University, (October 1957).
2. "Computation of Backwater Caused by Bridges." Preliminary Draft, Bureau of Public Roads, (October 1958).
3. Laursen, E.M., and Toch, A., "Scour Around Bridge Piers and Abutments." Bull. No. 4, Iowa HRB, (May 1956).
4. Laursen, E.M., "Scour at Bridge Crossings." Bull. No. 8, Iowa HRB, (unpublished).

Laboratory Observations of Scour at Bridge Abutments

H.K. LIU, Associate Civil Engineer, and
M.M. SKINNER, Assistant Research Engineer, Civil Engineering Department,
Colorado State University

The importance of being able to accurately predict the magnitude of scour at bridge abutments and piers cannot be overemphasized. Bridge design demands a knowledge of the scour phenomenon in order to insure a safe, economic structure. In the past, bridge designers have been forced to rely upon personal experience, judgment, and similar designs in determining the depth of the bridge foundations. Consequently, due to the limited amount of information on scour available to the designer, bridges are destroyed due to foundation failures each year during peak runoff periods.

Both laboratory and field studies are needed to increase the knowledge for determining the scour depth. This report is based upon a laboratory investigation of scour at abutments, currently being undertaken in the Hydraulics Laboratory of the Colorado State University. The project is sponsored by the Bureau of Public Roads.

CLASSIFICATION OF THE SCOUR PROBLEM

● THE PROBLEM of scour at bridge abutments is similar to the problem at any obstruction in an alluvial channel; for example, embankments, jetties, and piers. In any case the flow in the process of moving past the obstruction must undergo a certain change in direction with consequent increasing turbulence and eddy action. This action becomes evident in the erosion or scouring at the abutments and piers.

The depth of the scouring action, according to which the foundations must be designed, depends upon the flow conditions, shape of the obstruction, alignment and spacing of abutments or piers, bed material and sediment supply. Flow conditions involve the interrelated variables of slope, depth of flow, bed roughness, velocity, and discharge. The shape and alignment of the abutment or pier is obviously also important in determining the eddies that are produced in the flow—a more streamlined shape producing less disturbance and a reduction in scour. The spacing of abutments must also be considered as shown in Figures 1a and 1b. Closely spaced abutments may allow the localized scour areas at each abutment to interfere and cause a general lowering of the bed in the constriction. The properties of the bed material, such as size, gradation, and cohesiveness must be taken into consideration. As indicated in Figure 2, the presence of appreciable bed-load movement from upstream eventually produces an equilibrium scour depth. The scour rate in the absence of bed-load movement shown in Figure 2, appears to continue indefinitely.

The scour problem at best is quite complicated and requires investigation of many variables in order to understand the process and develop a workable criterion for the extent of the action.

PREVIOUS INVESTIGATIONS

Field Studies

Although numerous bridges have failed because of scour, information on such failures is very limited. The depth of scour observed after a flood usually does not re resent the maximum scour since the scour hole is often partially refilled during the time of the receding flood. Unless some type of continual depth sounding device is

used to indicate the complete history of the scour depth, the maximum scour depth often remains unknown. The Indian engineers have determined maximum scour depths by noticing the depth to which rip rap has been buried beneath the river bed. Although such depths of scour may have been affected by the presence of the rip rap, it does give some indication of the maximum depth of scour that occurred during flood stage. Some records of scour depths at certain bridges are available but the data are quite limited.

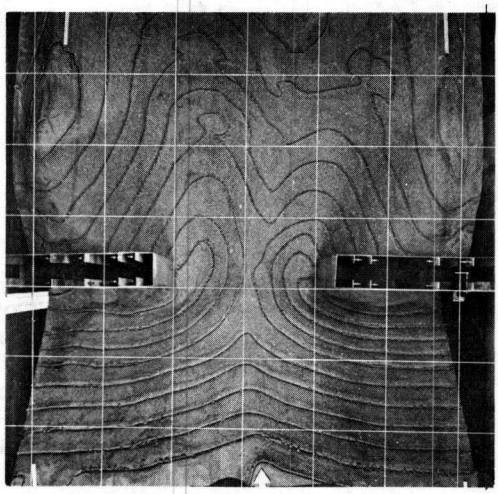

a. Interference of local scour

b. No interference of local scour

Figure 1. Contour view of local scour.

Laboratory Studies

Scour data from laboratory investigations are also quite scarce. Those studies that have been made are generally confined to conditions of no sediment supply. In the case of no sediment supply, as shown in Figure 2, the depths increase indefinitely with time. In the interest of determining the best shape of piers to reduce scour, Keutner (9) carried out an investigation early in 1934. This same approach was used by Ishihara (8). Tison (23, 24) studied the mechanics of scour at bridge piers. His study was also qualitative in nature. Although Straub (19) did not study the problem of local scour at piers or abutments, his analysis on the equilibrium condition of a contracted section is considered to be valuable in the general understanding of scour problems. He expressed the regime depth in the contracted section as a function of the approaching flow depth and the degree of contraction. Inglis (7) compared the depth of local scour with the regime depth in the contracted section based upon Lacy's regime theory. Inglis's analysis was based upon field data obtained in India. From the data, Inglis was able to draw the conclusion that the depth of local scour depends upon the discharge per foot of width adjacent to the extremity of the constriction and the size of the bed material. His approach was followed by Blench (5) and Ahmad (2).

In the United States, Laursen has done considerable work on the problem of scour at bridge piers and abutments. He studied the problem of scour both with and without sediment supply in the approaching flow. In the case where the flow is uniformly distributed across the channel, he concluded that the depth of scour for a given geometry of the obstruction, depends only on the width of the obstruction and on the depth of flow, provided that the sediment supply is appreciable.

The following publications should also be mentioned. The paper by Lane and Borland (10) on the depths of scour in a contracted section during flood; Posey's (17) investigation of scour around a circular cylinder; and Ahmad's (3) analysis of the model law

concerning the scour at piers and abutments is included in the references.

MODEL LAW OF LOCAL SCOUR

Considerable progress has been made in the past several decades on the technique of model study for hydraulic structures. Model studies of various types of hydraulic structures have provided many fruitful results.

Strictly speaking, an exact model should have complete similarity with the prototype, that is: (a) geometric similarity, (b) kinematic similarity, and (c) dynamic similarity. However, such a complete similarity is usually not obtainable. The model is usually chosen so that it retains the similarity of major factors. For example, for flow through a contraction, the Froude similarity is used and the Reynolds similarity is neglected. The geometric similarity is generally maintained except in some cases—for example, the sediment size relative to the flow depth and the width of the flood plain relative to the flow depth. If the size of the sand is to be modeled in the laboratory according to the same scale as the flow depth, the sand size has to be reduced so small that the dynamic similarity cannot be studied without encountering difficulties. If the model is reduced in size to include the entire flood plain, the flow depth will be reduced so small that both viscosity and surface tension become important in the study. Such a reduction should be avoided, and under such circumstances, a distorted model is normally employed.

Laboratory model studies can be divided into two categories: (a) a study for a specific engineering project, and (b) a general investigation of the mechanics of a certain phenomenon. In the specific model study the topographical conditions in the vicinity of the structure are also made similar in the model. Quantitative design information can be obtained through this type model study by using the technique of model verification. That is to say, if the past events in the prototype can be reproduced in the model, the results obtained from the model can be used as a guide in the design and construction of the prototype structure.

The second category of model study would apply to scour investigations. Each of the various variables, geometry, flow conditions, sediment supply, etc., needs to be studied independently to evaluate its effect and relative importance on the general over-all scour phenomenon. It is hoped that after such an understanding is achieved, a design criterion can be formulated.

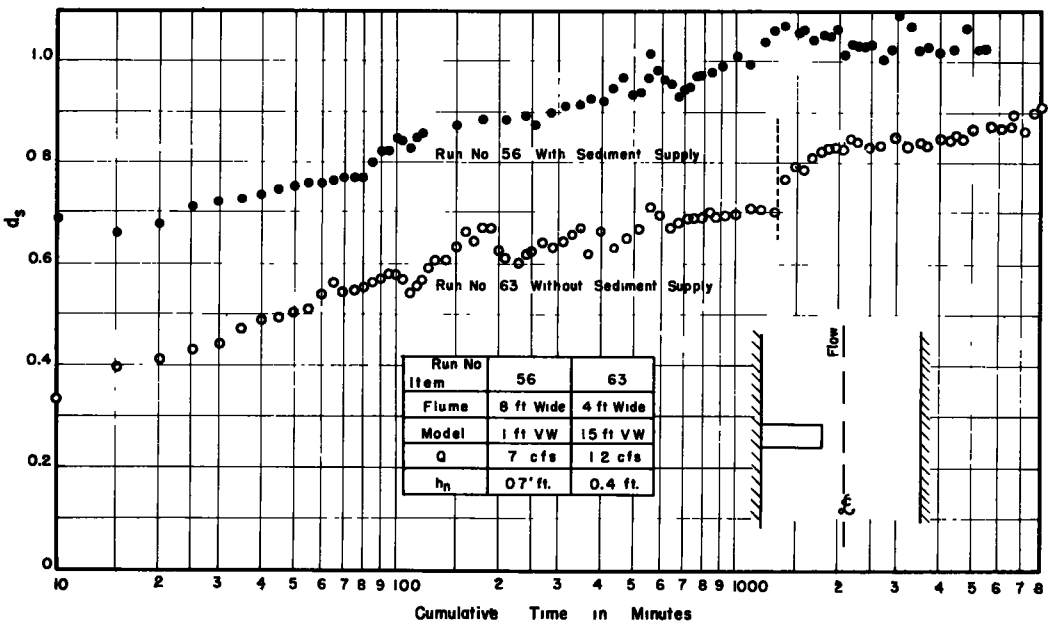

Figure 2. Scour rate curve.

LABORATORY EQUIPMENT

Two flumes were used in the tests. One was 8 ft wide, 160 ft long, and 2 ft deep. The slope of the rails on top of the flume wall and the slope of the flume were adjustable. A recess section located near the mid-point of the length of the flume allowed scour depths up to 5 ft deep. After enough water had been drawn from a sump located beneath the floor, it was recirculated along with sediment in a closed system. The bed material was regular pit run sand with a gradation as shown in Figure 3. A point gage attached to a wheeled carriage which traveled on top of the rails was used to measure the water surface, the bed surface, and the depth of scour. Discharge was measured by use of an offset orifice inserted in the pipe system.

A second flume used for the testing was 4 ft wide, 90 ft long and 2 ft deep. The facilities on this flume were similar to the 8-ft flume with the exception that sediment was not recirculated. A filter sand was used for bed material in this flume with the gradation as shown in Figure 3.

To provide a continuous history of the scour depth, an instrument called the Sonic Depth Sounder (Fig. 4) was utilized. In this instrument, high frequency or ultrasonic sound waves, produced by an electrically pulsed piezoelectric crystal, were used to measure the distance from the transducer to the sand bed. The crystal on being electrically pulsed vibrates at its natural frequency for a short period (a few cycles) resulting in a short burst of energy which travels through the water to the sand bed. Most of the wave is immediately reflected back to the transducer. The time interval between the start of the energy from the transducer and the return of the echo from the sand bed is proportional to the distance between the transducer face and the sand bed. The Sonic Depth Sounder measures the time interval and converts it to a voltage which varies linearly with time. This voltage is then used to operate a strip chart recorder. The piezoelectric element on the face of the transducer is concave in order to focus the energy waves. Depending on the distance to the original bed surface from the transducer face and the range of scour depths anticipated, the correct size and shape of piezoelectric element may be properly chosen. Figure 5 shows an actual recording produced by the instrument.

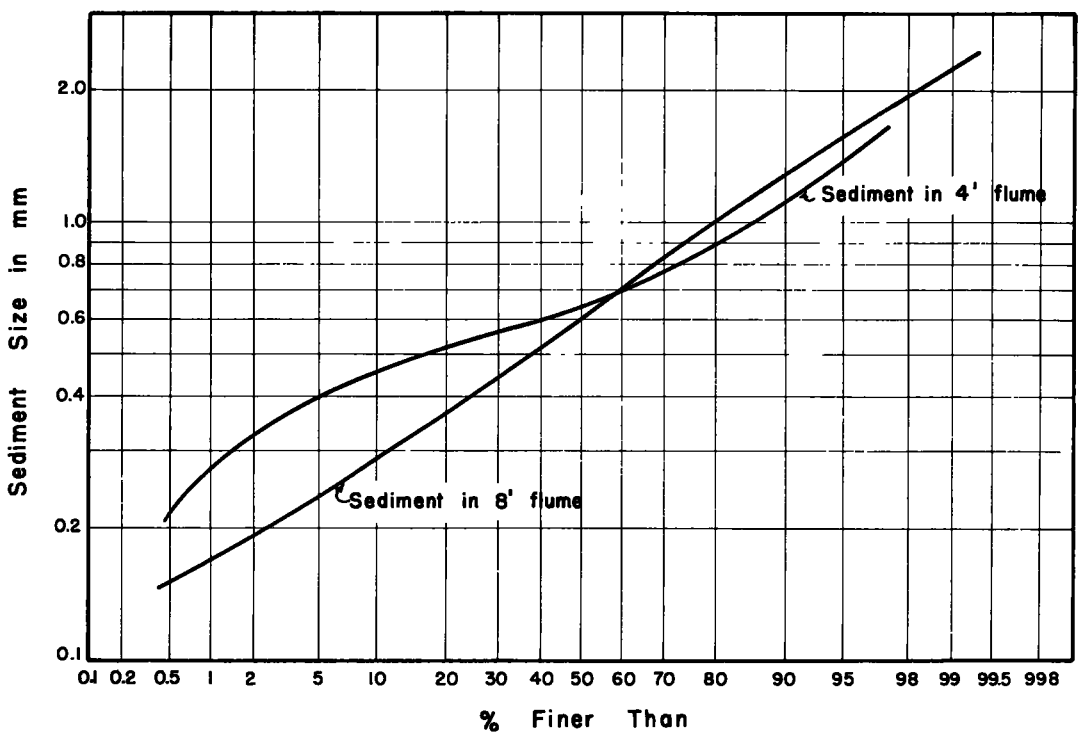

Figure 3. Sediment size analysis curve.

TESTING PROCEDURE

Before installing a model abutment, normal flow conditions were established in the flume. At this time, water surface, bed surface, discharge and depths were recorded. In the case of the 8-ft flume with sediment supply, the bed was normally in the ripple or dune regime depending upon the conditions of flow. In the 4-ft flume where no sediment was recirculated the bed was planed off with a screed and flow conditions established to just produce incipient bed movement. In both cases the datum for the scour depths was taken as the average elevation of the normal bed surface.

After normal flow conditions had been established, the abutment model was installed and readings started. Where sediment was being recirculated, equilibrium scour depths were usually obtained in two or three days. Since equilibrium scour depths could not be reached under conditions of no sediment supply, the 4-ft flume runs were of a comparative nature based on a five hour duration.

The backwater and also the drop of water surface across the embankment were measured. However, due to the movement of sand waves on the bed and also the rapid

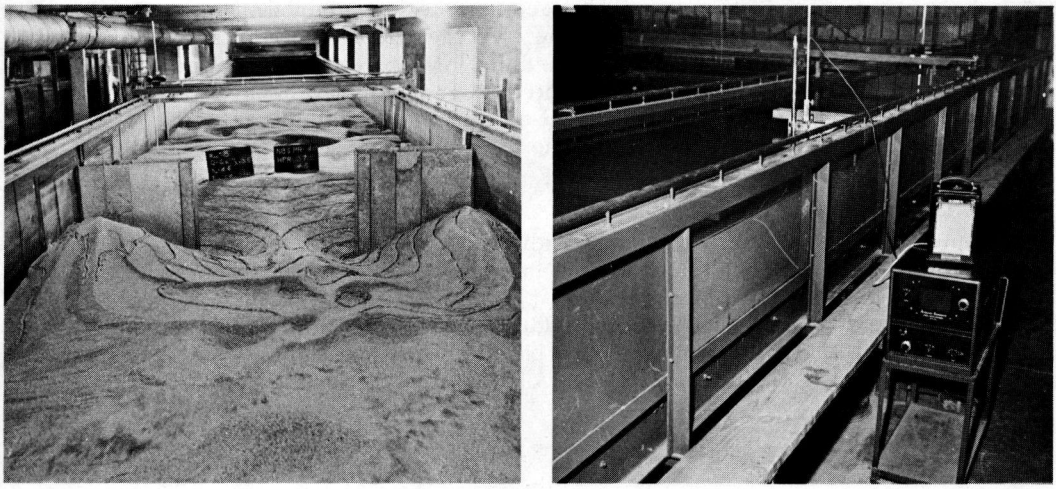

Figure 4. View of the 8-ft flume, 4-ft flume and the sonic depth sounder.

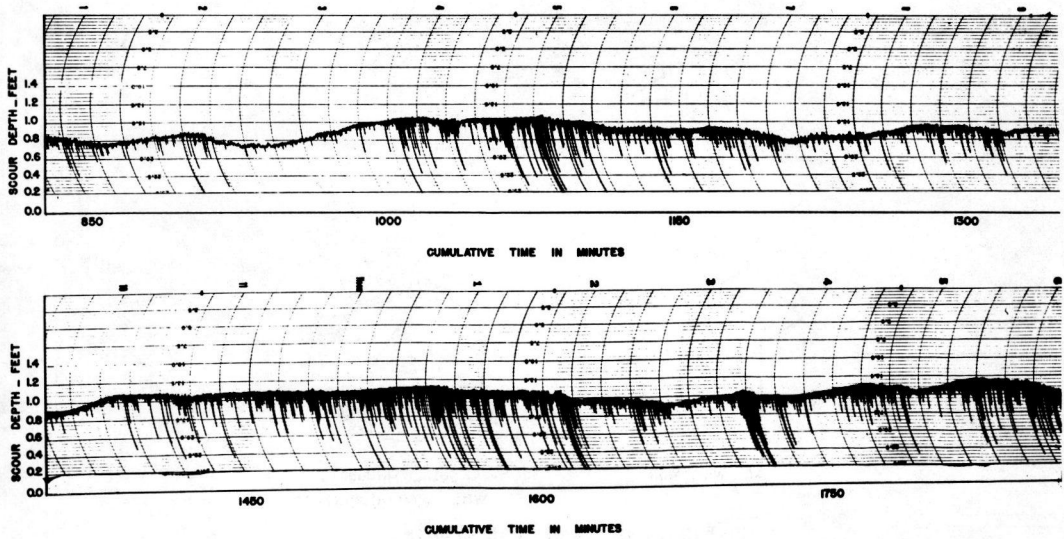

Figure 5. Scour depth recordings.

enlargement of the scour hole, many of the backwater measurements on the 8-ft flume were inconsistent. Better backwater measurements were obtained in the 4-ft flume studies.

After the flow was shut off the scour hole was contoured and a photograph was taken. Various types of abutments as depicted in Figure 6 were investigated for various degrees of contraction.

LABORATORY OBSERVATIONS OF SCOUR AT ABUTMENTS

Data obtained from the research up to the time of this writing are not sufficient to draw any definite conclusions, but some interesting observations have been made.

Geometry

Streamlining of the abutments reduces the extent of the scour depth. Figure 7 shows a comparison of scouring action for different abutment shapes under similar flow conditions; the more streamlined shapes produce the least scour while the vertical wall produces the most scour. As might be expected, a certain amount of properly placed rip rap material reduces the scouring action. On the other hand, the rip rap introduced considerable roughness on the bed in the constriction increasing the backwater upstream.

However, scour may eventually be inhibited by armor plating where the coarser fraction of the bed material is separated out by turbulence and eddies in the scour hole and deposited on the bottom of the hole in the form of a protective coating.

Sediment Supply and Bed Material

As pointed out earlier, the absence of sediment supply to the scour hole from upstream allows the scour depths to increase indefinitely. However, scour may eventually be inhibited by armor plating action. (The coarser fraction of the bed material becomes separated by the turbulence and eddies in the scour hole and then deposits in the form of a protective coating over the bottom of the hole.) Cohesive bed materials have not been investigated so the effect of the cohesion variable is still undetermined.

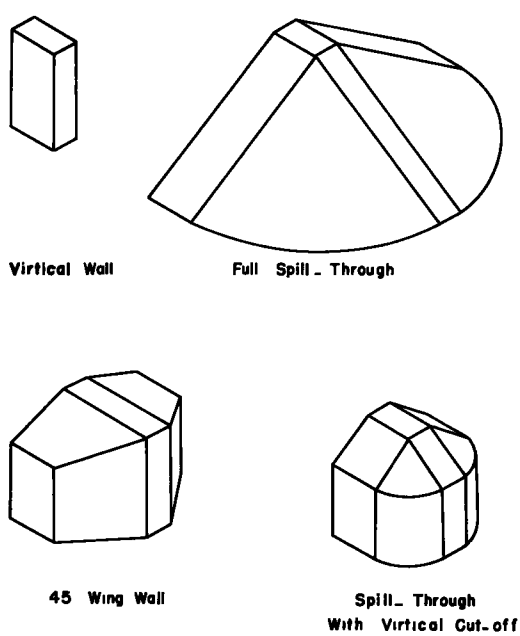

Figure 6. Abutment models.

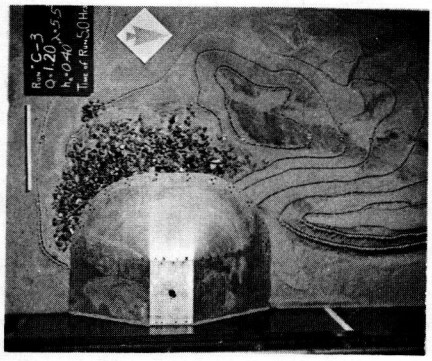

S.T. Vertical Cutoff
Rip Rapped

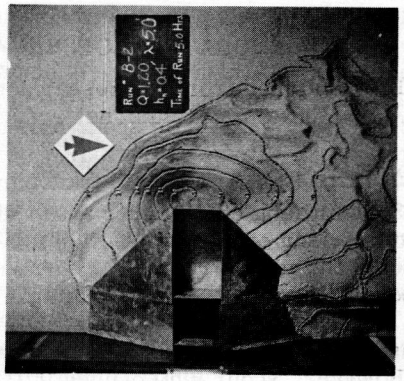

45 Deg Wing Wall

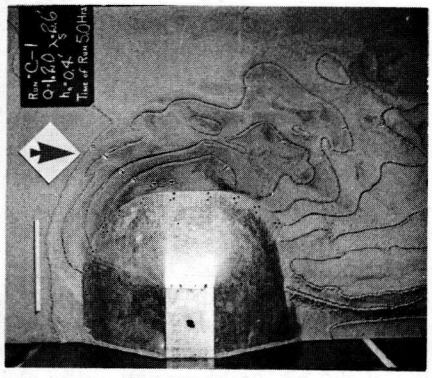

S.T. Vertical Cutoff

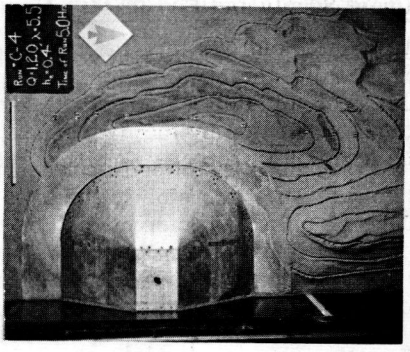

S.T. Apron

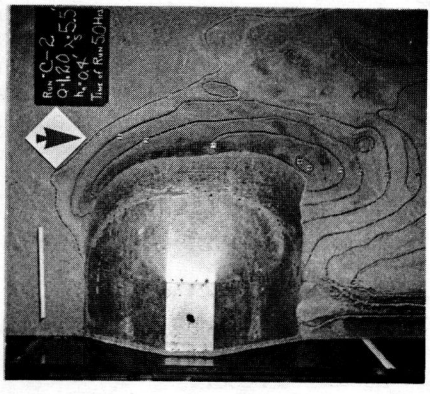

Full Spill-Through

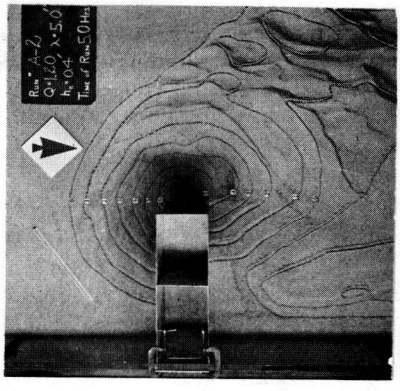

Vertical Wall

Figure 7. Comparison of scour for various models.

Development of the Scour Hole

The process of scour hole development and the accompanying flow patterns have been noted to be similar for the various models tested. Vertical wall and wing wall models develop the maximum scour depth at the upstream nose. The maximum scour for spill-through models occurs some distance downstream of the nose. In each case the maximum scour hole occurs at the point of flow separation.

The scoured material is transported from the scour hole in the form of suspended and bed load. Most of the scoured material is deposited in the vicinity of the downstream side of the abutment.

The pattern of flow in the scour hole is depicted in Figure 8. As flow approaches the abutment from upstream, a portion of the upper layer near the stream side of the abutment sweeps immediately around the nose while the other portion of the upper layer may circulate towards the bank and produce a stagnant pool. The lower layer of the approaching flow also tends to divide as it approaches the abutment with the portion of the stream side diving diagonally down around the nose and carrying with it quantities of bed material at this point. The bank side of the lower layer strikes the upstream face of the abutment and dives directly downward to the bottom of the scour hole and picks up material at this point. This diving jet produces a somewhat generally stable roller in the hole which deposits the scoured material on the sloping face on the upstream side of the scour hole. The material on the sloping upstream side of the scour hole tends to conform roughly to the angle of repose of the material. This portion of the material moves out of the scour hole mainly in the form of bed load.

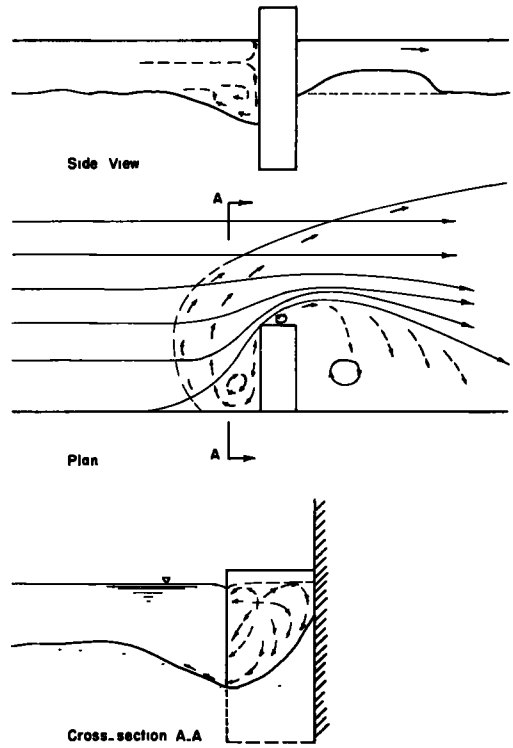

Figure 8. Flow patterns in the vicinity of the scour hole.

CONCLUSIONS

The laboratory study on scour around bridge abutments described here makes possible a much better understanding of the scour phenomenon. As to quantitative results, more time and testing will be required. Also satisfactory verification of model results with similar structures and conditions in the field are requisite before the information can be released for design purposes.

REFERENCES

1. Ahmad, Mushtag, "Spacing and Projection of Spurs for Bank Protection." Civil Eng., London, March and April (1951).
2. Ahmad, Mushtag, "Experiments on Design and Behavior of Spur Dikes." Proc., Minnesota International Hydraulics Convention, University of Minn. (1953).
3. Ahmad, Mushtag, "Effect of Scale Distortion, Size of Model Bed Material and Time Scale on the Geometrical Similarity of Localized Scour."
4. Andru, Peter, "Study of Scour at Obstructions in Non-Cohesive Bed." M.S. Thesis, University of Alberta, Canada (1956).
5. Blench, T., "Regime Behaviour of Canals and Rivers." Butterworths Scientific Pub., London (1957).

6. "Etude des Affouillements Autour des Piles de Ponts." Laboratoire National D'Hydraulique, Chatou (S. et-O), France, October (1956).
7. Ingles, C.C., "The Behaviour and Control of Rivers and Canals (With the Aid of Models)." p. 315 chapt. 8.
8. Ishihara, Toziro, "Experimental Study on Scour at Bridge Piers." Jap. Civil Eng., 24:1, 23-55 (1938), 28:9, 787-821 (1942), 1:11, 974-1007 (1942).
9. Keutner, Ch. "StroMungsVorgange und Stropfeilern von Verschiedener Grundissformen und Ihre Wirkung aut die Flussohle." Die Bautechnik, 161-170 (1932).
10. Lane, E.W. and Boland, W.M., "River Bed Scour During Floods." Trans. ASCE 119: 1069-89 (1954).
11. Laursen, E.M., "Progress Report of Model Studies of Scour Around Bridge Piers and Abutments." HRB Res. Rep. 13-B (1951).
12. Laursen, E.M., "Scour Around Bridge Piers and Abutments." Bull. No. 4, Iowa HRB, (May 1956).
13. Laursen, E.M., "Scour at Bridge Crossings." Bull. No. 4, Iowa HRB, (May 1956).
14. Laursen, E.M., "Observations on the Nature of Scour." Proc., 5th Hydraulics Conference, State University of Iowa (1953).
15. Laursen, E.M. and Toch, A., "A Generalized Model Study of Scour Around Bridge Piers and Abutments." Proc., Minn. Int'l. Hydraulics Convention, University of Minn. (1953).
16. Posey, C.J., Appel, D.W. and Chamness E., Jr., "Investigation of Flexible Mats to Reduce Scour Around Bridge Piers." HRB Res. Rep. 13-B (1951).
17. Posey, C.J., "Why Bridges Fall in Floods, Model Tests of Erosion Around Bridge Piers Indicate Depth of Scour in Erodible Material." Civil. Eng. 2: 42 (1949).
18. Straub, L.G., House Document 238, 738th Congress 2nd Session., U.S. Government Printing Office, Wash., D.C., Appen. XV, p. 1150.
19. Straub, L.G., "Effect of Channel-Contraction Works Upon Regimen of Movable Bed-Streams." Trans. AGU, pt. 2, p. 454 (1934).
20. Straub, L.G., "Approaches to the Study of Mechanics of Bed Movement." Proc. Hydraulics Conference, State University of Iowa (1940).
21. Sugimoto, Shiuichi and Inada, Yutaka, "On Separation Around Pier Wall." Jap. Civil Eng., 36:7, 21-25 (1951).
22. Sugimoto, Shiuichi and Inada, Yutaka, "Study on Hydrodynamics Around Pier." Jap. Civil Eng., 36: 10, 9-12 (1950).
23. Tison, L.J., "L'Erosion et le Transport des Materiaux Solides dans les Curs d' Eau." IVWBV. IAHSR (Int'l. Assoc. for Hyd. Str. Res.), AIRTH, Liege, Vol. II (1939).
24. Tison, L.J., "Erosion Autour de Piles de Ponts en Riviere." Annales des Travaux Publics de Belgique, p. 813-868 (1940).

THE NATIONAL ACADEMY OF SCIENCES—NATIONAL RESEARCH COUNCIL is a private, nonprofit organization of scientists, dedicated to the furtherance of science and to its use for the general welfare. The ACADEMY itself was established in 1863 under a congressional charter signed by President Lincoln. Empowered to provide for all activities appropriate to academies of science, it was also required by its charter to act as an adviser to the federal government in scientific matters. This provision accounts for the close ties that have always existed between the ACADEMY and the government, although the ACADEMY is not a governmental agency.

The NATIONAL RESEARCH COUNCIL was established by the ACADEMY in 1916, at the request of President Wilson, to enable scientists generally to associate their efforts with those of the limited membership of the ACADEMY in service to the nation, to society, and to science at home and abroad. Members of the NATIONAL RESEARCH COUNCIL receive their appointments from the president of the ACADEMY. They include representatives nominated by the major scientific and technical societies, representatives of the federal government, and a number of members at large. In addition, several thousand scientists and engineers take part in the activities of the research council through membership on its various boards and committees.

Receiving funds from both public and private sources, by contribution, grant, or contract, the ACADEMY and its RESEARCH COUNCIL thus work to stimulate research and its applications, to survey the broad possibilities of science, to promote effective utilization of the scientific and technical resources of the country, to serve the government, and to further the general interests of science.

The HIGHWAY RESEARCH BOARD was organized November 11, 1920, as an agency of the Division of Engineering and Industrial Research, one of the eight functional divisions of the NATIONAL RESEARCH COUNCIL. The BOARD is a cooperative organization of the highway technologists of America operating under the auspices of the ACADEMY–COUNCIL and with the support of the several highway departments, the Bureau of Public Roads, and many other organizations interested in the development of highway transportation. The purposes of the BOARD are to encourage research and to provide a national clearinghouse and correlation service for research activities and information on highway administration and technology.